UNIVERSIDADE FEDERAL DE CIÊNCIAS DA SAÚDE DE PORTO ALEGRE – UFCSPA
PROGRAMA DE PÓS-GRADUAÇÃO EM CIÊNCIAS DA SAÚDE

Roger Kist

Triagem virtual de potenciais inibidores para o complexo enzimático mTOR (m*echanistic target of rapamycin*) empregando modelos farmacofóricos

Porto Alegre
2018

Roger Kist

Triagem virtual de potenciais inibidores para o complexo enzimático mTOR (m*echanistic target of rapamycin*) empregando modelos farmacofóricos

Dissertação submetida ao Programa de Pós-Graduação em Ciências da Saúde da Universidade Federal de Ciências da Saúde de Porto Alegre como requisito para a obtenção do grau de Mestre.

Orientador: Prof. Dr. Rafael Andrade Caceres
Coorientadora: Profª Drª Helena Maria Tannhauser Barros

Porto Alegre
2018

Catalogação na Publicação

Kist, Roger
Triagem virtual de potenciais inibidores para o complexo enzimático mTOR (mechanistic target of rapamycin) empregando modelos farmacofóricos / Roger Kist. -- 2018.
94 p. : 30 cm.

Dissertação (mestrado) -- Universidade Federal de Ciências da Saúde de Porto Alegre, Programa de Pós-Graduação em Ciências da Saúde, 2018.

Orientador(a): Rafael Andrade Caceres ; coorientador(a): Helena Maria Tannhauser Barros.

1. mTOR. 2. Potenciais inibidores não competitivos ao ATP. 3. Modelos farmacofóricos baseados na estrutura do ligante. 4. Simulação de docagem molecular e determinação de propriedades ADMETox. 5. Dinâmica molecular. I. Título.

Sistema de Geração de Ficha Catalográfica da UFCSPA com os dados fornecidos pelo(a) autor(a).

Dedico este trabalho a todos que tornaram esta façanha realidade.

AGRADECIMENTOS

Aos meus pais, Nedi e Renato, meus formadores de caráter e sempre incansáveis para que eu atingisse êxito nos meus estudos.

À minha namorada, Natália, pelo companheirismo e por acreditar na nossa superação de desafios.

Ao amigo e professor Rafael, por toda a confiança depositada em mim desde a graduação, pela excelente orientação cedida durante o desenvolvimento do trabalho e pela autonomia que sempre possibilitou a mim.

À professora Helena que possibilitou a interface da nossa área de interesse com a farmacologia clássica a fim de integrar e disseminar o conhecimento.

Ao Luís pela imensa colaboração efetuada no trabalho e pelas discussões de estratégias aplicadas nos estudos efetuados.

Aos colegas da Santa Casa – onde descobri meu alvo de trabalho – pela parceria e auxílio nesta dupla jornada.

Aos secretários dos PPG – Cristiane, Maristela, Daniel e Simone – pela solicitude em toda e qualquer demanda.

Aos colegas e alunos com os quais pude compartilhar conhecimentos e auxiliá-los nos seus trabalhos.

Enfim, muito obrigado a todos que contribuíram de alguma forma para esta conquista.

“You rise.
You fall.
You're down, then you rise again.
What doesn't kill you make ya more strong.”

Broken, Beat & Scarred - Metallica

RESUMO

A via PI3K/Akt/mTOR é uma via de sinalização intracelular importante na regulação do ciclo celular que responde a múltiplas questões nutricionais e ambientais. A desregulação dessa via está envolvida em múltiplas patologias humanas. A mTOR (*mechanistic target of rapamycin*) constitui a principal enzima que exerce o controle intermediário da via de sinalização e a inibição clássica dessa quinase é efetuada pela rapamicina e seus derivados análogos – rapalogs – por meio do bloqueio alostérico do sítio catalítico de fosforilação. Atualmente, sabe-se que há limitações na eficácia dos rapalogs devido aos mecanismos de feedback, insensibilidade enzimática, rotas alternativas e mutações na via PI3K/Akt/mTOR. Considerando que os rapalogs ligam-se a um sítio alostérico não competitivo ao ATP e desempenham um papel fundamental na inibição enzimática da mTOR sem ocasionar efeitos colaterais comuns aos inibidores competidores ao ATP, neste trabalho empregamos triagem virtual aplicada em modelos farmacóforicos baseados na estrutura do ligante, docagem molecular, determinação de propriedades ADMETox das moléculas selecionadas e dinâmica molecular a fim de selecionar moléculas que possuem características favoráveis de se tornarem potenciais inibidores não competitivos ao ATP da mTOR.

Palavras-chave

mTOR. Potenciais inibidores não competitivos ao ATP. Modelos farmacofóricos baseados na estrutura do ligante. Simulação de docagem molecular. Determinação de propriedades ADMETox. Dinâmica molecular.

ABSTRACT

The PI3K/Akt/mTOR pathway is an important intracellular signaling pathway in cell cycle regulation that responds to multiple nutritional and environmental issues. Deregulation of this pathway is involved in multiple human pathologies. mTOR (*mechanistic target of rapamycin*) is the main enzyme that performs the intermediate control of the signaling pathway and the classic inhibition of this kinase is effected by rapamycin and its analogous derivatives - rapalogs – by allosteric locking of the catalytic phosphorylation site. Currently, there are limitations in the efficacy of rapalogs due to feedback mechanisms, enzymatic insensitivity, alternative routes and mutations in the PI3K/Akt/mTOR pathway. Considering that rapalogs bind to a non-ATP competitive allosteric site and perform a key role in mTOR enzymatic inhibition without causing side effects common to ATP-competitive inhibitors, in this work we employ ligand-based drug design, molecular docking, determination of ADMETox properties of the selected molecules and molecular dynamics in order to select molecules that have favorable characteristics of becoming potential non ATP-competitive of the mTOR.

Keywords

mTOR. Non-ATP competitive potential inhibitors. Ligand-based drug design. Molecular docking simulation. ADMETox properties. Molecular dynamics.

SUMÁRIO

1 REVISÃO BIBLIOGRÁFICA

1.1 A via de sinalização PI3K/Akt/mTOR

A via PI3K/Akt/mTOR (Figura 1) é uma via de sinalização intracelular importante na regulação do ciclo celular que responde a múltiplas questões nutricionais e ambientais, incluindo fatores de crescimento, níveis de energia, estresse celular e aminoácidos. A tradução destes sinais leva à promoção do crescimento celular por fosforilação de substratos que desencadeiam processos anabólicos como a tradução de ácido ribonucleico mensageiro (ARNm) e a síntese lipídica, ou limitam processos catabólicos como a autofagia. Resumidamente, a dinâmica da via reside na ativação por meio de substratos extra/intracelulares da fosfatidilinositol-3 quinase (PI3K) que fosforila e ativa a proteína quinase B (AKT) localizada na membrana plasmática. A AKT, além de ser capaz de desencadear outros processos fosforilativos celulares, ativa a mTOR (*mechanistic target of rapamycin*) (Soliman, 2013; Porta *et al.*, 2014; Zarogoulidis *et al.*, 2014).

A mTOR, formalmente denominada anteriormente de ser reconhecida como altamente conservada entre eucariotos como *mammalian Target Of Rapamycin* ou *FK506-binding protein 12-rapamycin-associated protein 1* (FRAP1), é uma quinase serina/treonina (EC 2.7.11.1) de 289 kDa pertencente à família das fosfatidilinositol-3 quinases (PI3K) e constitui a principal enzima que exerce o controle intermediário da via de sinalização também por meio do processo de fosfotransferência, possuindo a molécula de adenosina trifosfato (ATP) como doador de grupamentos fosfato (Guertin e Sabatini, 2007; Laplante e Sabatini, 2009; Soliman, 2013).

Estruturalmente, conforme a Figura 2, a quinase é composta de 2549 resíduos de aminoácidos que conta com um número distinto de domínios funcionais, incluindo (i) 32 repetições denominados "*Huntington, elongation factor 3, PR65/A, TOR"* (HEAT) (do resíduo de aminoácido 16 ao 1345), (ii) um domínio "*FRAP, ATM, TRRAP"* (FAT) (do resíduo de aminoácido 1382 ao 1982); (iii) uma região "FKBP12 *rapamycin-binding"* (FRB) (do resíduo de aminoácido 2012 ao 2144); (iv) um domínio catalítico "*kinase domain"* (KD) e regulador "*regulatory domain"* (RD) (do resíduo de aminoácido 2182 ao 2516) e (v) um domínio "*FRAP ATM TRRAP carboxy terminus"* (FATC) (do resíduo de aminoácido 2517 ao 2549). Os sítios fosforilativos são identificados na serinas 1265, 2448 e 2481, e na treonina 2446 (Watanabe *et al.*, 2011).

Figura 1. A via de sinalização PI3K/Akt/mTOR.

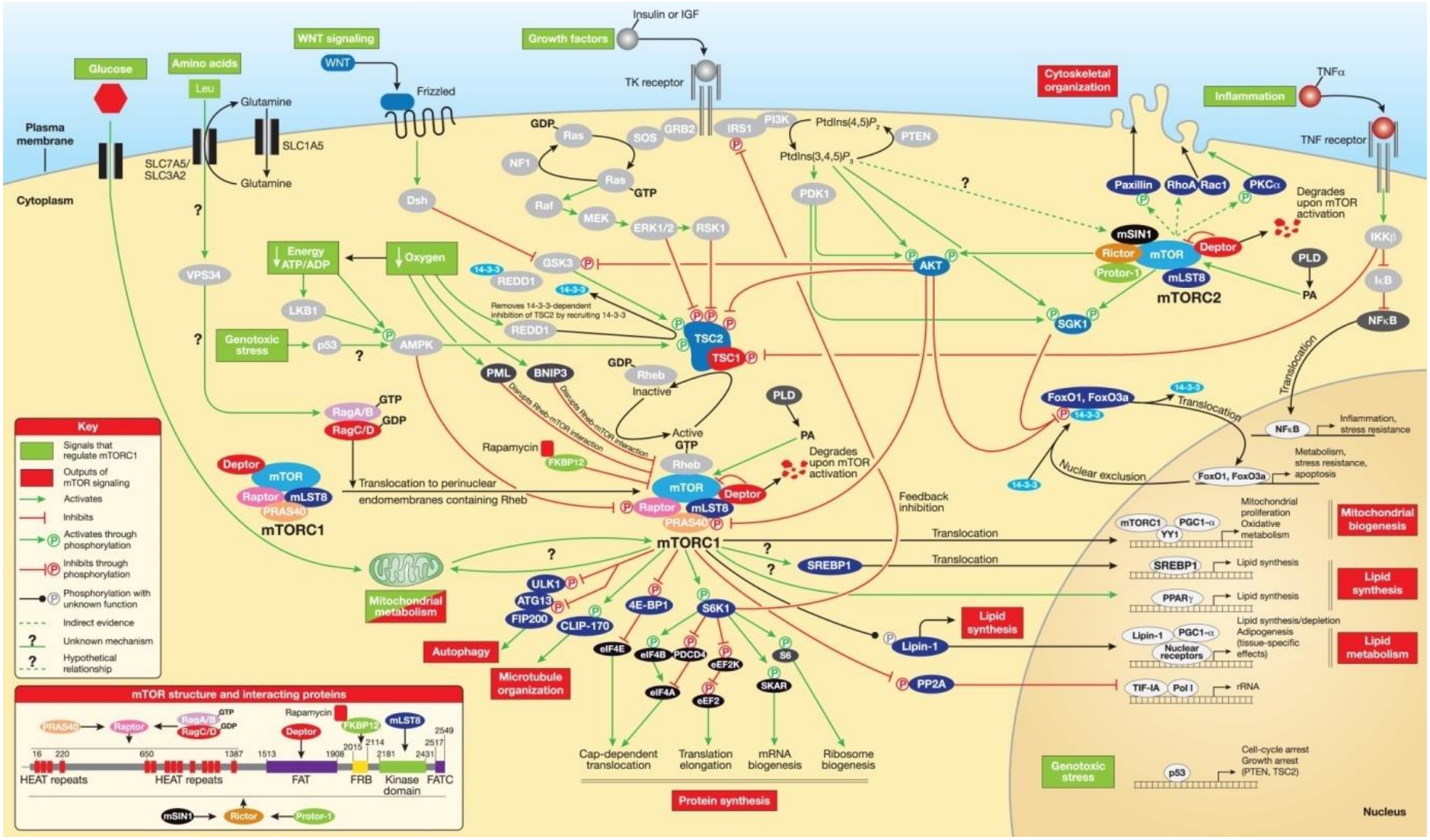

Fonte: Adaptada de Laplante e Sabatini (2009).

Esta quinase atípica está presente em dois complexos funcional e estruturalmente distintos, mTORC1 e mTORC2, localizados em diferentes compartimentos celulares, cada um contendo subunidades distintas e comuns necessárias à atividade e regulação catalíticas da enzima principal. O complexo mTORC1 transmite sinais de disponibilidade de nutrientes para controlar várias funções celulares, enquanto que o complexo mTORC2, regula principalmente a montagem do citoesqueleto por actina (Laplante e Sabatini, 2009; Watanabe *et al.*, 2011; Laplante e Sabatini, 2012; Betz e Hall, 2013).

O complexo mTORC1 possui cinco componentes: mTOR, que é a subunidade catalítica do complexo; "*regulatory-associated protein of* mTOR" (Raptor) e "*mammalian lethal with Sec13 protein 8"* (mLST8 ou GβL) que são as subunidades regulatórias positivas; "*prolinerich AKT substrate 40 kDa"* (PRAS40) e "*DEP-domain-containing mTOR-interacting protein"* (Deptor), que são as subunidades regulatórias negativas. Já o mTORC2 é composto por seis diferentes proteínas, muitas comuns à mTORC1 e mTORC2: mTOR; "*rapamycin-insensitive companion of* mTOR" (Rictor); "*mammalian stress-activated protein kinase interacting protein"* (mSIN1) e "*protein observed with* Rictor-1" (Protor-1) que desempenham o papel de estabilizar o complexo formado; mLST8; e Deptor (Laplante e Sabatini, 2009; Watanabe *et al.*, 2011; Laplante e Sabatini, 2012).

Figura 2. Diagrama estrutural da mTOR.

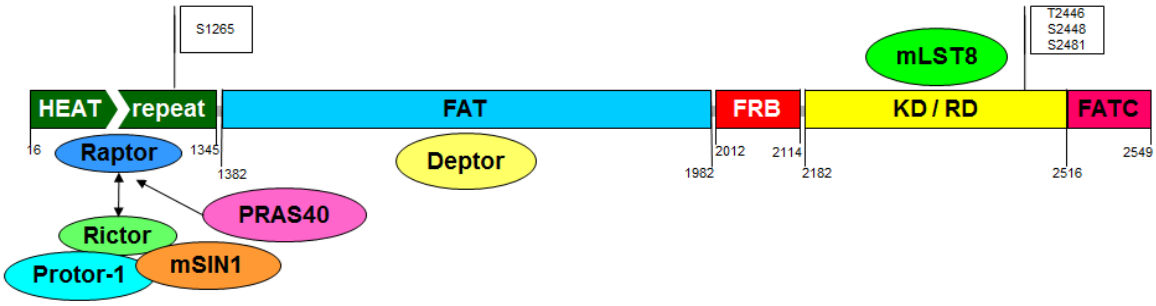

Fonte: Elaborada pelo autor.

1.2 Mecanismo de inibição da via mTOR

A inibição clássica da via da mTOR é efetuada pela rapamicina e seus derivados análogos, denominados *rapalogs*, que são considerados os inibidores de

primeira geração (Figura 3) (Sehgal, 2003; Abraham *et al.*, 2010; Santulli e Totary-Jain, 2013; Zheng e Jiang, 2015).

Figura 3. Estrutura molecular planar dos inibidores de primeira geração da mTOR. (A) rapamicina/sirolimo, (B) everolimo, (C) temsirolimo e (D) deforolimo.

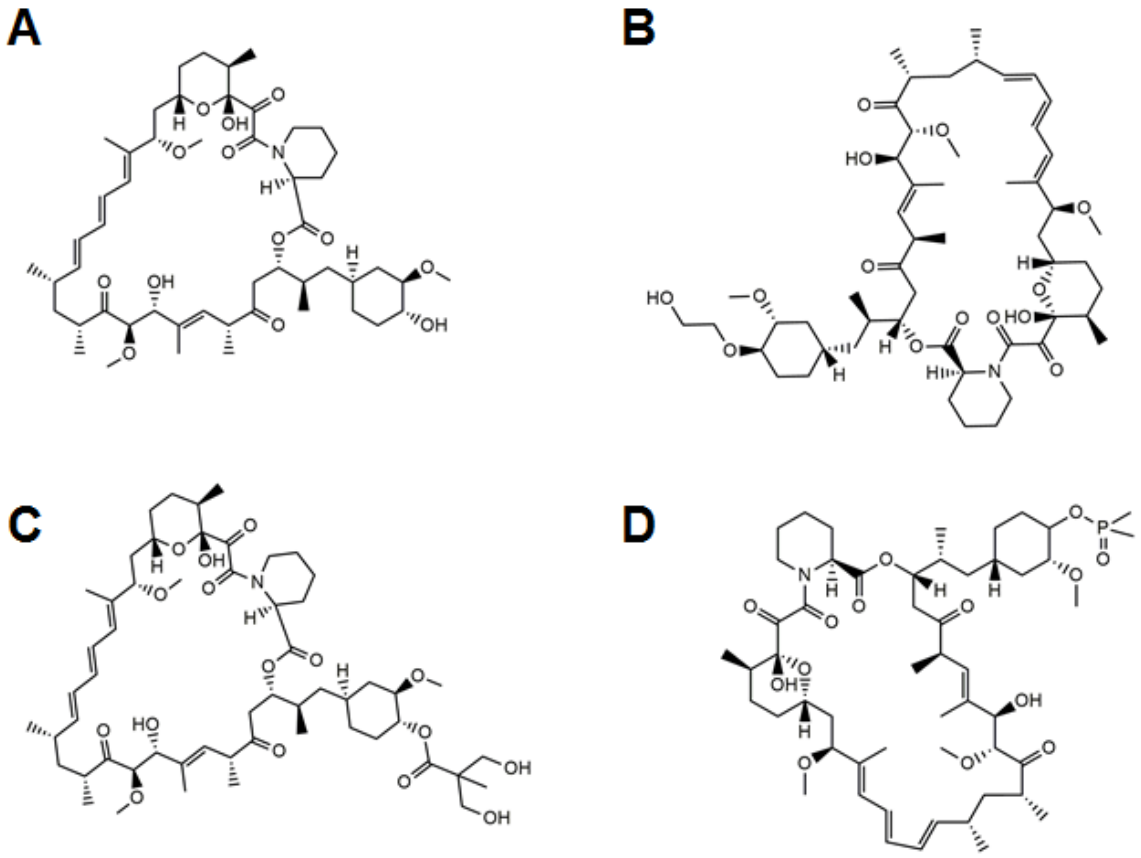

Fonte: Elaborada pelo autor.

A rapamicina ou sirolimo (Rapamune, Wyeth Pharmaceuticals), CAS 53123-88-9, fórmula molecular $C_{51}H_{79}NO_{13}$ e massa molecular de 914,17 g/mol, foi descoberta na Ilha da Páscoa, Chile, em 1972. Trata-se de um potente antibiótico macrolídeo produzido pelo micro-organismo *Streptomyces higroscopicus* e que, por possuir propriedades antifúngica, imunossupressora e antitumoral, é utilizado amplamente na terapêutica. Todavia, devido a suas propriedades desfavoráveis, como a sua baixa solubilidade em água e estabilidade em solução, foram desenvolvidos análogos moleculares, os *rapalogs*, como o everolimo (RAD001, Afinitor, Novartis Pharmaceuticals), temsirolimo (CCI-779, Torisel, Wyeth Pharmaceuticals) e ridaforolimo (AP23573; formalmente deforolimo, ARIAD Pharmaceuticals), os quais

melhoraram as propriedades farmacocinéticas sem alterar o mecanismo de ação (Santulli e Totary-Jain, 2013).

O mecanismo de inibição da mTOR pela rapamicina e seus análogos reside na ligação ao receptor intracelular da *FK506-binding protein* 12 kDa (FKBP12), formando o complexo rapamicina-FKBP12 que se liga direta e predominantemente ao domínio *FKBP12-rapamycin binding* (FRB), bloqueando de forma alostérica o sítio catalítico de fosforilação conforme demonstrado na Figura 4 (Laplante e Sabatini, 2009; Yang *et al.*, 2013; Shimobayashi e Hall, 2014).

Figura 4. A) Representação da superfície da estrutura do complexo mTOR-mLST8-ATP; B) Representação da superfície da estrutura do modelo mTOR-mLST8-ATP-rapamicina-FKBP12. Em ciano, domínio FAT; em vermelho, domínio FRB; em amarelo, domínio quinase; em magenta, domínio FATC; em verde, subunidade proteica mLST8; em azul, a subunidade proteica FKBP12.

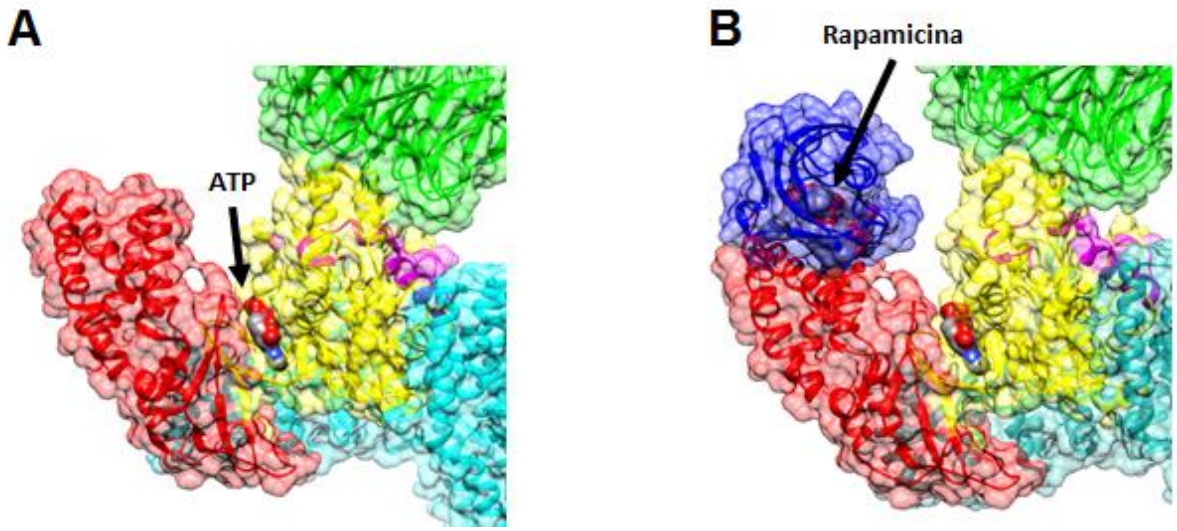

Fonte: Elaborada pelo autor utilizando o programa Chimera v.1.9 (Pettersen *et al.*, 2004), baseando-se em Yang e colaboradores (2013) (Yang *et al.*, 2013) nos modelos PDBID 1FAP e 4JSP.

Na prática, a partir de experimentos de Banaszynski e colaboradores (2005) revelou-se a constante de dissociação (K_d) moderadamente favorável entre a rapamicina e FRB (K_d = 26 ± 0,8 µM). No entanto, o complexo rapamicina-FKBP12 associa-se à FRB com uma afinidade 2000 vezes maior (K_d = 12 ± 0,8 nM) do que a rapamicina por si só. Além disso, nenhuma interação entre FKBP12 e FRB foi

detectada na ausência de rapamicina. Assim, sugere-se que a capacidade da rapamicina em se ligar à fração FRB e, por extensão, à mTOR na ausência de FKBP12, é de pouca importância sob condições fisiológicas. Além do mais, as interações proteína-proteína na interface FRB-FKBP12 desempenham um papel fundamental na estabilidade do complexo ternário (Banaszynski *et al.*, 2005).

A Figura 5 ilustra as interações entre os resíduos proteicos da porção FRB (do resíduo 108 a 201) e da porção FKBP12 (do resíduo 1 a 107) com a molécula de rapamicina. Adotou-se como parâmetros para ligação de hidrogênio, em angstroms (Å): distância máxima hidrogênio-aceptor de 3,2 Å e doador-aceptor de 4,0 Å; distância de contato mínima e máxima de 3,6 Å somente para contatos hidrofóbicos. Identifica-se interações hidrofóbicas com a porção FRB (cadeia B) nos resíduos Ser124, Phe128, Gly129, Thr187, Trp190 e Tyr194; interações hidrofóbicas com a porção FKBP12 (cadeia A) nos resíduos Phe36, Phe46, Val55, Trp59, Ile90; interações do tipo ligações de hidrogênio apenas com a porção FKBP12 (cadeia A) em Asp37 (2,76 Å); Gln53 (2,62 Å); Glu54 (2,88 Å); Ile56 (2,78 Å) e Tyr82 (2,71 Å).

Figura 5. Resíduos proteicos de FKBP12 (do resíduo 1 ao 107) e FRB (do resíduo 108 ao 202) que realizam interações com uma molécula de rapamicina.

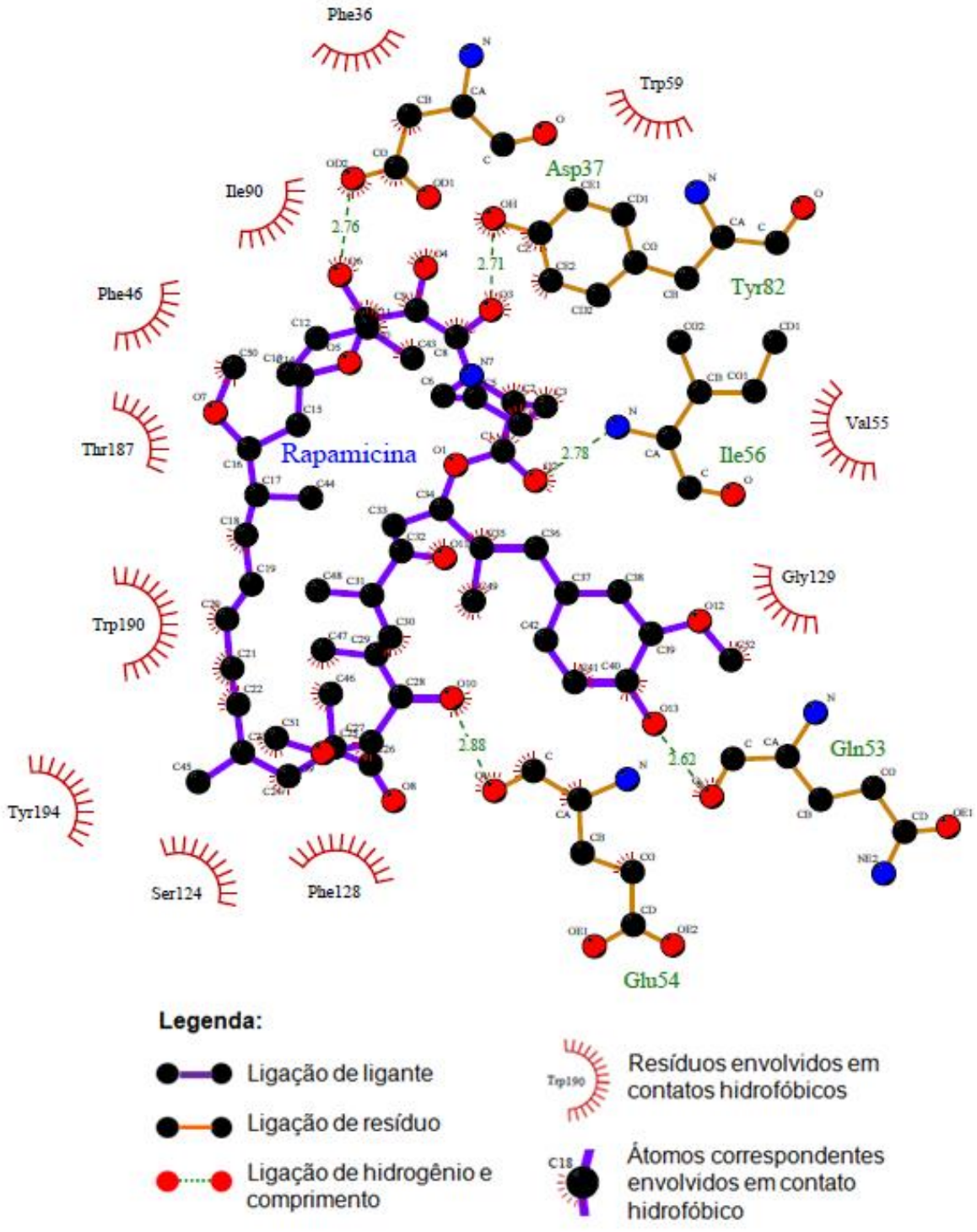

Fonte: Elaborada pelo autor utilizando o programa LigPlot⁺ v.1.4 (Banaszynski *et al.*, 2005).

1.3 Desafios dos inibidores de primeira geração e as inovações farmacológicas

Os *rapalogs* revelaram eficácia, segurança e tolerabilidade de eventos adversos na inibição da via da mTOR em uma série de estudos. Contudo, o sucesso desses inibidores de primeira geração tem demonstrado falhas especialmente devido ao mecanismo de *feedback* já que a inibição do complexo resulta na hiperativação da sinalização PI3K/Akt e incrementa a sobrevivência celular; determinada insensibilidade do mTORC1 aos *rapalogs* foi recentemente revelada, desafiando o dogma de que a rapamicina inibe completamente a atividade do mTORC1; vias alternativas e cruzamento de vias entre as quinases também poderia limitar a eficácia dos *rapalogs* e mutações na via PI3K/Akt/mTOR (Carracedo e Pandolfi, 2008; Choo *et al.*, 2008; Choo e Blenis, 2009; Guertin e Sabatini, 2009; Thoreen *et al.*, 2009; Di Nicolantonio *et al.*, 2010; Wacheck, 2010; Santulli e Totary-Jain, 2013).

Dessa forma, o esforço recente tem se baseado na busca por inibidores diretos do sítio catalítico de quinases, ou seja, ATP-competitivos. Nesse caso, pode-se citar fármacos com testes clínicos já iniciados como os inibidores duplos de segunda geração – mTOR/PI3K *dual inhibitors* (TPdIs) como, por exemplo, PF-0469150212, BEZ23513 e GSK212645814 e seletivos mTORC1/mTORC2 *dual inhibitors* (TORCdIs) como, por exemplo, OSI-0279, INK-12810 e CC-22311 (Knight *et al.*, 2010; Bhagwat *et al.*, 2011; Yuan *et al.*, 2011; Zask *et al.*, 2011; Mukherjee *et al.*, 2012; Guo e Kwiatkowski, 2013; Santulli e Totary-Jain, 2013; Zheng e Jiang, 2015).

Apesar de demonstrar certa seletividade e grande promessa na terapêutica, a maioria dos inibidores de quinases não são seletivos a um único alvo molecular. Tal fato aumenta potencialmente o risco de efeitos indesejáveis e toxicidade devido à interação com outras enzimas e à inibição de outras quinases essenciais ao metabolismo. Dessa forma, é importante a busca por inibidores cada vez mais seletivos a determinados alvos (Luo, 2005; Thaimattam *et al.*, 2007; Smyth e Collins, 2009; Wang *et al.*, 2016).

1.4 Bases metodológicas para o desenvolvimento de novos fármacos

O desenvolvimento de novos fármacos visa à identificação de compostos de interesse farmacológico que atendam tanto o tratamento de doenças quanto a melhoria da qualidade de vida do paciente. Atualmente, em termos gerais, o perfil de fármaco ideal a ser desenvolvido reside em três principais características: propriedades favoráveis de ADMETox (absorção, distribuição, metabolismo, excreção

e toxicidade); quesitos intrínsecos (seletividade, biodisponibilidade, facilidade de síntese e baixo custo); cumprimento da Regra de Lipinski dos Cinco (compostos com menos de 5 grupamentos doadores de pontes de hidrogênio; menos de 10 grupamentos receptores de pontes de hidrogênio; peso molecular menor que 500 Da e coeficiente de partição octanol/água (logP) menor que 5) e as Regras de Veber (um composto para apresentar biodisponibilidade oral deve satisfazer os critérios de ≤ 10 ligações flexíveis e área de superfície polar ≤ 140 (Lipinski *et al.*, 1997; Veber *et al.*, 2002; Lipinski, 2004; Bielska *et al.*, 2011; Leeson, 2012).

Candidatos a fármacos são moléculas orgânicas que geralmente compartilham características físico-químicas semelhantes. No intuito de avaliar experimentalmente esses compostos frente a um determinado alvo molecular, por exemplo, uma proteína-chave de determinada via metabólica de uma patologia, testes denominados de *high-throughput screening* ou triagem de alto desempenho são desenvolvidos. Dessa forma, os compostos são confrontados em relação ao alvo terapêutico em ensaios *in vitro* que empregam métodos analíticos de avaliação da atividade farmacológica desses compostos. Todavia a dimensão das bibliotecas torna esse método inviável financeiramente (Liu *et al.*, 2004; Bielska *et al.*, 2011; Ferreira *et al.*, 2011).

Uma alternativa à triagem de alto desempenho é a triagem virtual, cuja utilização de tecnologia computacional possibilita avaliar uma grande quantidade de compostos *in silico* em reduzidos tempo e custo em relação à triagem de alto desempenho. Além disso, possibilita não apenas testar as imensas bibliotecas, mas também adquirir ou sintetizar novas moléculas de acordo com a afinidade com o receptor e complementar a triagem de alto desempenho, identificando possíveis falso-negativos produzidos por testes experimentais a fim de aumentar a taxa de sucesso (Klebe, 2000; Bielska *et al.*, 2011).

De mesmo modo, a triagem virtual trata-se de uma metodologia baseada puramente em conhecimento prévio, sendo que a qualidade e a quantidade de informação exigida pelo sistema computacional se tornam fatores críticos quando se emprega essa tecnologia no desenvolvimento de novos candidatos a fármacos por computação assistida. De fato, o conhecimento sobre compostos químicos torna-se base para a procura por similaridade estrutural em relação ao ligante/substrato ou a pesquisa por farmacóforos. Se houver a disponibilidade da estrutura-alvo resolvida por cristalografia de raios X, ressonância magnética nuclear (RMN) ou microscopia eletrônica (EM), pode-se empregar o método de simulação por docagem molecular,

cujos compostos são atracados no sítio catalítico de determinado alvo-molecular e suas respectivas afinidades são avaliadas. Caso não haja estrutura-alvo resolvida, opta-se por realizar modelagem molecular por homologia também utilizando recursos computacionais (Bielska *et al.*, 2011; Cole *et al.*, 2011; Koeppen *et al.*, 2011; Rognan, 2011).

A análise dos resultados obtidos através da simulação da interação receptor-ligante é realizada de forma a obter a configuração dos possíveis ligantes dentro do sítio catalítico do receptor. Assim, emprega-se modelos computacionais baseados em algoritmos específicos que buscam predizer as interações intermoleculares entre a proteína e o ligante e, com isso, a afinidade entre estes. Além disso, a utilização de funções de avaliação permite estimar a energia livre de ligação do complexo formado com maior acurácia. Atualmente, essas funções são divididas em quatro grupos distintos: funções baseadas no campo de força; funções empíricas; funções baseadas em conhecimento e funções consenso (De Magalhães *et al.*, 2007; Sotriffer e Matter, 2011).

1.5 Modelos farmacofóricos como triagem virtual

Farmacóforos descrevem a disposição estrutural das características moleculares essenciais de uma interação entre um ligante e o seu receptor em que os principais desafios destes modelos são a identificação de uma disposição espacial representativa para a interação ligante-receptor e a identificação dos compostos em uma biblioteca química que satisfaçam este modelo (Langer e Krovat, 2003; Leach *et al.*, 2010; Mannhold *et al.*, 2011; Markt *et al.*, 2011).

Neste sentido, um exemplo trata-se do webserver ZINCPharmer, um mecanismo de pesquisa que emprega ligantes ativos que sejam conformacionalmente acessíveis a determinado espaço conformacional gerado. Dessa forma, o ZINCPharmer fornece um mecanismo para derivar uma hipótese de farmacóforo inicial diretamente a partir de estruturas dentro do PDB (Protein Data Bank), e também suporta a importação de definições de farmacóforos desenvolvidas usando abordagens computacionalmente mais exigentes implementadas em ferramentas de terceiros (Koes e Camacho, 2012).

1.6 Compreendendo o comportamento do alvo em relação ao ligante

Visto que proteínas são biomoléculas complexas que, em geral, demonstram uma ampla dinâmica envolvida na atividade e controle de vias metabólicas e que há

necessidade de entender tais processos dinâmicos, no desenvolvimento de fármacos por computação assistida emprega-se uma ferramenta importante denominada simulação computacional por dinâmica molecular (DM). Tal técnica permite determinar os movimentos das partículas de qualquer sistema do qual se conheçam o potencial de interação entre essas partículas e as equações que regem seu movimento. Dessa forma, possibilita a evolução temporal das configurações dos constituintes do sistema e, por intermédio das sequências de posições geradas, determinam-se as propriedades macroscópicas do sistema de acordo com os princípios de Mecânica Estatística (Martínez *et al.*, 2007; Namba *et al.*, 2008).

Nessa metodologia, partículas interagentes, inicialmente dispostas em uma configuração, movimentam-se sob a influência de potenciais intermoleculares. De posse dos dados relativos às posições e velocidades de todas as partículas envolvidas em um dado instante (t_0), pode-se computar as forças resultantes em cada partícula devido à interação com as demais e determinar posições e velocidades em um tempo posterior ($t_0 + \delta t$) por meio de equações de movimento Newtonianas. As novas posições são utilizadas para a computação de novas forças e posteriores posições e velocidades em ($t_0 + 2.\delta t$). Tal procedimento é realizado recursivo e intermitentemente gerando trajetórias moleculares para todo o sistema (Martínez *et al.*, 2007; Namba *et al.*, 2008).

Existem múltiplos fatores envolvidos na técnica de simulação por DM de macromoléculas, entre os quais a complexidade do sistema a ser compreendido torna-se o principal fator que influencia no tempo total da simulação. Esses fatores, como o cálculo das forças exercidas sobre cada partícula do sistema devido às interações intermoleculares; a movimentação das partículas; o estabelecimento dos protocolos e dos controles de simulação, a análise ou armazenamento das configurações devem ser cuidadosamente planejados e previamente avaliados para se obter resultados satisfatórios (Martínez *et al.*, 2007; Namba *et al.*, 2008).

1.7 Aplicabilidade de métodos *in silico* no caso da mTOR

Cada vez mais, a adoção de métodos computacionais vem auxiliando na concepção de novos candidatos a fármacos com maior agilidade e com menores custos. Conforme descrito previamente, o desenvolvimento *in silico* de moléculas consiste em uma coleção de ferramentas que colaboram na tomada de decisões racionais para as diferentes etapas do processo de descoberta de fármacos, tais como

a identificação de um alvo biomolecular de interesse terapêutico, a construção da estrutura do alvo, a identificação dos sítios de ligação a ligantes, a obtenção de uma biblioteca de compostos similares ao substrato ou de um inibidor já conhecido ou o desenvolvimento de novos compostos líderes e sua otimização para obtenção de melhor afinidade com o alvo, bem como as propriedades farmacocinéticas e farmacodinâmicas intrínsecas a cada molécula.

Nesse contexto, considerando a ligação de moléculas, por exemplo, a rapamicina com a subunidade FKBP12 e o domínio FRB da mTOR como ação central na inibição da rota metabólica, a busca e desenvolvimento de novas moléculas que sejam capazes de efetuar tal ligação e que possuam propriedades farmacológicas mais favoráveis torna-se essencial para o controle mais efetivo dessa importante via responsável por inúmeros mecanismos fisiológicos e que se encontra desregulada em determinadas patologias como, por exemplo, o câncer. Dessa forma, evidenciam-se estudos recentes com este intuito como Chen, Lee, Chen, & Chen (2014); Park, Choe, & Hong (2014); Nasr e colaboradores (2015); Wang e colaboradores (2016); e Kist & Caceres (2016) (Chen *et al.*, 2014; Park *et al.*, 2014; Nasr *et al.*, 2015; Kist e Caceres, 2016; Wang *et al.*, 2016). Entretanto, sabe-se que o complexo mTOR exibe uma dinâmica molecular que não deve ser desconsiderada, devendo-se aplicar métodos computacionais avançados para melhor avaliar o comportamento desse complexo e a mecanística de sua inibição.

REFERÊNCIAS BIBLIOGRÁFICAS

ABRAHAM, R., T.; GIBBONS, J. J.; GRAZIANI, E., I. Chemistry and Pharmacology of Rapamycin and Its Derivatives. In: HALL, M. N. e TAMANOI, F. (Ed.). **The Enzymes: Structure, Function and Regulation of TOR complexes from Yeasts to Mammals.**: Academic Press, v.27, 2010. p.329-356. ISBN 978-0-12-381539-2.

BANASZYNSKI, L. A.; LIU, C. W.; WANDLESS, T. J. Characterization of the FKBP.rapamycin.FRB ternary complex. **J Am Chem Soc,** v. 127, n. 13, p. 4715-21, Apr 2005. ISSN 0002-7863. Disponível em: < http://www.ncbi.nlm.nih.gov/pubmed/15796538 >.

BETZ, C.; HALL, M. N. Where is mTOR and what is it doing there? **J Cell Biol,** v. 203, n. 4, p. 563-74, Nov 2013. ISSN 1540-8140. Disponível em: < http://www.ncbi.nlm.nih.gov/pubmed/24385483 >.

BHAGWAT, S. V. et al. Preclinical characterization of OSI-027, a potent and selective inhibitor of mTORC1 and mTORC2: distinct from rapamycin. **Mol Cancer Ther,** v. 10, n. 8, p. 1394-406, Aug 2011. ISSN 1538-8514. Disponível em: < https://www.ncbi.nlm.nih.gov/pubmed/21673091 >.

BIELSKA, E. et al. Virtual screening strategies in drug design–methods and applications. ***Journal of Biotechnology Computational Biology and Bionanotechnology*Journal of Biotechnology Computational Biology and Bionanotechnology,** v. 92, n. 3, p. p 249-264, 2011.

CARRACEDO, A.; PANDOLFI, P. P. The PTEN-PI3K pathway: of feedbacks and cross-talks. **Oncogene,** v. 27, n. 41, p. 5527-41, Sep 2008. ISSN 1476-5594. Disponível em: < http://www.ncbi.nlm.nih.gov/pubmed/18794886 >.

CHEN, K.-C. et al. In Silico Investigation of Potential mTOR Inhibitors from Traditional Chinese Medicine for Treatment of Leigh Syndrome. **BioMed Research International,** v. 2014, p. 9, 2014. Disponível em: < http://dx.doi.org/10.1155/2014/139492 >.

CHOO, A. Y.; BLENIS, J. Not all substrates are treated equally: implications for mTOR, rapamycin-resistance and cancer therapy. **Cell Cycle,** v. 8, n. 4, p. 567-72, Feb 2009. ISSN 1551-4005. Disponível em: < http://www.ncbi.nlm.nih.gov/pubmed/19197153 >.

CHOO, A. Y. et al. Rapamycin differentially inhibits S6Ks and 4E-BP1 to mediate cell-type-specific repression of mRNA translation. **Proc Natl Acad Sci U S A,** v. 105, n. 45, p. 17414-9, Nov 2008. ISSN 1091-6490. Disponível em: < https://www.ncbi.nlm.nih.gov/pubmed/18955708 >.

COLE, J. C. et al. The Basis for Target-Based Virtual Screening: Protein Structures. In: (Ed.). **Virtual Screening**: Wiley-VCH Verlag GmbH & Co. KGaA, 2011. p.87-114. ISBN 9783527633326.

DE MAGALHÃES, C. S.; BARBOSA, H. J. C.; DARDENNE, L. E. Métodos de Docking Receptor-Ligante para o Desenho Racional de Compostos Bioativos. In:

MORGON, N. H. e COUTINHO, K. (Ed.). **Métodos de química teórica e modelagem molecular.** 1ª ed. São Paulo, 2007. cap. Cap. 14, p.p.489 - 532.

DI NICOLANTONIO, F. et al. Deregulation of the PI3K and KRAS signaling pathways in human cancer cells determines their response to everolimus. **J Clin Invest,** v. 120, n. 8, p. 2858-66, Aug 2010. ISSN 1558-8238. Disponível em: < https://www.ncbi.nlm.nih.gov/pubmed/20664172 >.

FERREIRA, R. S.; GLAUCIUS, O.; ANDRICOPULO, A. D. Integração das técnicas de triagem virtual e triagem biológica automatizada em alta escala: oportunidades e desafios em P&D de fármacos. **Química Nova,** v. 34, p. 1770-1778, 2011. ISSN 0100-4042. Disponível em: < http://www.scielo.br/scielo.php?script=sci_arttext&pid=S0100-40422011001000010&nrm=iso >.

GUERTIN, D. A.; SABATINI, D. M. Defining the role of mTOR in cancer. **Cancer Cell,** v. 12, n. 1, p. 9-22, Jul 2007. ISSN 1535-6108. Disponível em: < http://www.ncbi.nlm.nih.gov/pubmed/17613433 >.

GUERTIN, D. A.; SABATINI, D. M.. The pharmacology of mTOR inhibition. **Sci Signal,** v. 2, n. 67, p. pe24, Apr 2009. ISSN 1937-9145. Disponível em: < https://www.ncbi.nlm.nih.gov/pubmed/19383975 >.

GUO, Y.; KWIATKOWSKI, D. J. Equivalent benefit of rapamycin and a potent mTOR ATP-competitive inhibitor, MLN0128 (INK128), in a mouse model of tuberous sclerosis. **Mol Cancer Res,** v. 11, n. 5, p. 467-73, May 2013. ISSN 1557-3125. Disponível em: < https://www.ncbi.nlm.nih.gov/pubmed/23386687 >.

KIST, R.; CACERES, R. A. New potential inhibitors of mTOR: a computational investigation integrating molecular docking, virtual screening and molecular dynamics simulation. **Journal of Biomolecular Structure and Dynamics**, p. 1-14, 2016. ISSN 0739-1102. Disponível em: < http://dx.doi.org/10.1080/07391102.2016.1262279 >.

KLEBE, G. **Virtual Screening: an Alternative Or Complement to High Throughput Screening?** Springer, 2000. ISBN 0792366336.

KNIGHT, S. D. et al. Discovery of GSK2126458, a Highly Potent Inhibitor of PI3K and the Mammalian Target of Rapamycin. **ACS Med Chem Lett,** v. 1, n. 1, p. 39-43, Apr 2010. Disponível em: < https://www.ncbi.nlm.nih.gov/pubmed/24900173 >.

KOEPPEN, H. et al. Ligand-Based Virtual Screening. In: (Ed.). **Virtual Screening**: Wiley-VCH Verlag GmbH & Co. KGaA, 2011. p.61-85. ISBN 9783527633326.

KOES, D. R.; CAMACHO, C. J. ZINCPharmer: pharmacophore search of the ZINC database. **Nucleic Acids Res,** v. 40, n. Web Server issue, p. W409-14, Jul 2012. ISSN 1362-4962. Disponível em: < http://www.ncbi.nlm.nih.gov/pubmed/22553363 >.

LANGER, T.; KROVAT, E. M. Chemical feature-based pharmacophores and virtual library screening for discovery of new leads. **Curr Opin Drug Discov Devel,** v. 6, n. 3, p. 370-6, May 2003. ISSN 1367-6733. Disponível em: < https://www.ncbi.nlm.nih.gov/pubmed/12833670 >.

LAPLANTE, M.; SABATINI, D. M. mTOR signaling at a glance. **J Cell Sci,** v. 122, n. Pt 20, p. 3589-94, Oct 2009. ISSN 1477-9137. Disponível em: < http://www.ncbi.nlm.nih.gov/pubmed/19812304 >.

LAPLANTE, M.; SABATINI, D. M.. mTOR signaling in growth control and disease. **Cell,** v. 149, n. 2, p. 274-93, Apr 2012. ISSN 1097-4172. Disponível em: < http://www.ncbi.nlm.nih.gov/pubmed/22500797 >.

LEACH, A. R. et al. Three-dimensional pharmacophore methods in drug discovery. **J Med Chem,** v. 53, n. 2, p. 539-58, Jan 2010. ISSN 1520-4804. Disponível em: < https://www.ncbi.nlm.nih.gov/pubmed/19831387 >.

LEESON, P. Drug discovery: Chemical beauty contest. **Nature,** v. 481, n. 7382, p. 455-6, Jan 2012. ISSN 1476-4687. Disponível em: < https://www.ncbi.nlm.nih.gov/pubmed/22281594 >.

LIPINSKI, C. A. Lead-and drug-like compounds: the rule-of-five revolution. **Drug Discovery Today: Technologies,** v. v. 1, n. n. 4, p. p. 337-341, 2004.

LIPINSKI, C. A. et al. Experimental and computational approaches to estimate solubility and permeability in drug discovery and development settings. **Advanced Drug Delivery Reviews,** v. 23, n. 1, p. 3-25, 1997/01/15 1997. ISSN 0169-409X. Disponível em: < http://www.sciencedirect.com/science/article/pii/S0169409X96004231 >.

LIU, B.; LI, S.; HU, J. Technological advances in high-throughput screening. **Am J Pharmacogenomics,** v. 4, n. 4, p. 263-76, 2004. ISSN 1175-2203. Disponível em: < https://www.ncbi.nlm.nih.gov/pubmed/15287820 >.

LUO, Y. Selectivity assessment of kinase inhibitors: strategies and challenges. **Curr Opin Mol Ther,** v. 7, n. 3, p. 251-5, Jun 2005. ISSN 1464-8431. Disponível em: < https://www.ncbi.nlm.nih.gov/pubmed/15977423 >.

MANNHOLD, R.; KUBINYI, H.; FOLKERS, G. **Virtual Screening: Principles, Challenges, and Practical Guidelines**. 48. Wiley. com, 2011.

MARKT, P.; SCHUSTER, D.; LANGER, T. Pharmacophore Models for Virtual Screening. In: (Ed.). **Virtual Screening**: Wiley-VCH Verlag GmbH & Co. KGaA, 2011. p.115-152. ISBN 9783527633326.

MARTÍNEZ, L.; BORIN, I. A.; SKAT, M. S. Fundamentos de Simulação por Dinâmica Molecular. In: MORGAN, N. H. e COUTINHO, K. (Ed.). **Métodos de Química Teórica e Modelagem Molecular**. São Paulo, 2007. cap. 12, p.413-452.

MUKHERJEE, B. et al. The dual PI3K/mTOR inhibitor NVP-BEZ235 is a potent inhibitor of ATM- and DNA-PKCs-mediated DNA damage responses. **Neoplasia,** v. 14, n. 1, p. 34-43, Jan 2012. ISSN 1476-5586. Disponível em: < https://www.ncbi.nlm.nih.gov/pubmed/22355272 >.

NAMBA, A. M.; DA SILVA, V. B.; DA SILVA, C. H. T. P. Dinâmica molecular: teoria e aplicações em planejamento de fármacos. . **Eclética Química,** v. v. 33, n. n. 4, p. p. 13-24, 2008.

NASR, A. B. et al. Molecular Docking studies of FKBP12-mTOR inhibitors using binding predictions. **Bioinformation,** v. 11, n. 6, p. 307-15, 2015. Disponível em: < https://www.ncbi.nlm.nih.gov/pubmed/26229292 >.

PARK, H.; CHOE, H.; HONG, S. Virtual screening and biochemical evaluation to identify new inhibitors of mammalian target of rapamycin (mTOR). **Bioorganic & Medicinal Chemistry Letters,** v. 24, n. 3, p. 835-838, 2/1/ 2014. ISSN 0960-894X. Dis

PETTERSEN, E. F. et al. UCSF Chimera--a visualization system for exploratory research and analysis. **J Comput Chem,** v. 25, n. 13, p. 1605-12, Oct 2004. ISSN 0192-8651. Disponível em: < http://www.ncbi.nlm.nih.gov/pubmed/15264254 >.

PORTA, C.; PAGLINO, C.; MOSCA, A. Targeting PI3K/Akt/mTOR Signaling in Cancer. **Front Oncol,** v. 4, p. 64, 2014. Disponível em: < https://www.ncbi.nlm.nih.gov/pubmed/24782981 >.

ROGNAN, D. Docking Methods for Virtual Screening: Principles and Recent Advances. In: (Ed.). **Virtual Screening**: Wiley-VCH Verlag GmbH & Co. KGaA, 2011. p.153-176. ISBN 9783527633326.

SANTULLI, G.; TOTARY-JAIN, H. Tailoring mTOR-based therapy: molecular evidence and clinical challenges. **Pharmacogenomics,** v. 14, n. 12, p. 1517-26, Sep 2013. ISSN 1744-8042. Disponível em: < https://www.ncbi.nlm.nih.gov/pubmed/24024901 >.

SEHGAL, S. N. Sirolimus: its discovery, biological properties, and mechanism of action. **Transplant Proc,** v. 35, n. 3 Suppl, p. 7S-14S, May 2003. ISSN 0041-1345. Disponível em: < http://www.ncbi.nlm.nih.gov/pubmed/12742462 >.

SHIMOBAYASHI, M.; HALL, M. N. Making new contacts: the mTOR network in metabolism and signalling crosstalk. **Nat Rev Mol Cell Biol,** v. 15, n. 3, p. 155-162, 03//print 2014. ISSN 1471-0072. Disponível em: < http://dx.doi.org/10.1038/nrm3757 >.

SMYTH, L. A.; COLLINS, I. Measuring and interpreting the selectivity of protein kinase inhibitors. **J Chem Biol,** v. 2, n. 3, p. 131-51, Aug 2009. ISSN 1864-6158. Disponível em: < http://www.ncbi.nlm.nih.gov/pubmed/19568781 >.

SOLIMAN, G. A. The role of mechanistic target of rapamycin (mTOR) complexes signaling in the immune responses. **Nutrients,** v. 5, n. 6, p. 2231-57, Jun 2013. ISSN 2072-6643. Disponível em: < https://www.ncbi.nlm.nih.gov/pubmed/23783557 >.

SOTRIFFER, C.; MATTER, H. The Challenge of Affinity Prediction: Scoring Functions for Structure-Based Virtual Screening. In: (Ed.). **Virtual Screening**: Wiley-VCH Verlag GmbH & Co. KGaA, 2011. p.177-221. ISBN 9783527633326.

THAIMATTAM, R. et al. Protein kinase inhibitors: structural insights into selectivity. **Curr Pharm Des,** v. 13, n. 27, p. 2751-65, 2007. ISSN 1873-4286. Disponível em: < https://www.ncbi.nlm.nih.gov/pubmed/17897021 >.

THOREEN, C. C. et al. An ATP-competitive mammalian target of rapamycin inhibitor reveals rapamycin-resistant functions of mTORC1. **J Biol Chem,** v. 284, n. 12, p. 8023-32, Mar 2009. ISSN 0021-9258. Disponível em: < https://www.ncbi.nlm.nih.gov/pubmed/19150980 >.

VEBER, D. F. et al. Molecular properties that influence the oral bioavailability of drug candidates. **J Med Chem,** v. 45, n. 12, p. 2615-23, Jun 2002. ISSN 0022-2623. Disponível em: < http://www.ncbi.nlm.nih.gov/pubmed/12036371 >.

WACHECK, V. mTOR pathway inhibitors in cancer therapy: moving past rapamycin. **Pharmacogenomics,** v. 11, n. 9, p. 1189-91, Sep 2010. ISSN 1744-8042. Disponível em: < http://www.ncbi.nlm.nih.gov/pubmed/20860456 >.

WANG, L. et al. Discovering new mTOR inhibitors for cancer treatment through virtual screening methods and in vitro assays. **Scientific Reports,** v. 6, p. 18987, 01/06/online 2016. Disponível em: < http://dx.doi.org/10.1038/srep18987 >.

WATANABE, R.; WEI, L.; HUANG, J. mTOR signaling, function, novel inhibitors, and therapeutic targets. **J Nucl Med,** v. 52, n. 4, p. 497-500, Apr 2011. ISSN 1535-5667. Disponível em: < http://www.ncbi.nlm.nih.gov/pubmed/21421716 >.

YANG, H. et al. mTOR kinase structure, mechanism and regulation. **Nature,** v. 497, n. 7448, p. 217-23, May 2013. ISSN 1476-4687. Disponível em: < http://www.ncbi.nlm.nih.gov/pubmed/23636326 >.

YUAN, J. et al. PF-04691502, a potent and selective oral inhibitor of PI3K and mTOR kinases with antitumor activity. **Mol Cancer Ther,** v. 10, n. 11, p. 2189-99, Nov 2011. ISSN 1538-8514. Disponível em: < https://www.ncbi.nlm.nih.gov/pubmed/21750219 >.

ZAROGOULIDIS, P. et al. mTOR pathway: A current, up-to-date mini-review (Review). **Oncol Lett,** v. 8, n. 6, p. 2367-2370, Dec 2014. ISSN 1792-1074. Disponível em: < https://www.ncbi.nlm.nih.gov/pubmed/25360163 >.

ZASK, A.; VERHEIJEN, J. C.; RICHARD, D. J. Recent advances in the discovery of small-molecule ATP competitive mTOR inhibitors: a patent review. **Expert Opin Ther Pat,** v. 21, n. 7, p. 1109-27, Jul 2011. ISSN 1744-7674. Disponível em: < https://www.ncbi.nlm.nih.gov/pubmed/21591993 >.

ZHENG, Y.; JIANG, Y. mTOR Inhibitors at a Glance. **Mol Cell Pharmacol,** v. 7, n. 2, p. 15-20, 2015 2015. Disponível em: < https://www.ncbi.nlm.nih.gov/pubmed/27134695 >.

2 OBJETIVOS

2.1 Objetivo Principal

Selecionar possíveis novos inibidores, não competitivos ao ATP, do complexo enzimático mTOR.

2.2 Objetivos Específicos

- Construir modelos farmacofóricos da mTOR baseados na estrutura do ligante (LBDD);
- Obter um banco de dados de moléculas para ser usado na triagem virtual;
- Efetuar estudos de docagem molecular para avaliar questões energéticas da interação alvo-ligante;
- Executar a validação do protocolo de docagem;
- Selecionar moléculas triadas a partir das melhores propriedades ADMETox;
- Realizar a simulação por dinâmica molecular para evidenciar o comportamento das moléculas selecionadas.

3 ARTIGO

Journal

Journal of Molecular Graphics and Modelling

Title

Searching for potential mTOR inhibitors: Ligand-based drug design, docking and molecular dynamics studies of rapamycin binding site

Authors

Roger Kist[a], Luis Fernando Saraiva Macedo Timmers[b,c], Rafael Andrade Caceres[a,d]*

[a]Graduate Program in Health Sciences of Federal University of Health Sciences of Porto Alegre – UFCSPA, Porto Alegre City, Brazil.

[b]Laboratory for Bioinformatics, Modelling and Simulation of Biosystems – LABIO, Pontifical Catholic University of Rio Grande do Sul - PUCRS, Porto Alegre City, Brazil.

[c]Graduate Program in Cellular and Molecular Biology (PPGBCM), PUCRS, Porto Alegre, RS, Brazil

[d]Pharmacosciences Department of Federal University of Health Sciences of Porto Alegre – UFCSPA, Porto Alegre City, Brazil.

*Corresponding author. Email: rafaelca@ufcspa.edu.br. Phone number: +55 51 3303 8889.

Abstract

The PI3K/Akt/mTOR pathway is an important intracellular signaling pathway in cell cycle regulation and its dysregulation is associated with various types of diseases. mTOR (mechanistic or mammalian target of rapamycin) is the main enzyme that performs intermediate control of the signaling pathway through a phosphotransfer process. The classical inhibition of the mTOR pathway is effected by rapamycin and its analogous blocking allosterically the catalytic phosphorylation site, avoiding the deleterious side effects induced by ATP-competitive inhibitors. We employed ligand-based drug design strategies such as pharmacophore searching and analysis, molecular docking, absorption, distribution, metabolism, excretion and toxicity (ADMETox) properties filtering, and molecular dynamics to select potential molecules to become non-ATP competitive inhibitors of the mTOR complex. According to our findings, we propose eight novel potential mTOR inhibitors with similar or better properties than the classic inhibitor complex, rapamycin.

Graphical abstract

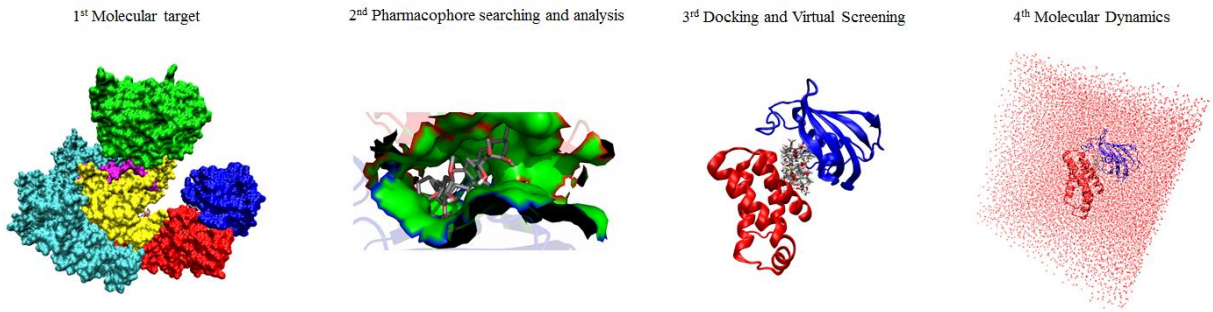

Highlights

- Through the virtual screening all selected molecules showed lower toxicity risk indicating drug-conform behavior.
- The presence of a ligand is central to the maintenance and stability of the ternary complex (FKBP12-ligand-FRB).
- Thermodynamically the exclusive interaction between FKBP12 and FRB fractions is not possible. However, the presence of a ligand, acting as a bridge, results in a favorable interaction.
- Evaluation of rapamycin binding pocket described the residues that were the major contributors to the binding.

Keywords

Mechanistic or mammalian target of rapamycin; ligand-based drug design; non-ATP competitive inhibitors; virtual screening; molecular dynamics.

This research did not receive any specific grant from funding agencies in the public, commercial, or not-for-profit sectors.

Introduction

The PI3K/Akt/mTOR pathway is an important intracellular signaling pathway in cell cycle responsible for regulating multiple nutritional and environmental factors, including growth factors, energy levels, cell stress and amino acids. However, its dysregulation has been implicated in major diseases such as cancer, metabolic disorders, neurological diseases and inflammation. The translation of these signals leads to the promotion of cell growth by substrates' phosphorylation triggering anabolic processes such as translation of messenger ribonucleic acid (mRNA) and lipid synthesis or by limiting the catabolic processes such as autophagy. Briefly, the dynamic of this pathway resides in the activation of phosphatidylinositol-3 kinase (PI3K) by extra/intracellular substrates that phosphorylates and activates protein kinase B (Akt), which is located on the plasma membrane. In addition, Akt is also able to activate the mTOR (mechanistic target of rapamycin) [1–5].

The mTOR - formerly called before being recognized as highly conserved among eukaryotes as a mammalian target of rapamycin or FK506-binding protein 12-rapamycin-associated protein 1 (FRAP1) - is a 289 kDa

serine/threonine kinase (EC 2.7.11.1) belonging to the phosphatidylinositol-3 kinase (PI3K) family. It is the main enzyme responsible for performing an intermediate control of the signaling pathway through a phosphotransfer process using adenosine triphosphate (ATP) as a phosphate donor [1,6,7].

Structurally, mTOR kinase is composed of 2549 amino acid residues (289 kDa) and organized into five distinct functional domains, (i) 32 replicates called "Huntington, elongation factor 3, PR65/A, TOR" (HEAT) (from amino acid residue 16 to 1345); (ii) domain "FRAP, ATM, TRRAP" (FAT) (from amino acid residue 1382 to 1982); (iii) region "FKBP12 rapamycin-binding" (FRB) (from amino acid residue 2012 to 2144); (iv) catalytic domain "kinase domain" (KD) and regulator "regulatory domain" (RD) (from amino acid residue 2182 to 2516); and (v) domain "FRAP ATM TRRAP carboxy terminus" (FATC) (from amino acid residue 2517 to 2549) [8].

This atypical kinase is present in two functional and structurally distinct complexes, mTORC1 and mTORC2, located in different cell compartments, each containing distinct and common subunits necessary for the catalytic activity and regulation of the main enzyme. The mTORC1 complex transmits signals of nutrient availability to control various cellular functions, while the mTORC2 complex regulates mainly the assembly of the cytoskeleton by actin [4,7–9].

The classical inhibition of the mTOR pathway is effected by rapamycin and its analogous, called rapalogs, which are considered the first-generation inhibitors [10–13]. The rapamycin, or sirolimus (Rapamune, Wyeth Pharmaceuticals), is a potent macrolide antibiotic produced by the microorganism *Streptomyces hygroscopicus* and it is widely used in therapy due to its immunosuppressive and antitumor properties [14]. However, because of their unfavorable properties, such as its low solubility in water and stability in solution, molecular analogues have been developed - the rapalogs - such as everolimo (RAD001, Afinitor, Novartis Pharmaceuticals), temsirolimus (CCI-779, Torisel, Wyeth Pharmaceuticals) and ridaforolimus (AP23573; formally called deforolimus, ARIAD Pharmaceuticals), which improved pharmacokinetic properties without altering the mechanism of action [12].

The inhibition mechanism of mTOR by rapamycin and its analogues occurs through the binding of the intracellular receptor of the FK506-binding protein 12 kDa (FKBP12), forming the rapamycin-FKBP12 complex. This association binds directly to the FKBP12-rapamycin binding (FRB) domain, blocking allosterically the catalytic phosphorylation site [7,15,16].

The rapalogs revealed efficacy, safety and tolerability of adverse events in inhibition of the mTOR pathway on treatment of many diseases [17,18]. However, the success of these first-generation inhibitors has shown flaws especially due to the feedback mechanism once that inhibition of the complex results in over activation of PI3K/Akt signaling and increases cell survival; a probable insensitivity of mTORC1 to rapalogs has recently been revealed, challenging the dogma that rapamycin completely inhibits the activity of mTORC1; alternative pathways and cross-pathways between the kinases could also limit the efficacy of rapalogs and mutations in the PI3K/Akt/mTOR pathway [12,19–25].

Recent effort has been based on the search for direct inhibitors of the catalytic kinases site – ATP competitive. In this case, it is possible to find drugs which are in clinical trials such as second-generation dual inhibitors - mTOR/PI3K dual inhibitors (TPdIs) for example, PF-0469150212, BEZ23513 and GSK212645814 and selective mTORC1/mTORC2 dual inhibitors (TORCdIs) as OSI-0279, INK-12810 and CC-22311 [12,13,26–30]. Although most kinase inhibitors present some selectivity and great potential in therapy, they are not selective to a single molecular target, since their unspecificity can potentially increase the risk of side effects and toxicity due to

interaction with other ATP-dependent enzymes. Therefore, it is important to search for inhibitors that are more selective for a single molecular target [31–34].

The development of new drugs aims at the identification of compounds with pharmacological interest, attending both treatment of diseases and improvement of patient's quality of life. Currently, the ideal drug profile resides in favorable ADMETox properties (absorption, distribution, metabolism, excretion and toxicity) and intrinsic requirements such as selectivity, bioavailability, ease of synthesis and low cost. Drug candidates are organic molecules that generally share similar physicochemical properties and that are grouped into large libraries. To experimentally evaluate these compounds against a particular molecular target, specific tests called high-throughput screening (HTS) are developed. Accordingly, compounds are compared to therapeutic targets in *in vitro* assays employing analytical methods for evaluating the pharmacological activity. The size, of the libraries, however, makes this method financially unfeasible to some laboratories [35–37].

An alternative to HTS is the virtual screening (VS), a computational approach (*in silico*) that allows the evaluation of a large number of compounds while reducing time and costs in relation to HTS. *In silico* techniques enable not only to test large libraries but also acquire and/or propose new molecules according to receptor affinity. In addition, VS method can also be used to identify false negatives in order to increase success [36,38].

Considering the binding of rapamycin to the FKBP12 subunit and the FRB domain as a central action to inhibit the metabolic pathway, the search and development of new molecules that are able to affect this mechanism while having more favorable pharmacological properties becomes essential for the more effective control of this important path, responsible for uncountable physiological mechanisms and deregulated in certain pathologies, such as cancer.

The aim of this work was to propose new potential inhibitors – non-ATP competitive – against the mTOR complex, employing ligand-based drug design, molecular docking, determination of ADMETox properties and molecular dynamics simulations in order to select molecules that present favorable features so as to become a potential non-ATP-competitive inhibitor of mTOR.

Material and methods

Protein structure selection

The crystallographic structure was retrieved from the Protein Data Bank [39,40] (PDBID: 1FAP). This is a structure of the ternary complex of human FKBP12 (from residue 1 to 107), rapamycin and the FKBP12-rapamycin-binding (FRB) domain of human mTOR (from residue 108 to 202) at a resolution of 2.7 Å [41].

Pharmacophore model

A pharmacophore describes the structural arrangement of essential molecular features of an interaction between a ligand and a receptor. The main challenge of this model is to identify a representative spatial arrangement for the ligand-receptor interaction and how this information can be used to search for new molecules in a chemical library that satisfies the model [42–45]. Since the majority of the contacts between FKBP12-rapamycin-FRB are hydrophobic [41], we employed a model composed of six hydrophobic contacts (C5, C19, C21, C43, C45, C49) of rapamycin (Fig. 1) as a template to construct the pharmacophore model in the ZincPharmer platform [46]. All pharmacophore points are shown in Table 1.

Pharmacophore/class	X coordinates	Y coordinates	Z coordinates	Radius (Å)
C5 – Hydrophobic	-8.20	23.65	41.43	1.00
C19 – Hydrophobic	-12.38	26.13	34.19	1.00
C21 – Hydrophobic	-11.65	26.22	31.88	1.00
C43 – Hydrophobic	-10.86	29.29	43.53	1.00
C45 – Hydrophobic	-11.17	26.30	28.46	1.00
C49 – Hydrophobic	-8.74	29.35	38.66	1.00

Table 1 Pharmacophore features employed as query search on ZincPharmer.

Elaborated using PyMol v.1.7.5.0 and ACD/ChemSketch Freeware.

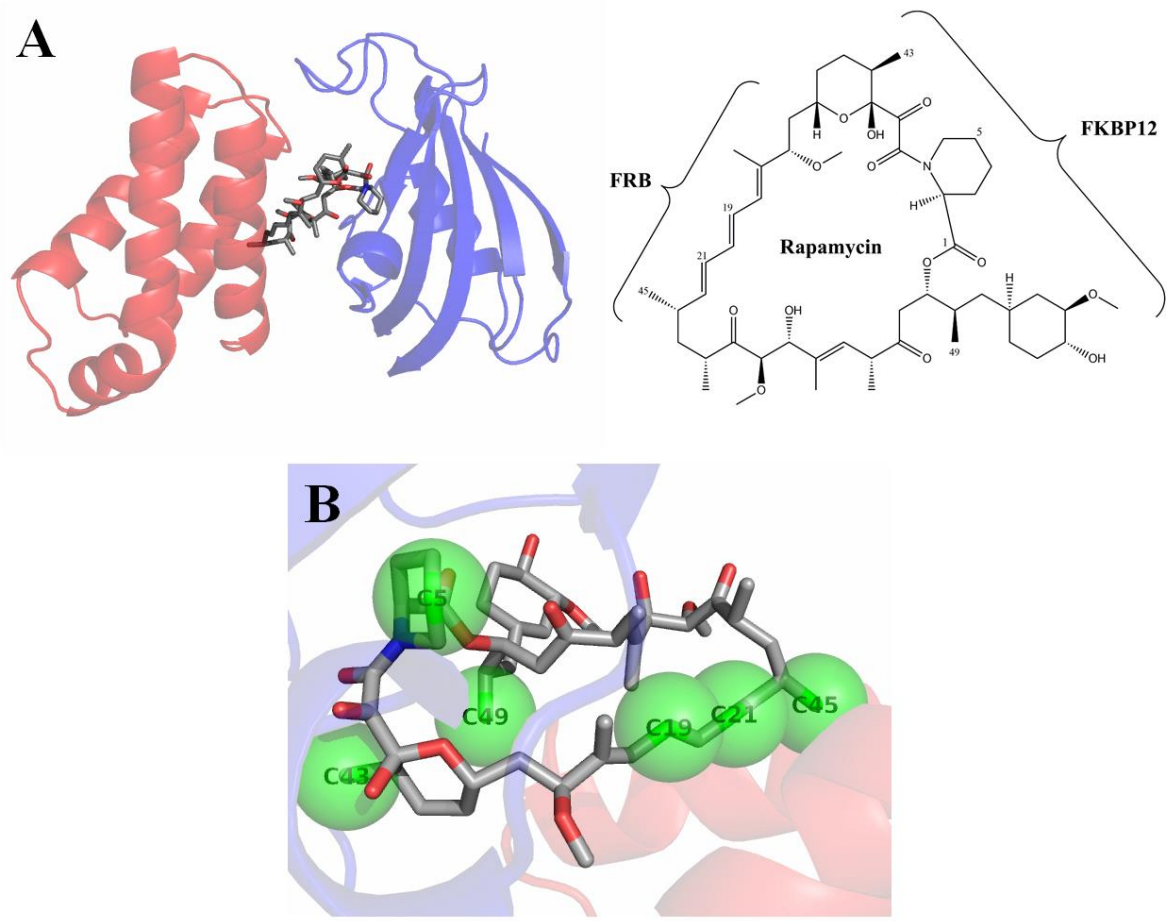

Fig. 1 Pharmacophore model employed for ZincPharmer search. (A) FKBP12-rapamycin-FRB complex. FKBP12 and FRB are drawn as cartoon and color in blue and red, respectively. The rapamycin molecule is shown as sticks and color by CPK. (B) The six hydrophobic pharmacophore points are colored in color in green and represented as sphere.

Molecular docking protocol and validation

Molecular docking experiments were carried out using AutoDock Vina [47] and MTiOpenScreen [48], which is based on AutoDock Vina. AutoDock Vina employs a gradient-based conformational search approach and defines the search space by a grid box defined by the box center coordinates and its dimensions of x, y and z in grid resolution internally assigned to 1Å [47]. We set the number of binding modes to 100 and exhaustiveness set to 200 in order to control how many times the calculations are repeated. The grid dimensions were 50 x 30 x 50 (x, y, z) points center on the rapamycin binding site -8.123 x 26.991 x 36.301 (x, y, z). The scoring of the generated docking poses and ranking of the ligands were based on the Vina empirical scoring function.

In addition to the ligands retrieved from ZincPharmer we used two more molecules as docking energy controls: crystal structure of rapamycin (PDBID 1FAP) and rapamycin. All water molecules were removed from the structure file as well as all ligands and ions.

To validate AutoDock Vina and MTiOpenScreen protocols we also used the AutoDock v.4.2 [49] in PyRx v.0.8 [50] program. We performed a redocking of the crystallographic structure 1FAP using a grid resolution of 0.375

Å and all others parameters follow the protocol applied to AutoDock Vina and MTiOpenScreen. Each simulation on AutoDock v.4.2 consisted of 10 independent runs of Lamarckian Genetic Algorithm (LGA) -number of generations set to 150; maximum number of energy assessments fixed at 25, elitism set to 1, mutation rate at 0.02 and crossover rate at 0.80.

Furthermore, a predictiveness' curve was created to evaluate the AutoDock Vina protocol ability to discriminate binders from nonbinding compounds employing protein target FKBP12 retrieved from the Database of Useful Decoys: Enhanced (DUD-E) [51]. The predictiveness' curve employs logistic regression models to calculate activity probabilities related to the scores obtained by each compound during VS experiments, providing an intuitive and graphical tool to compare the predictive power of VS methods [52].

ADMETox properties

All the molecules retrieved from ZincPharmer were submitted to DataWarrior webserver [53] based on DrugBank [54], FAF-Drugs [55]. The best scored molecules – lower docking energy and none mutagenic, tumorigenic, irritant and reproductive effect – were submitted to pkCSM webserver [56] to analyze the ADMETox properties. All those tools, when used together, generate a powerful mechanism, at least helpful, for selecting new mTOR inhibitors as well as the ability to select ligands.

MD simulations

Although extremely powerful, X-ray crystallography of biological macromolecules does not allow the investigation of a protein's flexibility. For this reason, molecular dynamics (MD) simulations is widely used to investigate structure and function of biomolecules, regarding its' motions. In addition, it is also applied to better understand protein-ligand interactions assisting in the computer assisted drug design (CADD) process [57].

MD simulations were performed using GROMACS v.4.6.7 package [58,59]. The top scored ligands – with no Lipinski Rules violation, lowest Autodock Vina/MTiOpenScreen docking energy and no mutagenic/tumorigenic/reproductive and irritant effects – were selected from VS and had hydrogen atoms added through PRODRG webserver [60] and were parameterized employing Automated Topology Builder server [61]. In addition, the systems FKBP12:FRB and FKBP12:rapamycin:FRB (PDBID: 1FAP) were also simulated as controls.

Each complex was immersed in a cubic-shaped box (x, y, and z) with volume 238.58 nm^3 and the minimum distance of 1 nm between the protein surface and the box edges. SPC/E water molecules were used to solvate the system. Periodic boundary conditions were assigned in all directions. The system net charge was neutralized by adding both Na^+ and Cl^- ions to mimic a physiological buffer (0.150 mM NaCl). These ions randomly substituted water molecules in suitable electrostatic potential positions. Two steps of energy minimization were used, employing a steepest descent algorithm with a tolerance of 1000 kJ mol^{-1} nm^{-1} followed by a conjugate gradient algorithm with a tolerance of 500 kJ mol^{-1} nm^{-1}. To relax strong solvent-solvent and solvent-protein non-bonded interactions, 1 ns (from 0 to 1 ns at 50 K) of MD simulation was performed restraining the protein structure. Initial velocities were assigned according to Maxwell distribution. All simulations were performed for 100 ns using an integration time step of 2 fs. Each system was heated with gradual increments in the following temperatures: 50 K (from 1 to 2 ns), 75 K (from 2 to 3 ns), 100 K (from 3 to 4 ns), 150 K (from 4 to 5 ns), 200 (from 5 to 6 ns), 250 K (from 6 to 7 ns), 300 K (from 7 to 8 ns) and after that (from 8 to 100 ns) the temperatures of the systems

were adjusted to 310.15 K. All simulations were performed using GROMOS96 53a6 force field [62]. Berendsen barostat and thermostat were applied to keep the pressure and temperature constant with a coupling time of τp = 0.5 ps, and τT = 1.0 ps, respectively. Long-range electrostatic interactions were calculated with the Ewald particle mesh method. The bond lengths were restrained employing Linear Constraint Solver algorithm (LINCS) [63], allowing an integration step of 2 fs. The principal components analysis (PCA) of FKBP12:FRB trajectory through 100 ns revealed 91.0 % of structure variance at the first ten principal components (1.7 % of 606 eigenvectors) thus showing that the parameter calculation of the simulation was well sampled [64].

Presentation software, data and statistical analysis

The structures generated by MD simulations were analyzed by visual inspection through PyMOL v.1.7.5.0 [65]. Trajectories of the MD simulations were analyzed using the analysis modules of the GROMACS program as root mean square deviation (RMSD), RMS fluctuations (RMSF), radius of gyration (Rg), free energy landscape (FEL) reported as the Gibbs Free Energy and porcupine plots.

The protein and protein-binding complexes stabilities were compared using RMSD measures, analyzing the difference between atom positions between two structures. The smaller the deviation, the more spatially equivalent the two structures are [66]. Besides, in biological terms, protein loops and disordered fragments are enriched with highly fluctuating residues, and this suggests that protein unfolding originates from highly fluctuating residues and their structural neighbors. So, structures with lower fluctuation (lower RMSF values) means a lower trend to be destabilized [67]. Otherwise, radius of gyration (Rg) is a parameter that defines the equilibrium of conformations in a total system in terms of compaction of protein structure with protein folding and unfolding [68]. Gibbs free energy calculation were performed employing RMSD *versus* Rg and plotted as free-energy landscape (FEL) that provides valuable information about proteins or complexes on its roughness and on how atomic trajectories evolve with time [69].

Molecular Mechanics Poisson–Boltzmann surface area (MM–PBSA) through the tool g_mmpbsa, which implements the MM–PBSA approach using subroutines written in-house or sourced from the GROMACS and APBS packages, was employed to estimate the binding energy contribution of each residue that performed bind with the ligands [70].

Statistical analysis was performed by IBM SPSS Statistics v. 22.0 (IBM Corp. Released, 2013) with normal distribution considered through the Kolmogorov-Smirnov Test of Normality (p value > 0.05) and statistical tests with $p < 0.05$ (CI 95 %) were considered significant.

Results

Binding pocket and pharmacophore model

From the searching of 215,407,096 conformations of 22,723,923 compounds from Zinc database, we retrieved 381 ligands that satisfied the query.

Fig. 2A shows the binding pocket analyzed through CASTp PyMOL plugin [71], which revealed 43 residues (THR21, TYR26, PHE36, ASP37, ARG42, LYS44, PRO45, PHE46, LYS47, PHE48, MET49, LYS52, GLN53, GLU54, VAL55, ILE56, TRP59, TYR82, HIS87, ILE90, ILE91, PHE99, GLU107, LEU121, GLU122, SER125, ARG126, PHE129, GLY130, ARG132, LYS185, THR188, GLN189, TRP191, ASP192, LEU193, TYR194, TYR195, HIS196, PHE198, ARG199, ARG200 and SER202) between the FKBP12:FRB interface. Furthermore,

the pharmacophore model's analysis (Fig. 2B) revealed that FKBP12 portion make contacts between PHE46 → C5 (7.3 Å) and ILE90 → C43 (6.2 Å), and FRB portion participate in contacts between GLU122 → C45 (4.1 Å), PHE129 → C49 (5.2 Å), ASP192 → C19 (6.2 Å), TYR195 → C19 (4.8 Å) and C21 (4.1 Å) and PHE198 → C45 (5.6 Å).

Elaborated using PyMol v.1.7.5.0.

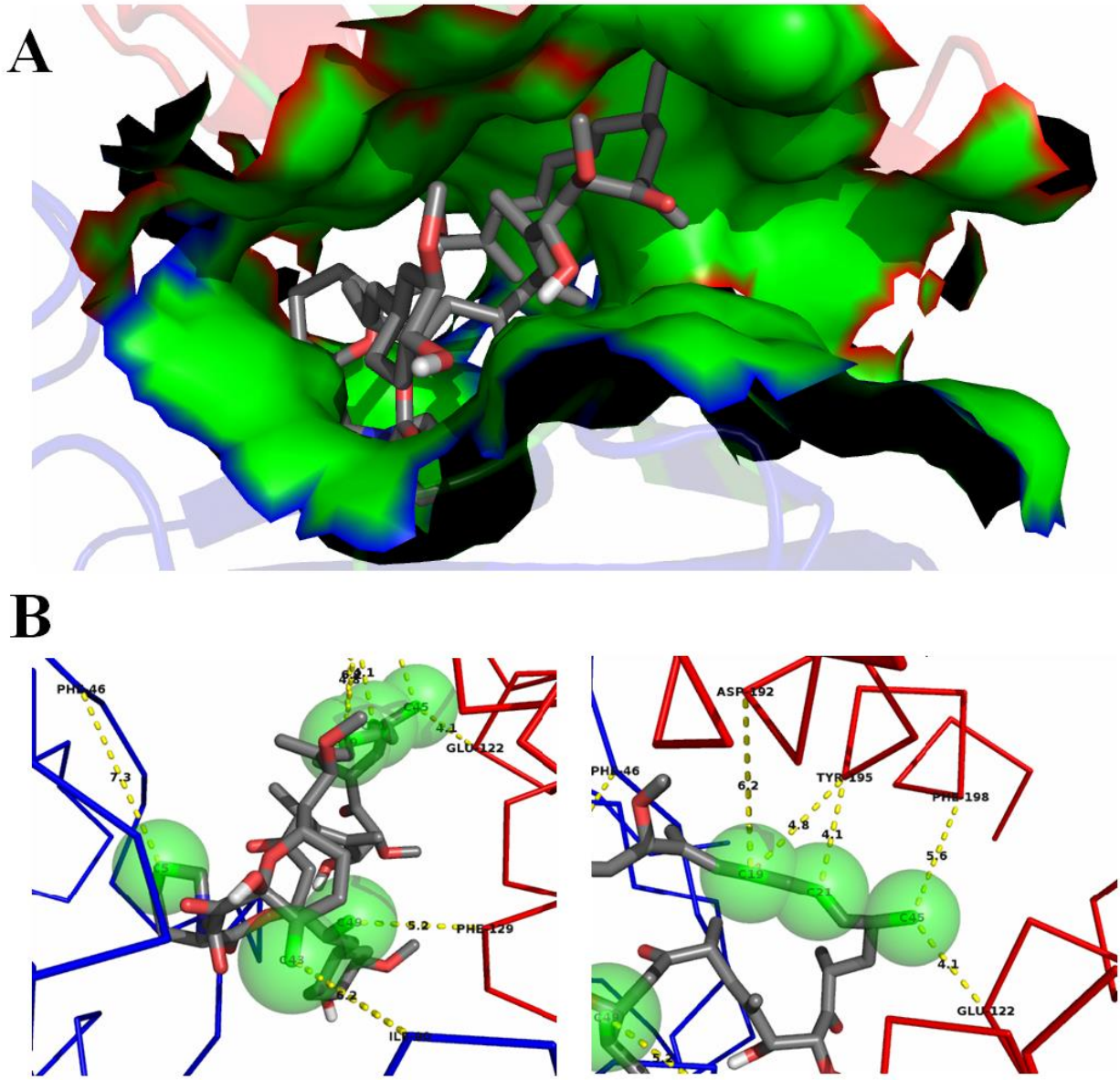

Fig. 2 (A) Binding pocket and (B) pharmacophore model analysis. FKBP12 and FRB are drawn as cartoon and color in blue and red, respectively. The rapamycin molecule is shown as sticks and color by CPK and binding pocket is shown as green surface.

Docking simulation and validation

According to statistical analysis, AutoDock Vina and MTiOpenScreen data distributions does not show difference ($p = 0.597$) through related-samples Wilcoxon test. Considering $n = 382$ (ligands and rapamycin), Spearman's correlation test coefficient was 0.904 ($p < 0.001$) and R square from linear regression was 0.818 ($p < 0.001$). Consequently, statistical analysis shows no difference between protocols, highlighting that docking energy results are strongly related.

The docking validation (assuming rapamycin crystallographic structure as reference) obtained the lowest energy of -18.10 (RMSD 7.808 Å), -18.10 kcal/mol (RMSD 7.572 Å), -19.76 kcal/mol (RMSD 6.724 Å) using the

AutoDock Vina, MTiOpenScreen and AutoDock programs, respectively. Fig. 3 presents the best pose of each protocol.

Elaborated using PyMol v.1.7.5.0.

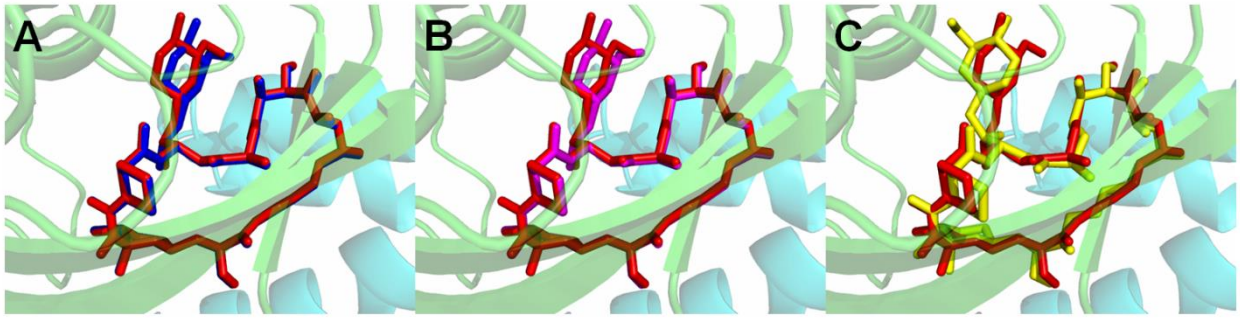

Fig. 3 Docking validation structures. Rapamycin crystallographic structure is shown in red, (A) AutoDock Vina in blue, (B) MTiOpenScreen in magenta and (C) AutoDock in yellow.

Considering the first step of mTOR inhibition is through the association of FKBP12-rapamycin, the ability of the AutoDock Vina protocol to discriminate binders from nonbinding compounds was evaluated in protein target FKBP12 [72] retrieved from DUD-E [73]. The screening was performed with 273 active molecules of FKBP12 binding and 2000 molecule decoys employing the same protocol used for the previous molecular docking experiments. Predictiveness curve reported area under the curve (AUC) equal to 0.879 (SE 0.0156; CI 95% from 0.865 to 0.893; $p < 0.0001$) with sensitivity as 75.5 %, specificity as 100.0 % and associated criterion (cut-off) equal to -10.10 kcal/mol. These results present good accuracy (AUC between 0.8 – 0.9) with a true positive rate of 75.5 %, a false positive rate of 0.0 % and a cut-off -10.10 kcal/mol from the protocol to discriminate binders from nonbinding compounds [74–76].

All the molecules were submitted to DataWarrior webserver and FAF-Drugs (Supplemental Material 1 and 2). The specific ADMETox properties, lower docking energy and none mutagenic, tumorigenic, irritant and reproductive effect properties of the eight top scored, including rapamycin crystallographic and docking structures are shown in Table 2.

Molecule	VINA Dock energy (kcal/mol)	MtiOpen Screen Dock energy (kcal/mol)	Molecular Weight (g/mol)	cLogP	cLogS	HBA	HBD	tPSA (Å)	RotB	RigB	Lipinski Violation	VEBER	EGAN
(i)	-18.1	-18.1	922.2	6.7	-7.7	14	3	195.4	6	49	3	Good	Low
(ii)	-10.1	-9.9	914.2	6.5	-6.7	14	3	195.4	6	49	3	Good	Low
A	-11.6	-11.4	485.3	5.3	-6.8	6	0	64.2	4	27	0	Good	Good
B	-10.5	-10.6	419.5	2.4	-5.2	8	2	97.9	5	19	0	Good	Good
C	-10.5	-10.2	478.5	3.4	-4.6	9	1	106.1	8	25	0	Good	Good
D	-10.5	-9.8	391.5	2.4	-3.9	7	2	88.7	5	22	0	Good	Good
E	-11.3	-11.1	419.4	3.6	-5.7	9	2	117.4	5	24	0	Good	Good
F	-11.3	-11.0	421.5	3.7	-5.6	9	2	117.4	5	23	0	Good	Good
G	-10.5	-10.6	421.5	2.1	-3.4	8	2	94.1	5	20	0	Good	Good
H	-10.6	-10.6	491.7	5.9	-7.9	7	2	106.4	9	25	0	Good	Good

Notes: (i) Rapamycin crystallographic structure; (ii) Rapamycin docking structure; cLogP: logarithm of the partition coefficient between n-octanol and water log ($c_{octanol}/c_{water}$); LogS: logarithm of the solubility measured in mol/L; HBD: Hydrogen Bound Donor; HBA: Hydrogen Bound Acceptor; tPSA: Topological Polar Surface Area in $Å^2$; RotB: Rotable Bounds; RigB: Rigid Bounds.

Table 2 ADMETox properties from selected ligands obtained from DataWarrior webserver and FAF-Drugs.

The ideal drug profile resides in three main characteristics: (i) favorable ADME/Tox properties, (ii) intrinsic requirements (for example, selectivity), and (iii) compliance with the Lipinski Rule-of-5 Violations (molecular weight ≤ 500; H-Bonds Donors ≤ 5 ; H-Bonds Acceptors ≤ 10 ; logP ≤ 5; where if two properties are out of range, a poor absorption or permeability is possible, one is acceptable); the Veber Rules (a compound to present oral bioavailability must meet the criteria of rotatable bonds ≤ 10 and tPSA ≤ 140 Å or H-Bonds Donors + H-Bonds Acceptors ≤ 12) and Egan Rules (0 ≥ tPSA ≤ 132 and -1 ≥ logP ≤ 6) [77–79]. All these considerations highlight the ideal drug profile of the top eight selected molecules, as shown in Table 2.

Furthermore, the specific ADMETox properties for ligands retrieved from pkCSM webserver revealed to be better than or similar to the rapamycin profile , for example, (i) intestinal absorption was higher for all ligands (up to 72.9 %) while rapamycin showed 62.0 %; (ii) volumes of distribution at steady-state (VDss) are lower than rapamycin (0.24 log L/Kg); (iii) specific hepatic metabolism showed a similar profile for all selected ligands as well as for rapamycin: non CYP2D6 substrates and CYP3A4 substrates; (iv) lower total clearance (log mL/min/Kg). These findings suggest that the compounds can have long plasma half-lives due to higher intestinal absorption, low VDss and low renal clearance meaning a lower dose to achieve the effect. Moreover, the specific hepatic metabolism can be helpful in improving the drug interaction with other medicines that are substrate for CYP2D6, for example.

MD simulations

The eight top scored ligands (Fig. 4) were selected from VS to perform MD simulations aiming to investigate the flexibility and stability of these complexes. In addition, FKBP12:FRB crystallographic structure and FKBP12:rapamycin:FRB docking pose were also simulated as control.

Elaborated using ACD/ChemSketch Freeware.

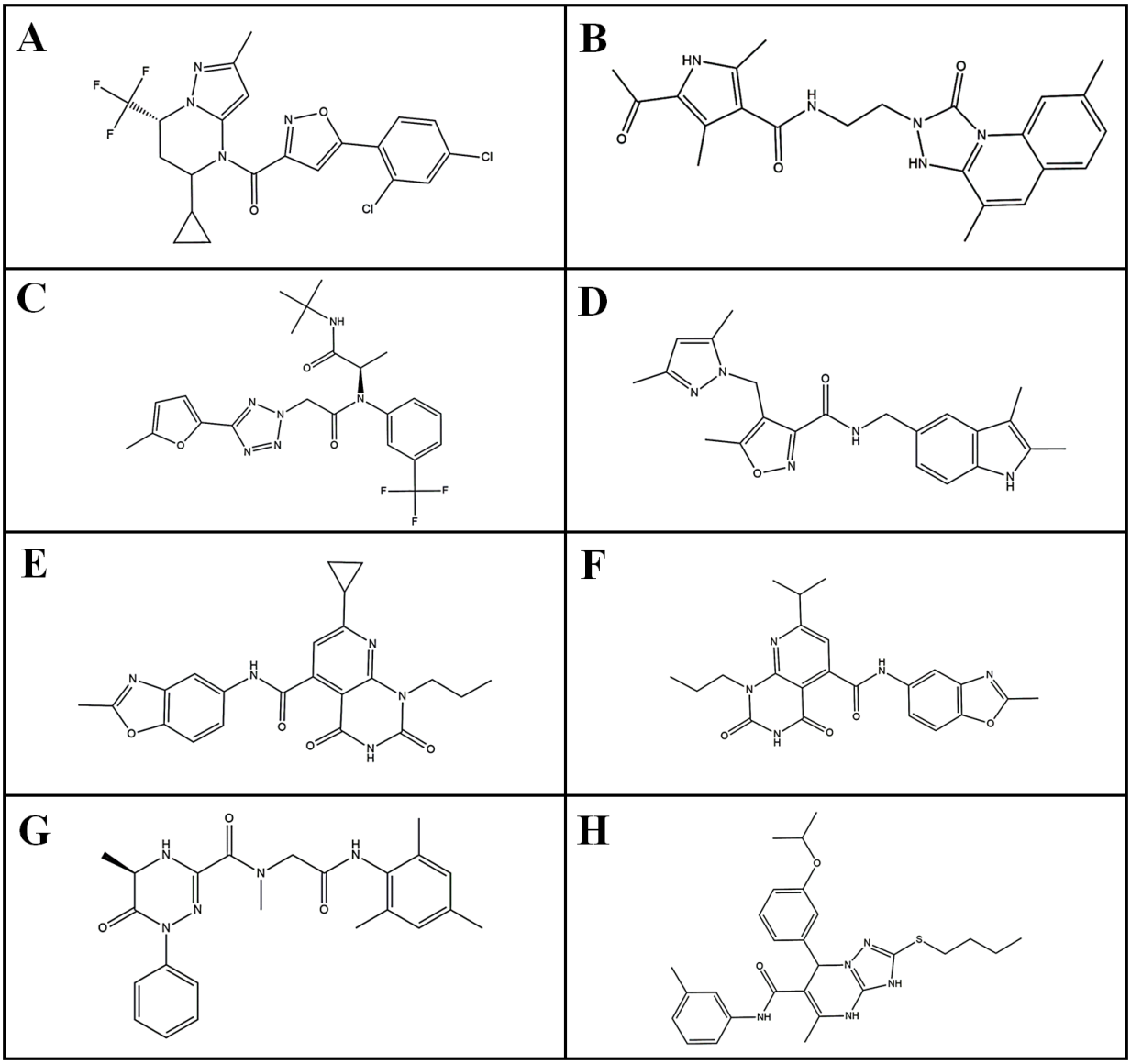

Fig. 4 The eight best scored ligands.

Elaborated using XMGRACE v.5.1.19.

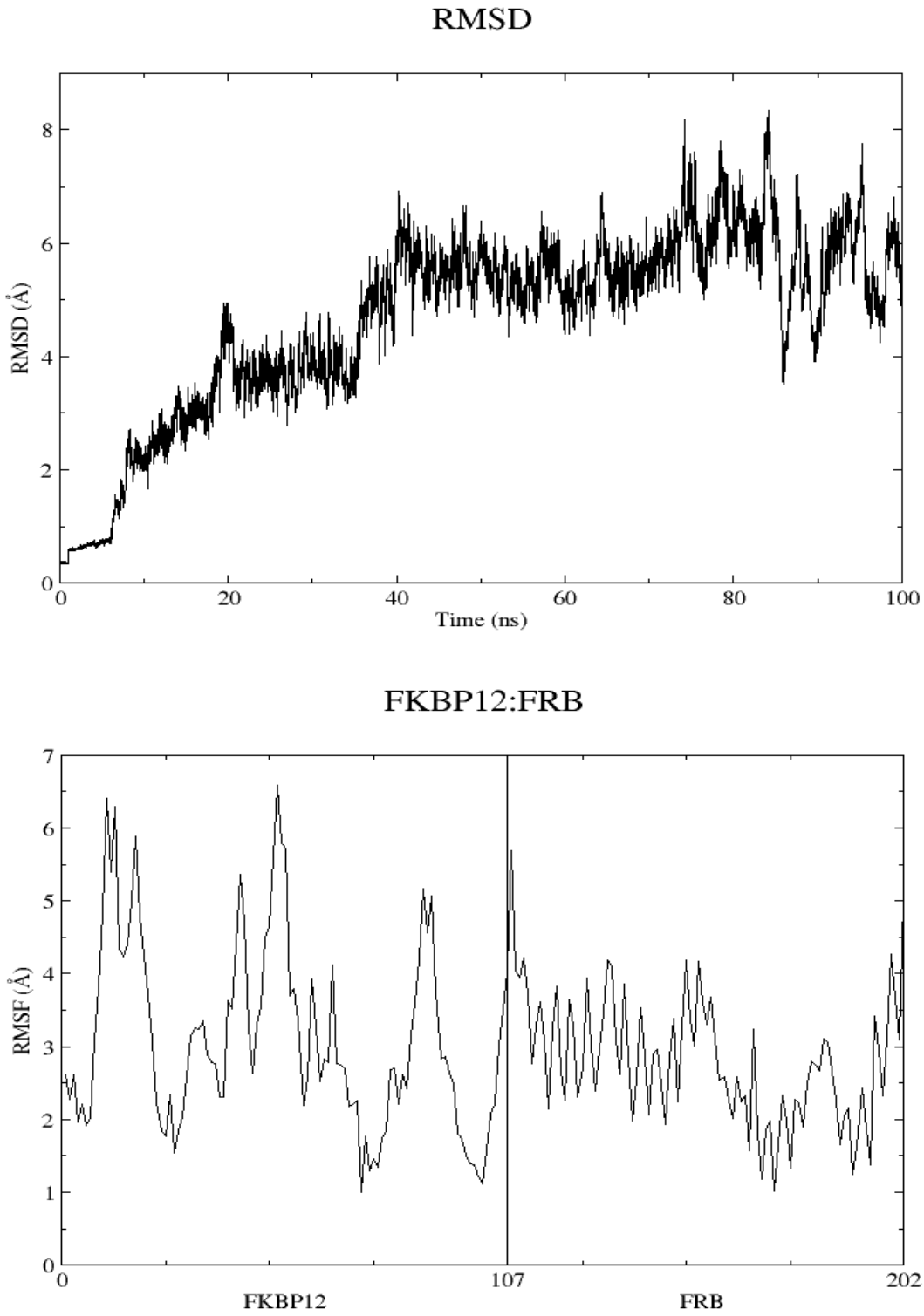

Fig. 5 RMSD and RMSF plots of Cα protein portions FKBP12:FRB system.

Elaborated using XMGRACE v.5.1.19.

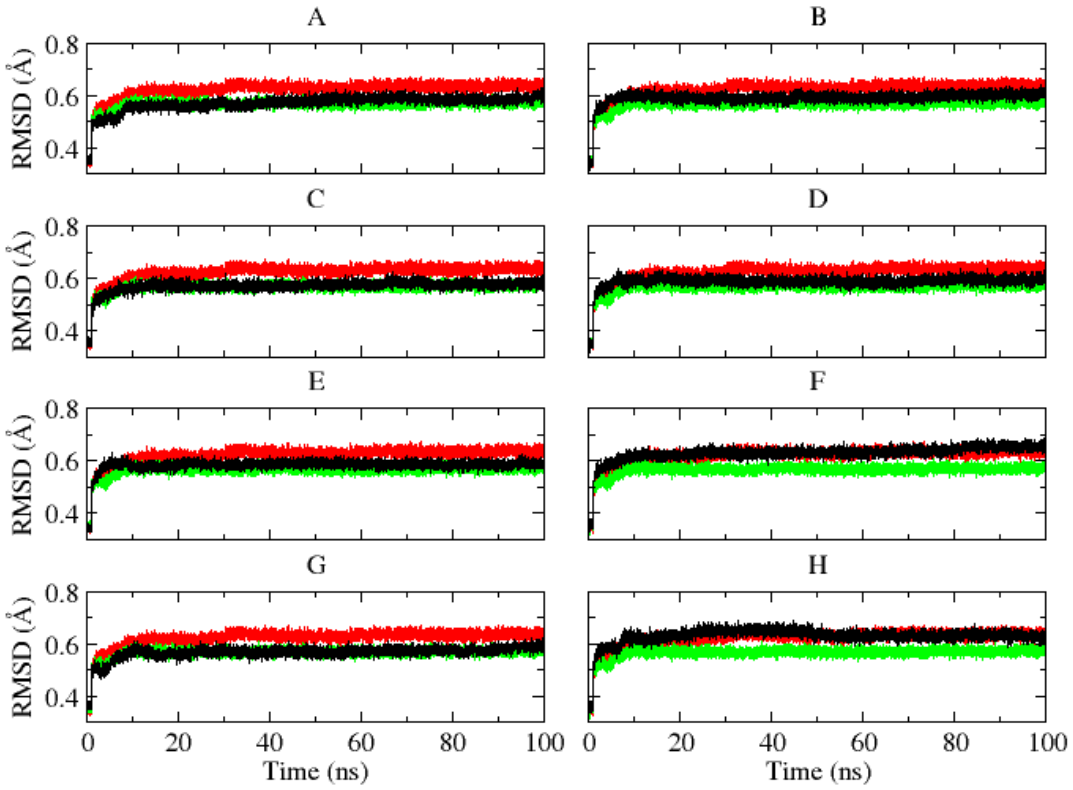

Fig. 6 RMSD plots of Cα protein portions of complexes FKBP12:X:FRB systems. Ligand (X) complex (black line); crystallographic rapamycin complex (green line) and docking rapamycin complex (red line).

Elaborated using XMGRACE v.5.1.19.

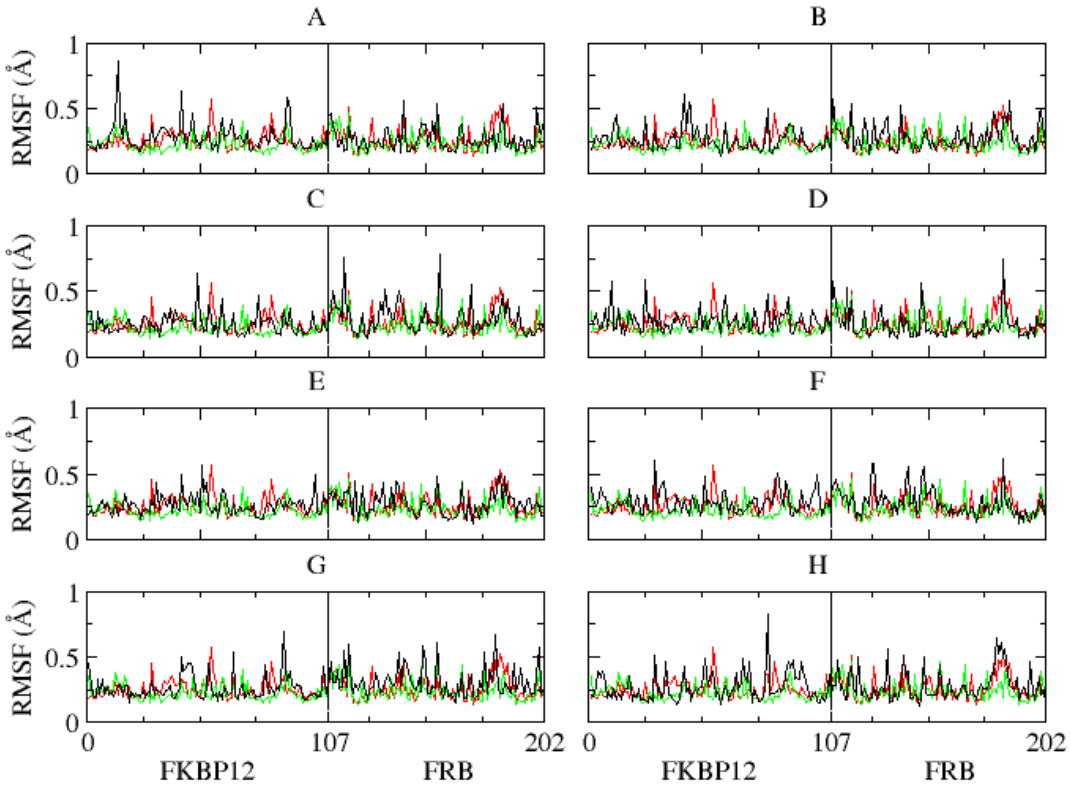

Fig. 7 RMSF plots of Cα protein portions of complexes FKBP12:X:FRB systems. Ligand (X) complex (black line); crystallographic rapamycin complex (green line) and docking rapamycin complex (red line).

Although a previous study employed a crystallographic structure other than FKBP12:FRB [80] (as shown on RMSD and RMSF plots), current results present higher evidence that the presence of a ligand is essential for the maintenance and stability of the ternary complex, reinforcing the results described by Banaszynski et al. (2005), which state the importance of the FKBP12-rapamycin in the stabilization of protein binding [81] and Choi et al. (1996), who report extensive interactions between rapamycin and FKBP12-FRB - but no interaction is observed, in absence of a ligand, between FKBP12 and the FRB domain of mTOR [41].

The analysis of the RMSF values of each residue revealed that the most part of the residues (> 93.0 %) of binding pocket showed low fluctuation (< 0.5 Å) during the simulation, meaning high stabilization in the presence of a ligand. Residues with fluctuation ≥ 0.5 Å were shown on VAL55 (FKBP12:rapamycin:FRB); ARG42 (FKBP12:A:FRB); ARG42, LYS44, PRO45 and ARG199 (FKBP12:B:FRB); MET49 and ARG132 (FKBP12:C:FRB); SER125 and ARG126 (FKBP12:D:FRB); ARG42, HIS87 and ARG200 (FKBP12:G:FRB); ARG132 (FKBP12:H:FRB). The systems FKBP12:D:FRB and FKBP12:E:FRB didn't show fluctuations ≥ 0.5 Å. Further information about residues RMSF can be found in Supplemental Material 3.

Elaborated using XMGRACE v.5.1.19.

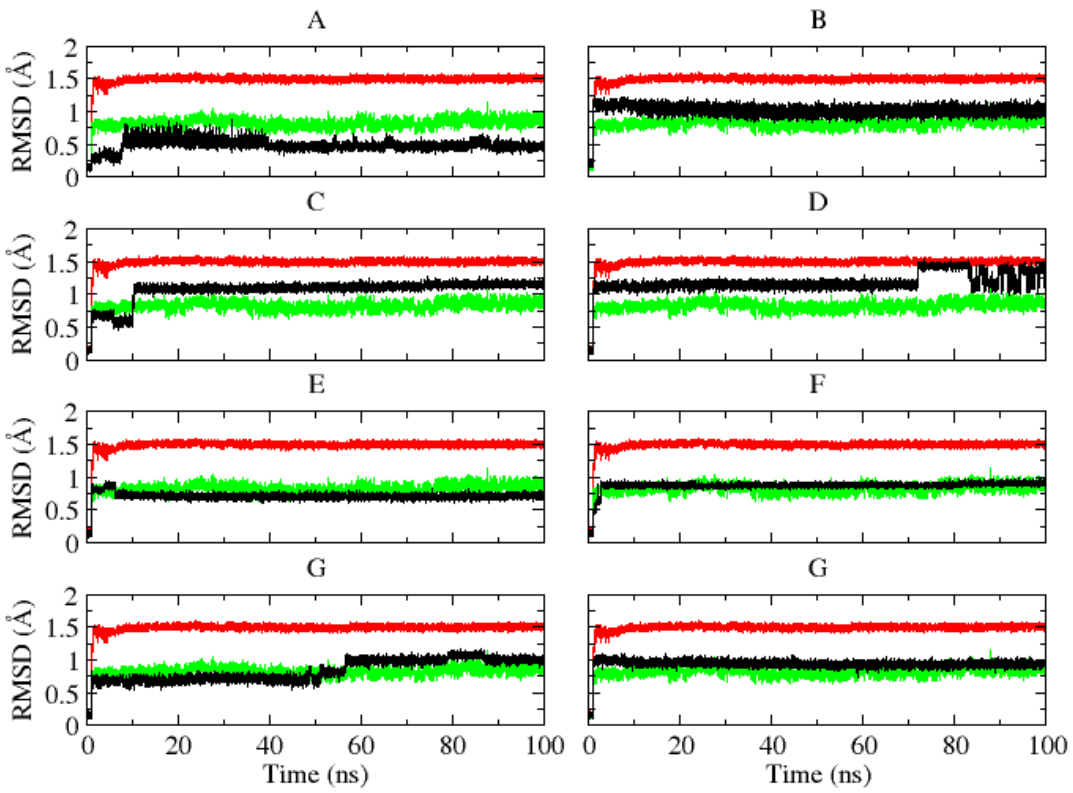

Fig. 8 RMSD plots of ligands. As a black line, ligand; as a green line, crystallographic rapamycin and, as a red line, docking rapamycin.

We used the RMSD to evaluate the ligand stability during simulation (Fig. 8). All selected molecules have better RMSD profile than docking rapamycin, which suggests a similar molecular stability of the ligand through the simulation. Although the compound D showed bigger fluctuation in the last 30 ns of MD compared to the others, this event seems insignificant (from 1.0 to 1.5 Å) since it didn't cause the exiting of the ligand from the binding site (Fig. 9).

Elaborated using PyMol v.1.7.5.0.

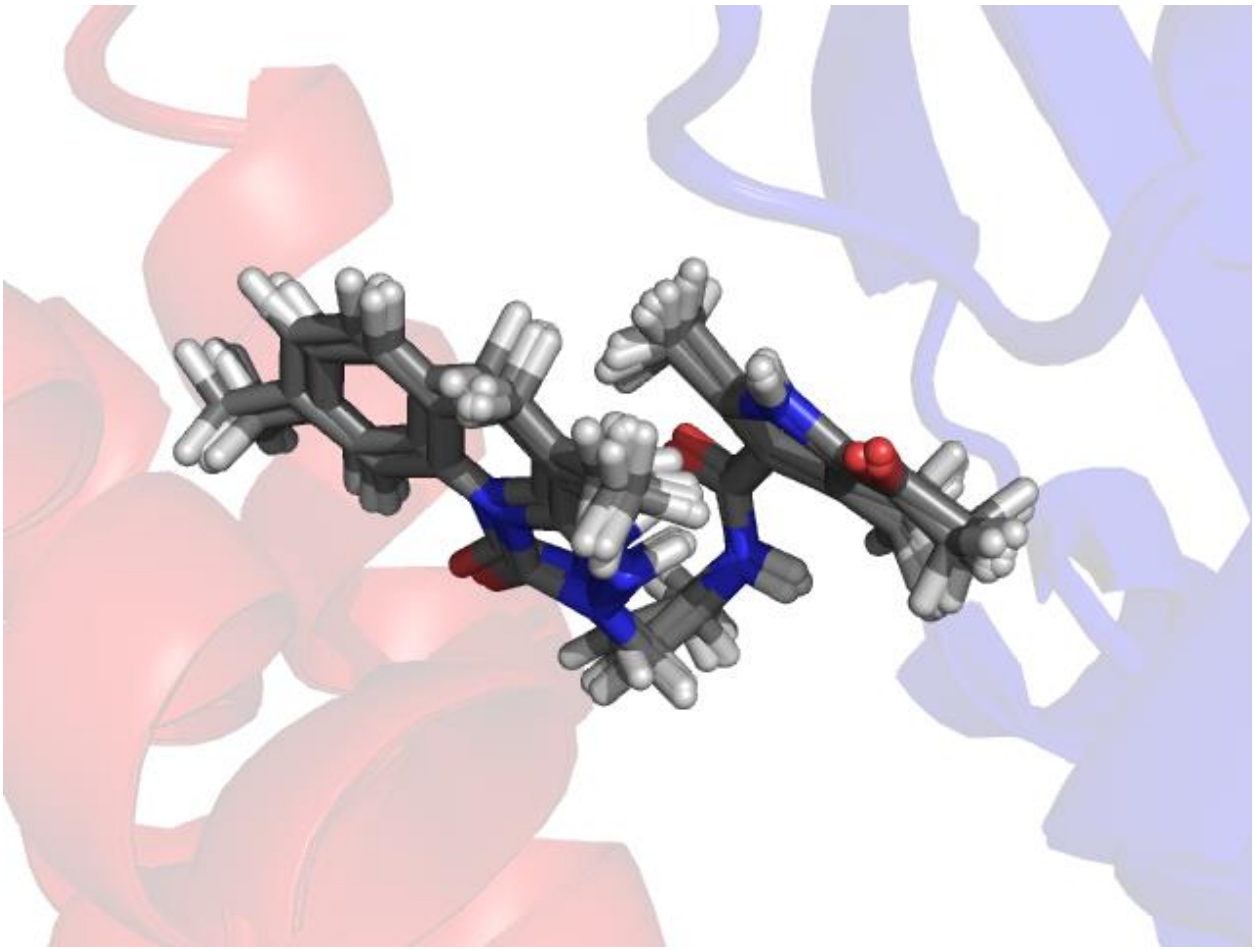

Fig. 9 Ligand D snapshots from 50; 60; 70; 80; 90 and 100 ns.

The binding energy profile, considering a binding energy cut-off of ≤ -1.0 kcal/mol, revealed that the complexes obtained using docking approach have more binding contacts with the FRB portion, mainly with the residues PHE129 and TYR195. However, the crystallographic system presents an equilibrium between residues of FKBP12 (TYR26, PHE36, PHE46, GLN53, GLU54, VAL55, ILE56, ILE90, PHE99) and FRB (LEU121, GLU122, PHE129, TRP191, ASP192, TYR195, PHE198). Fig. 10 presents the decomposition of binding energy per residue.

Elaborated using XMGRACE v.5.1.19.

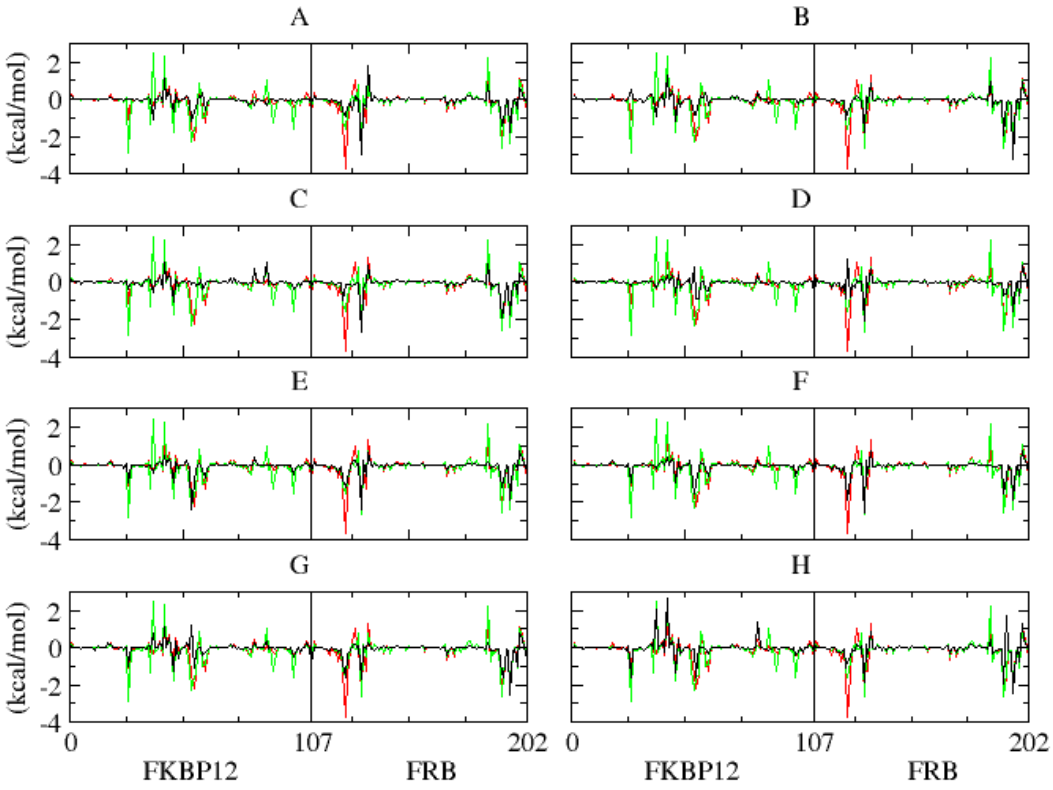

Fig. 10 Binding energy contribution of each residue. As a black line, ligand complex; as a green line, crystallographic rapamycin complex and, as red, docking rapamycin complex.

When analyzing the residues retrieved from the pharmacophore model (PHE46, ILE90, GLU122, PHE129, ASP192, TYR195, and PHE198), we can observe that the residues PHE46, GLU122, PHE129, ASP192 and TYR195 are the major contributors for the association between FKBP12:FRB domain and its ligands. Furthermore, considering the binding pocket analyzed through CASTp, the residues with lower binding energy belong to the pocket. Thus, these results confirm that all ligands are stable into the cavity delimited by the pharmacophore model and the lowest binding energy values belong to the binding pocket. For more information about the binding energy contribution of each residue, see Supplemental Material 4.

In Fig. 11, the Gibbs free energy based on RMSD and Rg (Supplemental Material 5 and 6) is plotted as FEL, providing valuable information about the protein structure flexibility. When FKBP12:FRB is not associated with a ligand, the system can better explore the conformational space. However, the presence of a ligand induces a protein stiffening, stabilizing the complexes in a similar conformation. In addition, all docking complexes exhibit a similar profile to rapamycin structure.

Elaborated using Gnuplot.

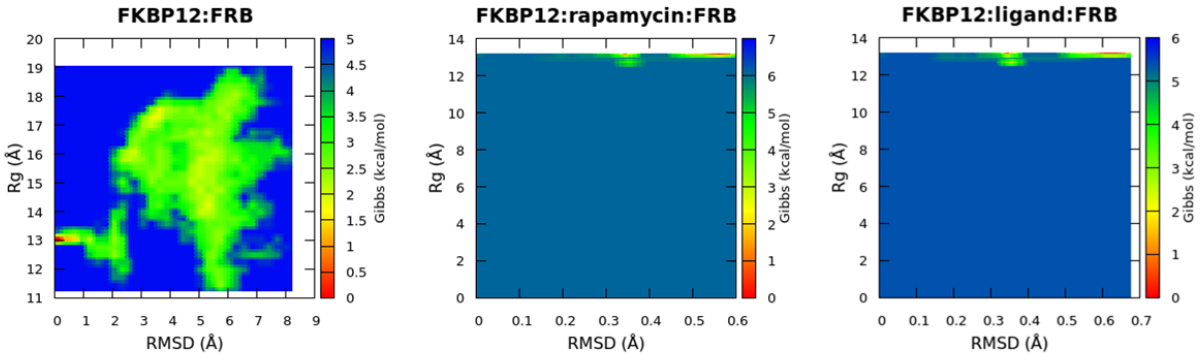

Fig. 11 Free energy landscapes from molecular dynamics.

The first prominent characteristic motions (PC1) during the simulation were analyzed through principal component analysis (PCA). The first eigenvectors corresponding to the PC1 accounted 64.2 % for FKBP12:FRB system; 65.5 % for FKBP12:A:FRB, 61.9 % for FKBP12:B:FRB, 57.7 % for FKBP12:C:FRB, 59.4 % for FKBP12:D:FRB, 66.0 % for FKBP12:E:FRB, 66.8 % for FKBP12:F:FRB, 58.3 % for FKBP12:G:FRB and 61.0 % for FKBP12:H:FRB system. We focused our analyses on the rapamycin pocket, especially on the mobility of the loops. We found that the motions were more pronounced in the FKBP12:FRB system, whereas in the presence of a ligand these motions were drastically reduced. Fig. 12 shows the tendency of eigenvectors for all complexes.

Elaborated using PyMol v.1.7.5.0.

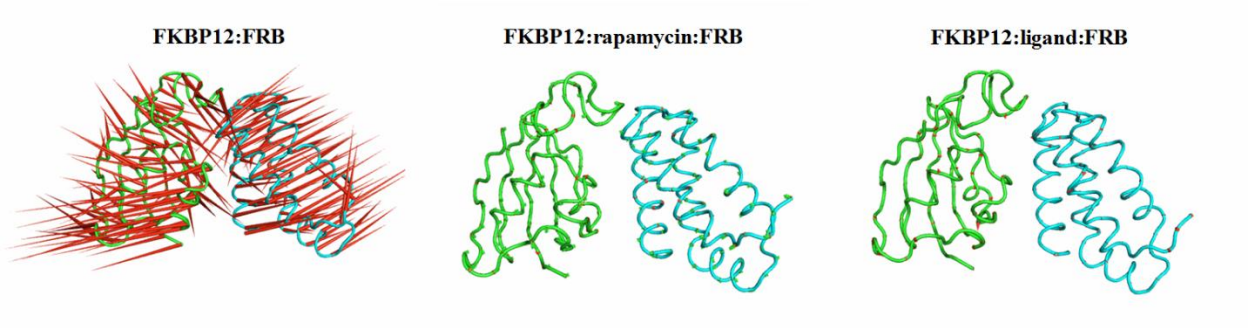

Fig. 12 Porcupine plots of FKBP12:FRB and ligands complexes during the simulation.

Conclusion

Computational techniques are widely used by the pharmaceutical industry to reduce time and financial resources in the process of drug discovery and development. Here we present an initial step to find new molecules to act as potential non-ATP competitive inhibitors to mTOR pathway. We were able to propose eight molecules presenting better energetic and pharmacokinetics profiles than rapamycin. In addition, MD simulations showed that all ligands induce a protein structure stiffening and its feature is also observed on the FKBP12:FRB associated with rapamycin. These conformational changes were confirmed by PCA and FEL analysis, allowing us to understand important features of the rapamycin's association with FKBP12:FRB. Furthermore, we were able to describe the residues PHE46, GLU122, PHE129, ASP192, and TYR195 as the major contributors to the binding. Then, the next step is to carry out experimental (*in vitro*) studies to confirm the inhibition profile of these ligands.

REFERENCES

[1] G.A. Soliman, The role of mechanistic target of rapamycin (mTOR) complexes signaling in the immune responses, Nutrients. 5 (2013) 2231–2257. doi:10.3390/nu5062231.

[2] C. Porta, C. Paglino, A. Mosca, Targeting PI3K/Akt/mTOR Signaling in Cancer, Front Oncol. 4 (2014) 64. doi:10.3389/fonc.2014.00064.

[3] P. Zarogoulidis, S. Lampaki, J.F. Turner, H. Huang, S. Kakolyris, K. Syrigos, K. Zarogoulidis, mTOR pathway: A current, up-to-date mini-review (Review), Oncol Lett. 8 (2014) 2367–2370. doi:10.3892/ol.2014.2608.

[4] M. Laplante, D.M. Sabatini, mTOR signaling in growth control and disease, Cell. 149 (2012) 274–293. doi:10.1016/j.cell.2012.03.017.

[5] E. Dazert, M.N. Hall, mTOR signaling in disease, Curr Opin Cell Biol. 23 (2011) 744–755. doi:10.1016/j.ceb.2011.09.003.

[6] D.A. Guertin, D.M. Sabatini, Defining the role of mTOR in cancer, Cancer Cell. 12 (2007) 9–22. doi:10.1016/j.ccr.2007.05.008.

[7] M. Laplante, D.M. Sabatini, mTOR signaling at a glance, J Cell Sci. 122 (2009) 3589–3594. doi:10.1242/jcs.051011.

[8] R. Watanabe, L. Wei, J. Huang, mTOR signaling, function, novel inhibitors, and therapeutic targets, J Nucl Med. 52 (2011) 497–500. doi:10.2967/jnumed.111.089623.

[9] C. Betz, M.N. Hall, Where is mTOR and what is it doing there?, J Cell Biol. 203 (2013) 563–574. doi:10.1083/jcb.201306041.

[10] S.N. Sehgal, Sirolimus: its discovery, biological properties, and mechanism of action, Transpl. Proc. 35 (2003) 7S–14S.

[11] R. Abraham T., J.J. Gibbons, E. Graziani I., Chemistry and Pharmacology of Rapamycin and Its Derivatives., in: M.N. Hall, F. Tamanoi (Eds.), Enzym. Struct. Funct. Regul. TOR Complexes Yeasts Mamm., Academic Press, 2010: pp. 329–356.

[12] G. Santulli, H. Totary-Jain, Tailoring mTOR-based therapy: molecular evidence and clinical challenges, Pharmacogenomics. 14 (2013) 1517–1526. doi:10.2217/pgs.13.143.

[13] Y. Zheng, Y. Jiang, mTOR Inhibitors at a Glance, Mol Cell Pharmacol. 7 (2015) 15–20.

[14] S.N. Sehgal, K. Molnar-Kimber, T.D. Ocain, B.M. Weichman, Rapamycin: A novel immunosuppressive macrolide, Med. Res. Rev. 14 (1994) 1–22. doi:10.1002/med.2610140102.

[15] H. Yang, D.G. Rudge, J.D. Koos, B. Vaidialingam, H.J. Yang, N.P. Pavletich, mTOR kinase structure, mechanism and regulation, Nature. 497 (2013) 217–223. doi:10.1038/nature12122.

[16] M. Shimobayashi, M.N. Hall, Making new contacts: the mTOR network in metabolism and signalling crosstalk, Nat Rev Mol Cell Biol. 15 (2014) 155–162. doi:10.1038/nrm3757.

[17] M. Dufour, A. Dormond-Meuwly, N. Demartines, O. Dormond, Targeting the Mammalian Target of Rapamycin (mTOR) in Cancer Therapy: Lessons from Past and Future Perspectives, Cancers. 3 (2011) 2478–2500. doi:10.3390/cancers3022478.

[18] J. Li, S.G. Kim, J. Blenis, Rapamycin: one drug, many effects, Cell Metab. 19 (2014) 373–379. doi:10.1016/j.cmet.2014.01.001.

[19] A. Carracedo, P.P. Pandolfi, The PTEN-PI3K pathway: of feedbacks and cross-talks, Oncogene. 27 (2008) 5527–5541. doi:10.1038/onc.2008.247.

[20] A.Y. Choo, S.O. Yoon, S.G. Kim, P.P. Roux, J. Blenis, Rapamycin differentially inhibits S6Ks and 4E-BP1 to mediate cell-type-specific repression of mRNA translation, Proc Natl Acad Sci U A. 105 (2008) 17414–17419. doi:10.1073/pnas.0809136105.

[21] A.Y. Choo, J. Blenis, Not all substrates are treated equally: implications for mTOR, rapamycin-resistance and cancer therapy, Cell Cycle. 8 (2009) 567–572.

[22] D.A. Guertin, D.M. Sabatini, The pharmacology of mTOR inhibition, Sci Signal. 2 (2009) pe24. doi:10.1126/scisignal.267pe24.

[23] C.C. Thoreen, S.A. Kang, J.W. Chang, Q. Liu, J. Zhang, Y. Gao, L.J. Reichling, T. Sim, D.M. Sabatini, N.S. Gray, An ATP-competitive mammalian target of rapamycin inhibitor reveals rapamycin-resistant functions of mTORC1, J Biol Chem. 284 (2009) 8023–8032. doi:10.1074/jbc.M900301200.

[24] F. Di Nicolantonio, S. Arena, J. Tabernero, S. Grosso, F. Molinari, T. Macarulla, M. Russo, C. Cancelliere, D. Zecchin, L. Mazzucchelli, T. Sasazuki, S. Shirasawa, M. Geuna, M. Frattini, J. Baselga, M. Gallicchio, S. Biffo, A. Bardelli, Deregulation of the PI3K and KRAS signaling pathways in human cancer cells determines their response to everolimus, J Clin Invest. 120 (2010) 2858–2866. doi:10.1172/JCI37539.

[25] V. Wacheck, mTOR pathway inhibitors in cancer therapy: moving past rapamycin, Pharmacogenomics. 11 (2010) 1189–1191. doi:10.2217/pgs.10.113.

[26] S.D. Knight, N.D. Adams, J.L. Burgess, A.M. Chaudhari, M.G. Darcy, C.A. Donatelli, J.I. Luengo, K.A. Newlander, C.A. Parrish, L.H. Ridgers, M.A. Sarpong, S.J. Schmidt, G.S. Van Aller, J.D. Carson, M.A. Diamond, P.A. Elkins, C.M. Gardiner, E. Garver, S.A. Gilbert, R.R. Gontarek, J.R. Jackson, K.L. Kershner, L. Luo, K. Raha, C.S. Sherk, C.M. Sung, D. Sutton, P.J. Tummino, R.J. Wegrzyn, K.R. Auger, D. Dhanak, Discovery of GSK2126458, a Highly Potent Inhibitor of PI3K and the Mammalian Target of Rapamycin, ACS Med Chem Lett. 1 (2010) 39–43. doi:10.1021/ml900028r.
[27] S. V Bhagwat, P.C. Gokhale, A.P. Crew, A. Cooke, Y. Yao, C. Mantis, J. Kahler, J. Workman, M. Bittner, L. Dudkin, D.M. Epstein, N.W. Gibson, R. Wild, L.D. Arnold, P.J. Houghton, J.A. Pachter, Preclinical characterization of OSI-027, a potent and selective inhibitor of mTORC1 and mTORC2: distinct from rapamycin, Mol Cancer Ther. 10 (2011) 1394–1406. doi:10.1158/1535-7163.MCT-10-1099.
[28] J. Yuan, P.P. Mehta, M.J. Yin, S. Sun, A. Zou, J. Chen, K. Rafidi, Z. Feng, J. Nickel, J. Engebretsen, J. Hallin, A. Blasina, E. Zhang, L. Nguyen, M. Sun, P.K. Vogt, A. McHarg, H. Cheng, J.G. Christensen, J.L. Kan, S. Bagrodia, PF-04691502, a potent and selective oral inhibitor of PI3K and mTOR kinases with antitumor activity, Mol Cancer Ther. 10 (2011) 2189–2199. doi:10.1158/1535-7163.MCT-11-0185.
[29] B. Mukherjee, N. Tomimatsu, K. Amancherla, C. V Camacho, N. Pichamoorthy, S. Burma, The dual PI3K/mTOR inhibitor NVP-BEZ235 is a potent inhibitor of ATM- and DNA-PKCs-mediated DNA damage responses, Neoplasia. 14 (2012) 34–43.
[30] Y. Guo, D.J. Kwiatkowski, Equivalent benefit of rapamycin and a potent mTOR ATP-competitive inhibitor, MLN0128 (INK128), in a mouse model of tuberous sclerosis, Mol Cancer Res. 11 (2013) 467–473. doi:10.1158/1541-7786.MCR-12-0605.
[31] Y. Luo, Selectivity assessment of kinase inhibitors: strategies and challenges, Curr Opin Mol Ther. 7 (2005) 251–255.
[32] R. Thaimattam, R. Banerjee, R. Miglani, J. Iqbal, Protein kinase inhibitors: structural insights into selectivity, Curr Pharm Des. 13 (2007) 2751–2765.
[33] L.A. Smyth, I. Collins, Measuring and interpreting the selectivity of protein kinase inhibitors, J Chem Biol. 2 (2009) 131–151. doi:10.1007/s12154-009-0023-9.
[34] L. Wang, L. Chen, M. Yu, L.-H. Xu, B. Cheng, Y.-S. Lin, Q. Gu, X.-H. He, J. Xu, Discovering new mTOR inhibitors for cancer treatment through virtual screening methods and in vitro assays, Sci. Rep. 6 (2016) 18987. doi:10.1038/srep18987 http://www.nature.com/articles/srep18987#supplementary-information.
[35] B. Liu, S. Li, J. Hu, Technological advances in high-throughput screening, Am J Pharmacogenomics. 4 (2004) 263–276.
[36] E. Bielska, X. Lucas, A. Czerwoniec, J.M. Kasprzak, K.H. Kaminska, J.M. Bujnicki, Virtual screening strategies in drug design–methods and applications., J. Biotechnol. Comput. Biol. Bionanotechnol. 92 (2011) p 249-264.
[37] R.S. Ferreira, O. Glaucius, A.D. Andricopulo, Integração das técnicas de triagem virtual e triagem biológica automatizada em alta escala: oportunidades e desafios em P&D de fármacos, Quím. Nova. 34 (2011) 1770–1778.
[38] G. Klebe, Virtual Screening: an Alternative Or Complement to High Throughput Screening?, Springer, 2000.
[39] H.M. Berman, J. Westbrook, Z. Feng, G. Gilliland, T.N. Bhat, H. Weissig, I.N. Shindyalov, P.E. Bourne, The Protein Data Bank, Nucleic Acids Res. 28 (2000) 235–242.
[40] F.C. Bernstein, T.F. Koetzle, G.J. Williams, E.F. Meyer, M.D. Brice, J.R. Rodgers, O. Kennard, T. Shimanouchi, M. Tasumi, The Protein Data Bank: a computer-based archival file for macromolecular structures, Arch Biochem Biophys. 185 (1978) 584–591.
[41] J. Choi, J. Chen, S.L. Schreiber, J. Clardy, Structure of the FKBP12-rapamycin complex interacting with the binding domain of human FRAP, Science. 273 (1996) 239–242.
[42] T. Langer, E.M. Krovat, Chemical feature-based pharmacophores and virtual library screening for discovery of new leads, Curr Opin Drug Discov Devel. 6 (2003) 370–376.
[43] A.R. Leach, V.J. Gillet, R.A. Lewis, R. Taylor, Three-dimensional pharmacophore methods in drug discovery, J Med Chem. 53 (2010) 539–558. doi:10.1021/jm900817u.
[44] R. Mannhold, H. Kubinyi, G. Folkers, Virtual Screening: Principles, Challenges, and Practical Guidelines, 48th ed., Wiley. com, 2011.
[45] P. Markt, D. Schuster, T. Langer, Pharmacophore Models for Virtual Screening, in: Virtual Screen., Wiley-VCH Verlag GmbH & Co. KGaA, 2011: pp. 115–152. doi:10.1002/9783527633326.ch5.
[46] D.R. Koes, C.J. Camacho, ZINCPharmer: pharmacophore search of the ZINC database, Nucleic Acids Res. 40 (2012) W409-14. doi:10.1093/nar/gks378.
[47] O. Trott, A.J. Olson, AutoDock Vina: improving the speed and accuracy of docking with a new scoring function, efficient optimization, and multithreading, J Comput Chem. 31 (2010) 455–461. doi:10.1002/jcc.21334.

[48] C.M. Labbé, J. Rey, D. Lagorce, M. Vavruša, J. Becot, O. Sperandio, B.O. Villoutreix, P. Tufféry, M.A. Miteva, MTiOpenScreen: a web server for structure-based virtual screening, Nucleic Acids Res. 43 (2015) W448-54. doi:10.1093/nar/gkv306.
[49] G.M. Morris, R. Huey, W. Lindstrom, M.F. Sanner, R.K. Belew, D.S. Goodsell, A.J. Olson, AutoDock4 and AutoDockTools4: Automated docking with selective receptor flexibility, J Comput Chem. 30 (2009) 2785–2791. doi:10.1002/jcc.21256.
[50] S. Dallakyan, PyRx-python prescription v. 0.8, Scripps Res. Inst. 2010 (2008).
[51] M.M. Mysinger, M. Carchia, J.J. Irwin, B.K. Shoichet, Directory of useful decoys, enhanced (DUD-E): better ligands and decoys for better benchmarking, J Med Chem. 55 (2012) 6582–6594. doi:10.1021/jm300687e.
[52] C. Empereur-mot, H. Guillemain, A. Latouche, J.-F. Zagury, V. Viallon, M. Montes, Predictiveness curves in virtual screening, J. Cheminformatics. 7 (2015) 52. doi:10.1186/s13321-015-0100-8.
[53] T. Sander, J. Freyss, M. von Korff, C. Rufener, DataWarrior: an open-source program for chemistry aware data visualization and analysis, J Chem Inf Model. 55 (2015) 460–473. doi:10.1021/ci500588j.
[54] D.S. Wishart, C. Knox, A.C. Guo, S. Shrivastava, M. Hassanali, P. Stothard, Z. Chang, J. Woolsey, DrugBank: a comprehensive resource for in silico drug discovery and exploration, Nucleic Acids Res. 34 (2006) D668-72. doi:10.1093/nar/gkj067.
[55] M.A. Miteva, S. Violas, M. Montes, D. Gomez, P. Tuffery, B.O. Villoutreix, FAF-Drugs: free ADME/tox filtering of compound collections, Nucleic Acids Res. 34 (2006) W738-44. doi:10.1093/nar/gkl065.
[56] D.E. Pires, T.L. Blundell, D.B. Ascher, pkCSM: Predicting Small-Molecule Pharmacokinetic and Toxicity Properties Using Graph-Based Signatures, J Med Chem. 58 (2015) 4066–4072. doi:10.1021/acs.jmedchem.5b00104.
[57] J.D. Durrant, J.A. McCammon, Molecular dynamics simulations and drug discovery, BMC Biol. 9 (2011) 71. doi:10.1186/1741-7007-9-71.
[58] E. Lindahl, B. Hess, D. Van der Spoel, GROMACS 3.0: A package for molecular simulation and trajectory analysis., J. Mol. Model. v. 7 (2001) 306–317.
[59] D. Van Der Spoel, E. Lindahl, B. Hess, G. Groenhof, A.E. Mark, H.J. Berendsen, GROMACS: fast, flexible, and free, J Comput Chem. 26 (2005) 1701–1718. doi:10.1002/jcc.20291.
[60] A.W. Schüttelkopf, D.M. van Aalten, PRODRG: a tool for high-throughput crystallography of protein-ligand complexes, Acta Crystallogr Biol Crystallogr. 60 (2004) 1355–1363. doi:10.1107/S0907444904011679.
[61] K.B. Koziara, M. Stroet, A.K. Malde, A.E. Mark, Testing and validation of the Automated Topology Builder (ATB) version 2.0: prediction of hydration free enthalpies, J Comput Aided Mol Des. 28 (2014) 221–233. doi:10.1007/s10822-014-9713-7.
[62] C. Oostenbrink, A. Villa, A.E. Mark, W.F. van Gunsteren, A biomolecular force field based on the free enthalpy of hydration and solvation: the GROMOS force-field parameter sets 53A5 and 53A6, J Comput Chem. 25 (2004) 1656–1676. doi:10.1002/jcc.20090.
[63] B. Hess, H. Bekker, H.J.C. Berendsen, J.G.E.M. Fraaije, LINCS: A linear constraint solver for molecular simulations, Journal of Computational Chemistry Volume 18, Issue 12, J. Comput. Chem. 18 (1997) 1463–1472.
[64] A. Amadei, A.B. Linssen, H.J. Berendsen, Essential dynamics of proteins, Proteins. 17 (1993) 412–425. doi:10.1002/prot.340170408.
[65] W.L. Delano, The PyMOL Molecular Graphics System, (2002).
[66] V.N. Maiorov, G.M. Crippen, Significance of root-mean-square deviation in comparing three-dimensional structures of globular proteins, J. Mol. Biol. 235 (1994) 625–634.
[67] A.M. Ruvinsky, T. Kirys, A. V Tuzikov, I.A. Vakser, Structure fluctuations and conformational changes in protein binding, J Bioinform Comput Biol. 10 (2012) 1241002. doi:10.1142/S0219720012410028.
[68] M.I.. Lobanov, N.S. Bogatyreva, O. V Galzitskaia, [Radius of gyration is indicator of compactness of protein structure], Mol Biol Mosk. 42 (2008) 701–706.
[69] I. Tavernelli, S. Cotesta, E.E. Di Iorio, Protein dynamics, thermal stability, and free-energy landscapes: a molecular dynamics investigation, Biophys J. 85 (2003) 2641–2649. doi:10.1016/S0006-3495(03)74687-6.
[70] R. Kumari, R. Kumar, A. Lynn, O.S.D.D. Consortium, g_mmpbsa--a GROMACS tool for high-throughput MM-PBSA calculations, J Chem Inf Model. 54 (2014) 1951–1962. doi:10.1021/ci500020m.
[71] J. Dundas, Z. Ouyang, J. Tseng, A. Binkowski, Y. Turpaz, J. Liang, CASTp: computed atlas of surface topography of proteins with structural and topographical mapping of functionally annotated residues, Nucleic Acids Res. 34 (2006) W116-8. doi:10.1093/nar/gkl282.
[72] F. Sun, P. Li, Y. Ding, L. Wang, M. Bartlam, C. Shu, B. Shen, H. Jiang, S. Li, Z. Rao, Design and Structure-Based Study of New Potential FKBP12 Inhibitors, Biophys. J. 85 (2003) 3194–3201.

[73] M.M. Mysinger, M. Carchia, J.J. Irwin, B.K. Shoichet, Directory of Useful Decoys, Enhanced (DUD-E): Better Ligands and Decoys for Better Benchmarking, J. Med. Chem. 55 (2012) 6582–6594. doi:10.1021/jm300687e.
[74] D.K. McClish, Analyzing a portion of the ROC curve, Med Decis Mak. 9 (1989) 190–195. doi:10.1177/0272989X8900900307.
[75] M.H. Zweig, G. Campbell, Receiver-operating characteristic (ROC) plots: a fundamental evaluation tool in clinical medicine, Clin Chem. 39 (1993) 561–577.
[76] N. Triballeau, F. Acher, I. Brabet, J.P. Pin, H.O. Bertrand, Virtual screening workflow development guided by the "receiver operating characteristic" curve approach. Application to high-throughput docking on metabotropic glutamate receptor subtype 4, J Med Chem. 48 (2005) 2534–2547. doi:10.1021/jm049092j.
[77] C.A. Lipinski, F. Lombardo, B.W. Dominy, P.J. Feeney, Experimental and computational approaches to estimate solubility and permeability in drug discovery and development settings, Adv Drug Deliv Rev. 46 (2001) 3–26.
[78] D.F. Veber, S.R. Johnson, H.Y. Cheng, B.R. Smith, K.W. Ward, K.D. Kopple, Molecular properties that influence the oral bioavailability of drug candidates, J Med Chem. 45 (2002) 2615–2623.
[79] W.J. Egan, Merz Kenneth M., J.J. Baldwin, Prediction of Drug Absorption Using Multivariate Statistics, J. Med. Chem. 43 (2000) 3867–3877. doi:10.1021/jm000292e.
[80] R. Kist, R.A. Caceres, New potential inhibitors of mTOR: a computational investigation integrating molecular docking, virtual screening and molecular dynamics simulation, J. Biomol. Struct. Dyn. 35 (2016) 3555–3568. doi:10.1080/07391102.2016.1262279.
[81] L.A. Banaszynski, C.W. Liu, T.J. Wandless, Characterization of the FKBP.rapamycin.FRB ternary complex, J Am Chem Soc. 127 (2005) 4715–4721. doi:10.1021/ja043277y.

Supplemental Material 1

Descriptive results obtained from DataWarrior webserver and FAF-Drugs.

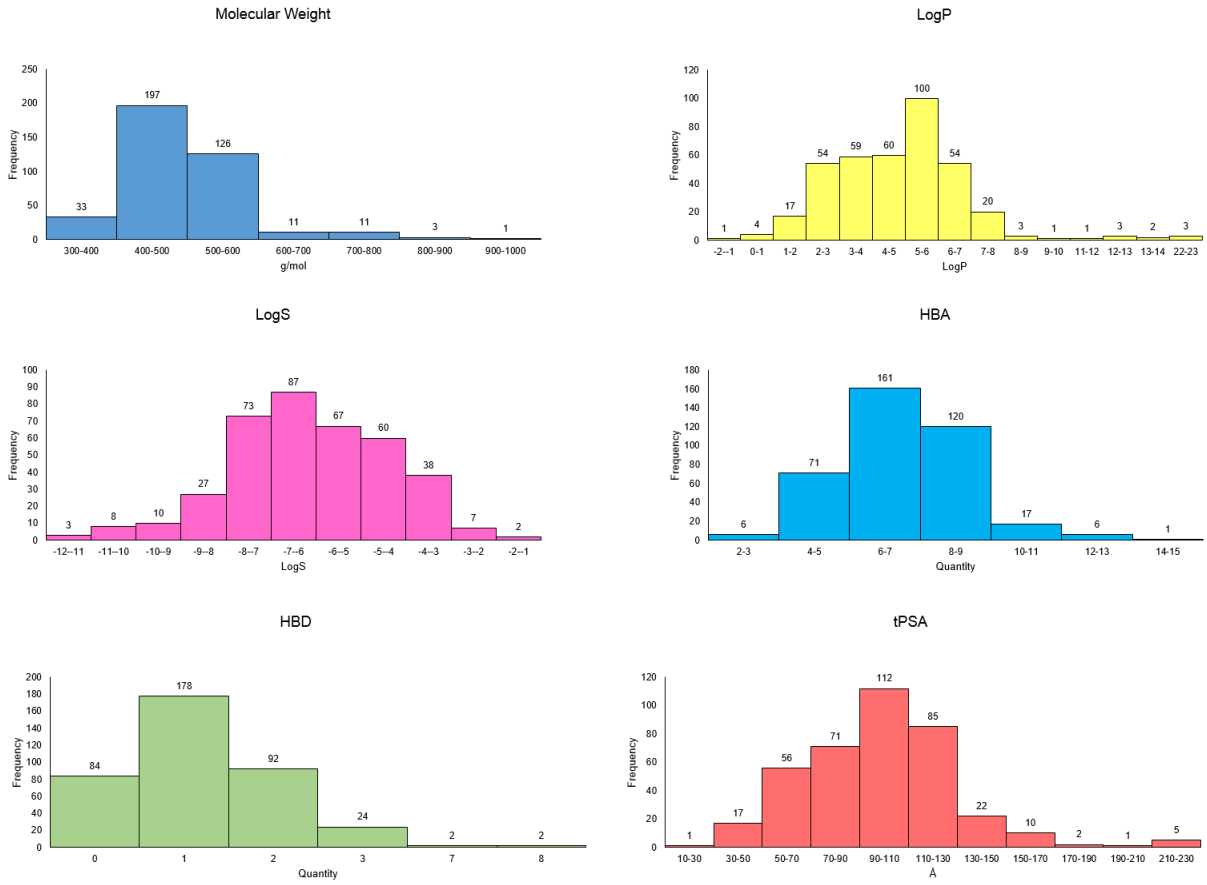

Supplemental Material 2

ADMETox properties from all compounds obtained from DataWarrior webserver and FAF-Drugs.

Molecule	VINA Dock energy (kcal/mol)	MtiOpen Screen Dock energy (kcal/mol)	Molecular Weight (g/mol)	cLogP	cLogS	HBA	HBD	tPSA (Å)	RotB	RigB	Lipinski Violation	VEBER	EGAN	Mutagenic Profile	Tumorigenic Profile	Reproductive Effective Profile	Irritant Profile
(i)	-18.1	-18.1	922.2	6.7	-7.7	14	3	195.4	6	49	3	Good	Good	None	None	None	None
(ii)	-10.1	-9.9	914.2	6.5	-6.7	14	3	195.4	6	49	3	Good	Good	None	None	None	None
A	-11.6	-11.4	485.3	5.3	-6.8	6	0	64.2	4	26	1	Good	Good	None	None	None	None
B	-10.5	-10.6	419.5	2.4	-5.2	8	2	97.9	5	24	0	Good	Good	None	None	None	None
C	-10.5	-10.2	478.5	3.4	-4.6	9	1	106.2	8	20	0	Good	Good	None	None	None	None
D	-10.5	-9.8	391.5	2.4	-4.0	7	2	88.7	5	22	0	Good	Good	None	None	None	None
E	-11.3	-11.1	419.4	3.6	-5.7	9	2	117.4	5	28	0	Good	Good	None	None	None	None
F	-11.3	-11.0	421.5	3.7	-5.7	9	2	117.4	5	25	0	Good	Good	None	None	None	None
G	-10.5	-10.6	421.5	2.1	-3.4	8	2	94.1	5	23	0	Good	Good	None	None	None	None
H	-10.6	-10.6	491.7	6.0	-7.9	7	2	106.4	9	24	1	Good	Good	None	None	None	None
9	-8.1	-8.2	316.4	2.1	-3.9	5	3	56.5	8	12	0	Good	Good	None	None	None	High
10	-8.5	-8.2	330.5	2.5	-4.2	5	3	56.5	9	12	0	Good	Good	None	None	None	High
11	-9.4	-9.4	330.5	5.4	-7.6	2	0	17.3	3	18	1	Good	Good	None	High	None	Low
12	-7.9	-7.6	332.5	0.9	-2.7	5	1	52.9	8	11	0	Good	Good	None	None	None	None
13	-7.8	-7.6	346.4	1.7	-3.1	7	2	77.4	8	14	0	Good	Good	None	None	None	None
14	-8.2	-8.1	346.4	2.0	-2.2	4	0	34.5	8	12	0	Good	Good	None	None	None	None
15	-8.2	-8.0	348.8	2.0	-3.4	6	1	69.0	5	14	0	Good	Good	None	None	None	None
16	-8.4	-8.3	359.5	2.1	-3.2	6	3	101.5	8	16	0	Good	Good	None	None	None	High
17	-8.8	-8.4	361.4	2.7	-5.0	5	3	94.5	7	15	0	Good	Good	None	None	High	Low
18	-8.8	-8.8	361.9	5.2	-5.5	4	1	47.6	6	14	1	Good	Good	None	None	None	None
19	-8.5	-8.3	362.9	3.5	-4.7	5	0	53.4	7	13	0	Good	Good	High	None	Low	High
20	-8.4	-8.5	367.3	2.4	-4.4	5	1	50.2	4	17	0	Good	Good	None	None	None	None
21	-8.8	-9.2	368.4	2.3	-1.5	7	0	78.6	7	17	0	Good	Good	None	None	Low	None

22	-9.2	-8.8	369.4	1.2	-2.8	8	2	102.1	6	19	0	Good	Good	None	None	None	None
23	-8.7	-9.2	369.4	1.2	-2.8	8	2	102.1	6	19	0	Good	Good	High	None	None	None
24	-8.1	-8.0	373.5	1.9	-3.4	6	0	92.1	6	17	0	Good	Good	None	None	None	None
25	-8.0	-8.0	373.5	2.0	-3.2	6	0	92.1	7	17	0	Good	Good	None	None	None	None
26	-8.2	-9.3	373.7	4.3	-4.8	5	2	59.0	4	14	0	Good	Good	High	None	Low	Low
27	-8.4	-9.5	373.8	1.8	-3.2	6	0	63.9	6	18	0	Good	Good	None	None	None	None
28	-8.7	-8.7	382.3	5.4	-5.9	4	1	47.6	6	14	1	Good	Good	None	None	None	High
29	-10.0	-10.0	382.5	3.8	-3.4	5	1	66.6	5	23	0	Good	Good	None	None	None	None
30	-8.3	-8.3	385.8	2.7	-3.8	5	0	57.5	8	13	0	Good	Good	None	None	Low	None
31	-7.9	-7.8	386.4	-1.5	-3.1	9	0	117.2	7	18	0	Good	Good	Low	None	None	None
32	-8.8	-8.5	387.5	3.7	-4.0	6	1	105.5	8	17	0	Good	Good	None	None	None	None
33	-8.7	-8.7	387.5	2.4	-3.3	6	0	92.1	6	17	0	Good	Good	None	None	None	High
34	-8.5	-9.3	387.9	2.3	-3.2	6	0	63.9	6	18	0	Good	Good	None	None	None	High
35	-8.7	-8.3	388.9	2.0	-5.4	7	2	76.9	6	19	0	Good	Good	None	None	None	None
36	-9.5	-9.8	391.5	3.4	-3.9	5	0	47.4	6	19	0	Good	Good	None	None	None	High
37	-7.6	-7.8	392.5	3.7	-3.8	6	2	100.9	10	14	0	Good	Good	None	None	None	High
38	-7.6	-7.8	392.5	3.7	-3.8	6	2	100.9	10	14	0	Good	Good	None	None	None	High
39	-10.1	-10.5	394.5	2.1	-5.1	7	1	85.6	6	19	0	Good	Good	None	None	High	None
40	-10.2	-10.4	399.9	2.2	-4.0	6	0	63.9	5	23	0	Good	Good	None	None	None	None
41	-8.0	-7.8	401.3	4.3	-5.7	4	2	107.8	7	15	1	Good	Good	None	None	High	None
42	-8.1	-8.0	402.6	1.9	-3.9	4	1	87.0	11	12	0	Good	Good	None	None	None	None
43	-8.5	-8.2	404.4	2.4	-3.3	7	1	76.5	10	17	0	Good	Good	None	Low	None	Low
44	-8.6	-8.7	406.3	5.3	-5.6	4	1	47.6	6	14	1	Good	Good	None	None	None	None
45	-8.6	-8.2	406.9	3.7	-4.4	5	1	83.9	8	16	0	Good	Good	None	None	None	None
46	-8.5	-9.8	408.3	2.4	-4.0	6	0	63.9	6	18	0	Good	Good	None	None	None	Low
47	-8.0	-8.0	411.3	3.6	-4.7	5	1	67.8	7	14	0	Good	Good	None	None	None	None
48	-9.5	-9.4	413.5	2.9	-3.7	6	0	92.1	6	22	0	Good	Good	None	None	None	High
49	-8.2	-8.1	415.4	1.4	-3.5	9	0	103.3	9	18	0	Good	Good	Low	None	None	None

50	-9.6	-9.5	415.5	2.7	-3.6	7	0	105.9	7	23	0	Good	Good	None	None	None	None
51	-7.4	-7.4	416.5	4.5	-6.1	7	1	103.6	10	17	1	Good	Good	None	None	High	None
52	-7.7	-7.8	416.5	4.4	-6.1	7	1	103.6	10	17	0	Good	Good	None	None	High	None
53	-8.4	-10.3	416.6	4.8	-5.8	4	1	130.1	7	19	1	Good	Good	None	High	None	None
54	-10.3	-10.2	418.5	4.8	-5.9	6	1	67.4	6	25	0	Good	Good	Low	High	None	High
55	-7.9	-7.6	418.6	4.4	-4.4	6	2	100.9	12	15	0	Good	Good	None	None	None	High
56	-10.0	-9.1	420.4	3.6	-4.3	9	3	138.2	7	19	0	Good	Good	None	None	Low	None
57	-9.3	-10.9	420.5	3.4	-4.6	6	0	70.4	7	23	0	Good	Good	None	None	None	None
58	-10.0	-10.2	421.4	2.2	-1.9	7	1	81.4	6	18	0	Good	Good	None	None	Low	None
59	-9.7	-9.4	422.3	4.4	-6.5	5	2	95.9	5	20	0	Good	Good	None	None	Low	Low
60	-9.7	-11.0	422.5	3.1	-4.2	7	0	69.0	6	23	0	Good	Good	None	None	None	None
61	-9.9	-9.7	424.9	4.6	-6.0	6	1	67.4	5	25	0	Good	Good	High	High	Low	High
62	-10.2	-10.1	425.6	3.5	-4.5	6	0	90.5	6	24	0	Good	Good	None	None	None	None
63	-8.2	-8.0	425.6	2.5	-4.3	7	2	150.4	10	14	0	Low	Low	None	None	None	High
64	-8.6	-8.6	426.7	5.5	-6.0	4	1	47.6	6	14	1	Good	Good	None	None	None	High
65	-8.0	-8.2	427.4	4.0	-4.8	5	1	83.9	8	16	0	Good	Good	None	None	High	None
66	-7.9	-8.1	430.6	4.8	-6.5	7	1	103.6	10	17	1	Good	Good	None	None	High	None
67	-7.9	-8.2	430.6	4.7	-6.4	7	1	103.6	10	17	0	Good	Good	None	None	High	None
68	-7.7	-8.0	430.6	4.9	-6.4	7	1	103.6	11	17	1	Good	Good	None	None	High	None
69	-8.0	-8.0	430.6	4.8	-6.5	7	1	103.6	10	17	1	Good	Good	None	None	None	None
70	-8.3	-9.3	432.3	2.4	-3.3	6	0	63.9	6	18	0	Good	Good	None	None	None	High
71	-7.9	-7.4	432.5	4.0	-5.8	8	1	112.8	10	17	0	Good	Good	None	None	None	None
72	-9.7	-9.4	434.3	2.8	-4.7	6	0	63.9	5	23	0	Good	Good	None	None	None	Low
73	-8.3	-8.3	435.3	2.7	-4.7	7	1	83.1	8	15	0	Good	Good	None	None	None	High
74	-8.9	-11.3	435.5	2.7	-3.1	8	1	87.8	8	23	0	Good	Good	None	None	None	None
75	-10.1	-10.7	435.5	4.4	-4.0	6	0	65.1	6	25	0	Good	Good	None	None	None	None
76	-9.1	-10.4	435.5	3.2	-5.1	6	0	92.1	7	23	0	Good	Good	None	None	None	None
77	-7.4	-7.1	435.6	0.3	-2.4	7	3	99.4	14	13	0	Good	Good	None	None	None	None

78	-9.4	-11.1	436.6	2.4	-3.8	8	0	76.4	6	24	0	Good	Good	None	None	None	None
79	-7.6	-7.6	436.6	3.7	-3.8	7	2	110.1	13	14	0	Good	Good	None	None	None	High
80	-11.0	-10.9	437.3	6.7	-8.6	4	1	50.7	5	25	1	Good	Good	High	High	High	High
81	-9.5	-9.5	438.6	5.1	-5.6	5	2	91.7	10	20	1	Good	Good	None	None	None	High
82	-9.3	-10.2	442.3	5.4	-6.8	5	0	66.2	6	20	1	Good	Good	High	High	High	High
83	-9.6	-9.7	442.5	4.4	-7.2	6	1	94.3	7	23	0	Good	Good	None	None	None	None
84	-7.6	-7.8	442.6	5.2	-6.6	7	1	103.6	12	18	1	Good	Good	None	None	High	High
85	-9.4	-9.5	443.0	6.0	-6.2	4	1	91.7	5	24	1	Good	Good	None	None	None	None
86	-8.7	-8.3	443.6	4.8	-5.0	6	1	96.3	10	20	0	Good	Good	None	None	None	None
87	-9.7	-10.0	444.3	2.3	-4.1	6	0	63.9	5	23	0	Good	Good	None	None	None	None
88	-9.0	-9.0	444.5	3.1	-4.8	6	1	56.9	7	23	0	Good	Good	None	None	None	None
89	-8.4	-8.3	444.6	5.2	-6.8	7	1	103.6	10	17	1	Good	Good	None	None	None	None
90	-7.8	-8.0	444.6	5.2	-6.7	7	1	103.6	11	17	1	Good	Good	None	None	High	None
91	-7.6	-8.0	444.6	5.3	-6.6	7	1	103.6	12	17	1	Good	Good	None	None	High	None
92	-7.8	-7.8	444.6	5.3	-6.6	7	1	103.6	12	17	1	Good	Good	None	None	None	High
93	-9.1	-9.5	445.0	5.8	-6.9	5	1	85.2	7	23	1	Good	Good	None	None	None	None
94	-8.5	-8.7	445.6	4.1	-3.2	6	0	83.7	11	17	0	Good	Good	None	None	None	High
95	-7.9	-8.0	446.6	4.4	-6.1	8	1	112.8	11	17	0	Good	Good	None	None	None	None
96	-10.4	-9.1	448.5	4.4	-4.2	9	3	138.2	8	19	0	Good	Good	None	None	Low	None
97	-10.0	-9.8	448.6	1.0	-2.7	8	1	77.2	8	26	0	Good	Good	None	None	None	None
98	-10.3	-10.4	449.9	3.5	-5.1	7	0	73.1	5	28	0	Good	Good	None	None	None	None
99	-10.3	-10.4	449.9	3.5	-5.1	7	0	73.1	5	28	0	Good	Good	None	None	None	None
100	-10.2	-10.2	450.3	3.5	-4.5	5	0	54.7	5	24	0	Good	Good	None	None	None	None
101	-10.1	-10.0	450.5	2.2	-5.2	8	1	85.6	10	20	0	Good	Good	None	None	None	None
102	-9.7	-9.8	450.5	2.6	-4.3	8	1	115.7	5	27	0	Good	Good	High	None	None	None
103	-8.8	-8.8	450.7	3.1	-5.9	5	3	94.5	7	15	0	Good	Good	High	None	High	None
104	-9.7	-9.8	452.6	5.0	-7.6	6	1	94.3	7	23	1	Good	Good	None	None	High	Low
105	-9.1	-9.0	453.7	5.8	-5.6	4	1	59.8	11	18	1	Good	Good	None	None	None	None

106	-9.6	-10.7	455.0	1.2	-4.3	7	2	75.7	7	25	0	Good	Good	High	None	None	None
107	-10.3	-10.2	455.4	6.5	-7.6	3	1	78.2	6	21	1	Good	Good	None	None	High	None
108	-9.0	-9.2	455.6	4.7	-5.9	7	1	116.3	9	20	1	Good	Good	Low	High	None	Low
109	-9.3	-9.2	457.5	2.9	-4.6	9	1	145.5	7	25	0	Good	Good	None	None	None	None
110	-8.8	-8.9	457.5	1.5	-3.5	7	0	100.7	11	19	0	Good	Good	High	High	None	High
111	-9.2	-9.8	458.1	4.6	-6.2	4	1	50.7	5	15	0	Good	Good	None	None	None	None
112	-8.3	-8.3	458.5	3.9	-4.8	8	0	107.6	8	23	0	Good	Good	High	None	None	None
113	-8.2	-8.3	458.6	5.6	-6.9	7	1	103.6	12	17	1	Good	Good	None	None	High	High
114	-7.8	-8.1	458.6	5.8	-6.9	7	1	103.6	13	17	1	Good	Good	None	None	None	High
115	-9.9	-9.8	458.9	4.7	-6.5	5	1	74.9	6	23	1	Good	Good	None	High	None	None
116	-9.7	-9.5	458.9	4.9	-7.6	6	1	94.3	7	23	1	Good	Good	None	None	None	None
117	-9.4	-9.4	458.9	4.9	-7.6	6	1	94.3	7	23	1	Good	Good	None	None	None	None
118	-8.3	-8.2	460.6	4.9	-6.3	8	1	112.8	12	17	1	Good	Good	None	None	None	None
119	-7.9	-8.1	460.6	4.7	-6.5	8	1	112.8	11	17	1	Good	Good	None	None	None	None
120	-7.8	-7.9	460.6	4.8	-6.4	8	1	112.8	12	17	1	Good	Good	None	None	None	None
121	-8.3	-8.3	460.6	4.7	-6.5	8	1	112.8	11	17	1	Good	Good	None	None	None	None
122	-7.8	-7.8	460.6	4.8	-6.4	8	1	112.8	12	17	1	Good	Good	None	None	None	None
123	-8.0	-8.2	460.6	4.7	-6.5	8	1	112.8	11	17	1	Good	Good	None	None	None	None
124	-9.2	-9.6	461.4	6.3	-7.3	5	1	85.2	7	23	1	Good	Good	None	None	None	None
125	-9.9	-9.9	461.5	1.8	-4.1	9	1	98.1	7	25	0	Good	Good	None	None	High	None
126	-10.6	-10.5	463.3	6.7	-7.9	5	1	68.3	5	29	1	Good	Good	None	High	High	None
127	-10.8	-10.7	463.3	6.0	-7.3	6	1	73.0	4	29	1	Good	Good	None	High	High	Low
128	-10.7	-10.7	464.6	2.9	-3.0	7	0	67.7	4	30	0	Good	Good	None	None	None	Low
129	-10.3	-9.8	464.6	5.2	-5.4	5	1	74.9	6	22	1	Good	Good	None	None	None	None
130	-10.5	-10.6	465.3	4.4	-5.9	5	1	93.3	7	19	0	Good	Good	None	None	None	High
131	-10.5	-10.6	465.3	4.4	-5.9	5	1	93.3	7	19	0	Good	Good	None	None	None	High
132	-10.5	-9.7	466.0	2.7	-5.2	9	0	116.9	6	28	0	Good	Good	None	None	None	None
133	-9.5	-12.3	466.6	3.8	-5.0	8	3	130.6	8	24	0	Good	Good	None	None	None	None

134	-9.4	-9.7	467.6	0.9	-3.6	8	2	74.9	8	25	0	Good	Good	None	None	Low	None
135	-9.6	-10.4	467.7	6.2	-5.4	3	1	52.3	9	24	1	Good	Good	None	None	High	Low
136	-8.2	-8.4	467.7	6.2	-5.9	4	1	59.8	12	18	1	Good	Good	None	None	None	None
137	-9.7	-10.6	468.3	5.9	-8.7	8	3	135.5	7	20	0	Good	Good	None	High	High	Low
138	-7.9	-7.7	468.7	9.6	-7.7	4	2	58.2	20	12	1	Good	Good	None	None	None	High
139	-9.7	-9.7	469.0	5.5	-8.0	6	1	94.3	7	23	1	Good	Good	None	None	High	Low
140	-10.4	-10.4	470.0	3.4	-4.9	6	0	80.7	5	27	0	Good	Good	None	None	None	None
141	-10.2	-10.2	470.2	5.4	-6.5	4	1	85.6	3	23	1	Good	Good	High	None	None	None
142	-10.4	-10.2	471.6	5.0	-5.7	7	1	85.8	10	24	1	Good	Good	None	None	High	None
143	-8.7	-8.7	471.6	4.9	-5.3	7	3	120.8	15	17	1	Good	Good	None	None	High	High
144	-8.3	-7.8	472.6	4.3	-5.1	8	0	107.6	9	23	0	Good	Good	None	None	Low	None
145	-9.6	-9.8	473.3	4.5	-6.1	6	1	67.4	5	25	0	Good	Good	Low	None	None	High
146	-8.7	-8.3	474.1	4.2	-5.9	5	1	59.9	6	15	0	Good	Good	Low	None	High	None
147	-9.2	-9.2	474.3	3.8	-6.0	7	0	84.2	10	18	0	Good	Good	None	None	None	High
148	-10.4	-10.6	474.6	5.5	-6.7	6	2	76.7	8	22	1	Good	Good	None	None	None	None
149	-8.0	-8.1	474.6	4.4	-5.7	7	0	123.7	8	23	0	Good	Good	None	None	None	None
150	-7.8	-8.0	474.6	5.2	-6.7	8	1	112.8	13	17	1	Good	Good	None	None	None	None
151	-8.1	-7.7	474.6	5.1	-6.8	8	1	112.8	12	17	1	Good	Good	None	None	None	None
152	-8.2	-8.2	474.6	5.2	-6.8	8	1	112.8	12	17	1	Good	Good	None	None	None	None
153	-8.5	-8.4	474.6	5.3	-6.6	8	1	112.8	13	17	1	Good	Good	None	None	None	High
154	-9.8	-9.2	475.4	4.1	-7.0	6	1	81.2	7	23	1	Good	Good	None	None	None	None
155	-9.5	-9.9	476.5	3.3	-6.3	9	2	118.1	9	26	0	Good	Good	None	None	None	None
156	-8.6	-8.0	476.6	0.8	-4.5	11	2	165.9	8	21	1	Good	Good	None	None	None	None
157	-10.1	-10.3	476.6	3.4	-4.9	8	0	135.6	6	25	0	Good	Good	None	None	None	None
158	-9.6	-9.5	476.9	5.0	-7.9	6	1	94.3	7	23	1	Good	Good	None	None	None	None
159	-8.5	-8.6	477.6	4.0	-5.4	6	2	94.9	9	25	0	Good	Good	None	None	Low	None
160	-9.6	-9.6	477.6	5.7	-7.4	7	2	106.4	10	24	1	Good	Good	None	None	High	None
161	-10.0	-9.7	477.6	5.6	-7.5	7	2	106.4	9	24	1	Good	Good	None	None	None	None

162	-10.3	-10.3	478.0	4.0	-4.7	8	0	72.1	5	28	1	Good	Good	None	None	None	None
163	-10.2	-9.7	478.6	4.0	-4.1	9	2	119.4	6	25	0	Good	Good	High	High	None	None
164	-9.2	-9.3	478.6	5.9	-6.4	7	0	102.7	9	25	1	Good	Good	None	High	None	High
165	-9.5	-9.7	479.6	2.6	-6.7	9	1	127.0	8	25	0	Good	Good	None	None	High	Low
166	-10.0	-10.1	479.6	3.8	-7.7	6	0	89.2	8	24	0	Good	Good	None	None	Low	High
167	-11.1	-10.8	479.6	2.9	-5.8	6	3	103.2	7	25	0	Good	Good	None	High	None	Low
168	-10.3	-11.8	479.6	4.9	-6.9	8	3	126.6	8	24	1	Good	Good	None	None	None	None
169	-10.3	-11.8	479.6	4.9	-6.9	8	3	126.6	8	24	1	Good	Good	None	None	None	None
170	-9.2	-9.0	480.5	2.5	-4.3	9	1	125.0	6	27	0	Good	Good	High	None	None	None
171	-9.7	-9.7	480.5	2.5	-4.3	9	1	125.0	6	27	0	Good	Good	High	None	None	None
172	-10.0	-10.1	480.9	4.6	-6.8	5	1	74.9	6	23	1	Good	Good	None	None	None	None
173	-11.0	-10.9	481.3	6.1	-7.6	6	1	73.0	4	29	1	Good	Good	None	High	High	Low
174	-9.8	-9.4	483.6	2.0	-4.9	9	1	110.7	7	27	0	Good	Good	None	None	Low	None
175	-9.5	-9.4	483.6	4.9	-5.2	7	3	112.9	11	21	0	Good	Good	None	None	None	High
176	-10.7	-10.8	485.6	5.2	-6.4	7	2	121.3	5	30	1	Good	Good	None	None	Low	None
177	-9.1	-8.7	485.6	2.8	-3.0	10	1	153.0	8	24	0	Good	Good	None	High	Low	None
178	-10.1	-11.6	485.6	2.7	-3.8	7	2	141.9	7	24	0	Good	Good	None	None	None	None
179	-9.8	-10.7	486.6	3.6	-5.7	7	1	84.9	8	27	0	Good	Good	None	None	Low	Low
180	-10.7	-10.8	486.6	3.6	-5.7	7	1	84.9	8	27	0	Good	Good	None	None	Low	Low
181	-9.7	-9.8	486.6	2.9	-4.3	8	1	85.2	10	28	0	Good	Good	None	None	None	None
182	-9.4	-9.6	487.0	4.4	-5.9	6	2	130.3	6	24	1	Good	Good	None	High	None	Low
183	-9.4	-9.7	488.1	1.1	-4.0	8	2	74.9	8	25	0	Good	Good	None	None	None	None
184	-10.7	-10.2	488.6	4.4	-6.7	8	0	110.8	7	29	0	Good	Good	None	None	High	Low
185	-8.5	-8.3	488.7	5.6	-7.0	8	1	112.8	13	17	1	Good	Good	None	None	None	High
186	-7.8	-8.0	488.7	5.7	-6.9	8	1	112.8	14	17	1	Good	Good	None	None	None	High
187	-8.1	-8.2	488.7	5.6	-7.1	8	1	112.8	13	17	1	Good	Good	None	None	None	None
188	-10.6	-9.8	489.4	5.6	-7.2	5	1	74.9	6	23	1	Good	Good	None	High	None	Low
189	-8.9	-12.7	489.6	5.2	-6.2	5	2	85.7	10	25	1	Good	Good	High	High	None	Low

190	-10.7	-10.8	490.5	3.4	-5.6	7	1	84.9	8	27	0	Good	Good	None	None	None	None
191	-10.7	-10.5	490.6	5.9	-8.2	6	0	125.7	7	29	1	Good	Good	High	Low	None	None
192	-8.8	-8.8	490.6	5.4	-4.7	4	1	31.5	14	16	1	Good	Good	None	None	None	Low
193	-9.6	-9.1	490.7	5.4	-5.8	6	0	78.9	9	23	0	Good	Good	None	None	None	None
194	-9.5	-9.5	490.7	5.9	-5.6	7	0	67.2	10	25	1	Good	Good	None	None	High	High
195	-10.9	-11.0	491.4	6.7	-7.8	6	1	73.0	5	29	1	Good	Good	Low	High	High	Low
196	-9.7	-9.8	491.6	2.9	-4.3	7	1	69.5	10	24	0	Good	Good	None	None	None	High
197	-10.1	-10.1	491.7	6.1	-7.8	7	2	106.4	10	24	1	Good	Good	None	None	High	None
198	-10.2	-10.1	491.7	6.0	-7.9	7	2	106.4	9	24	1	Good	Good	None	None	None	Low
199	-9.7	-9.7	491.7	6.1	-7.8	7	2	106.4	10	24	1	Good	Good	None	None	High	Low
200	-9.7	-9.8	491.7	6.1	-7.8	7	2	106.4	10	24	1	Good	Good	None	None	High	None
201	-10.6	-10.6	491.7	6.0	-7.9	7	2	106.4	9	24	1	Good	Good	None	None	None	None
202	-9.7	-9.7	491.7	6.0	-7.9	7	2	106.4	9	24	1	Good	Good	None	None	None	None
203	-9.9	-9.9	491.7	4.8	-5.5	5	1	115.3	9	25	1	Good	Good	None	None	None	None
204	-10.0	-10.0	492.0	3.2	-4.5	8	1	91.0	8	25	0	Good	Good	None	None	None	None
205	-10.0	-10.0	492.0	3.2	-4.5	8	1	91.0	8	25	0	Good	Good	None	None	None	None
206	-11.0	-10.7	492.4	7.1	-10.0	4	1	46.9	8	25	1	Good	Good	High	High	None	None
207	-8.8	-9.5	492.6	3.2	-5.2	8	2	121.3	8	25	0	Good	Good	None	None	None	None
208	-10.5	-10.1	492.6	4.4	-4.4	9	2	119.4	6	25	0	Good	Good	High	High	None	None
209	-10.7	-10.5	493.3	5.9	-7.3	7	1	82.2	5	29	1	Good	Good	None	High	High	Low
210	-9.6	-9.7	493.6	3.1	-4.4	7	1	69.5	10	23	0	Good	Good	None	None	None	None
211	-9.6	-9.5	493.6	5.2	-7.2	8	2	115.6	10	24	1	Good	Good	None	None	None	None
212	-10.5	-11.9	493.6	5.2	-7.3	8	3	126.6	8	24	1	Good	Good	None	None	None	High
213	-9.5	-9.5	493.6	5.2	-7.2	8	2	115.6	10	24	1	Good	Good	None	None	None	None
214	-11.2	-11.5	494.5	5.8	-8.9	7	1	107.7	7	29	1	Good	Good	None	High	None	None
215	-8.9	-8.8	494.6	2.2	-3.5	9	1	94.4	12	23	0	Good	Good	None	None	None	None
216	-9.0	-8.9	494.6	3.0	-4.6	9	1	125.0	7	27	0	Good	Good	None	None	Low	None
217	-9.8	-10.9	494.6	4.3	-5.7	8	0	147.5	8	28	0	Good	Good	None	None	None	None

218	-10.9	-11.1	495.6	4.2	-3.4	8	0	96.8	3	32	0	Good	Good	High	High	None	None
219	-8.7	-8.6	495.8	5.0	-5.7	4	2	55.0	13	18	1	Good	Good	None	None	None	None
220	-8.9	-9.1	496.6	2.9	-5.2	8	2	121.3	8	25	0	Good	Good	None	None	None	None
221	-9.9	-10.0	496.6	4.0	-6.4	8	2	139.0	8	26	1	Good	Good	None	None	None	High
222	-9.7	-9.8	496.6	4.0	-6.4	8	2	139.0	8	26	1	Good	Good	None	None	None	High
223	-10.6	-10.4	496.6	3.6	-4.7	8	1	89.1	11	28	0	Good	Good	None	None	None	None
224	-9.7	-9.0	497.1	6.3	-6.4	6	0	88.5	9	23	1	Good	Good	None	None	None	High
225	-10.5	-10.3	497.8	7.3	-8.6	5	1	68.3	5	29	1	Good	Good	None	High	High	None
226	-10.8	-10.9	497.8	6.6	-8.1	6	1	73.0	4	29	1	Good	Good	None	High	High	Low
227	-9.2	-9.3	498.2	5.3	-6.4	5	1	59.9	7	15	1	Good	Good	Low	None	High	None
228	-8.1	-8.1	498.4	3.0	-4.0	7	0	96.7	8	20	0	Good	Good	None	None	None	Low
229	-10.3	-10.4	498.9	4.7	-7.1	5	1	74.9	6	23	1	Good	Good	None	None	None	None
230	-10.0	-9.8	499.6	5.8	-5.9	7	2	91.6	10	27	1	Good	Good	None	None	None	High
231	-8.3	-8.1	500.6	5.1	-5.7	8	0	107.6	11	23	2	Good	Good	High	None	None	None
232	-11.3	-10.6	501.9	6.1	-8.8	8	3	135.5	8	20	1	Good	Good	None	None	Low	High
233	-10.5	-10.5	502.1	7.4	-10.6	4	1	71.7	7	26	2	Good	Good	None	None	High	None
234	-10.3	-10.2	502.4	6.5	-7.8	6	0	103.4	7	23	2	Good	Good	High	None	None	None
235	-8.4	-8.3	502.7	6.0	-7.3	8	1	112.8	14	17	2	Good	Good	None	None	None	High
236	-8.3	-7.9	502.7	6.2	-7.2	8	1	112.8	15	17	2	Good	Good	None	None	None	High
237	-8.4	-8.3	502.7	6.1	-7.3	8	1	112.8	14	17	2	Good	Good	None	None	None	High
238	-9.6	-9.6	503.4	5.0	-7.7	6	1	94.3	7	23	2	Good	Good	None	None	None	None
239	-10.0	-11.1	503.6	5.1	-8.0	10	2	144.6	9	25	1	Good	Good	None	None	Low	None
240	-10.1	-8.8	503.7	6.2	-6.4	6	2	102.8	13	23	2	Good	Good	None	None	High	High
241	-9.9	-10.0	504.6	2.4	-6.0	7	0	151.9	6	28	2	Good	Good	None	None	Low	None
242	-11.4	-11.0	505.4	7.2	-8.2	6	1	73.0	5	29	2	Good	Good	None	High	High	Low
243	-9.6	-9.4	505.6	6.9	-10.8	4	0	126.6	8	23	2	Good	Good	None	None	None	None
244	-9.2	-9.3	505.6	4.8	-6.0	6	2	94.9	11	25	1	Good	Good	High	High	None	Low
245	-10.2	-10.2	505.7	6.4	-8.1	7	2	106.4	10	24	2	Good	Good	None	None	High	High

246	-10.2	-10.6	505.7	6.3	-8.2	7	2	106.4	9	24	2	Good	Good	None	None	None	High
247	-9.6	-9.6	506.3	3.7	-5.4	8	1	136.2	6	25	1	Good	Good	High	None	None	None
248	-12.1	-12.1	506.7	8.0	-7.1	3	1	32.3	5	30	2	Good	Good	High	Low	None	None
249	-10.8	-11.0	507.1	5.4	-6.4	7	1	103.1	8	28	2	Good	Good	None	None	None	None
250	-10.8	-11.0	507.1	5.4	-6.4	7	1	103.1	8	28	2	Good	Good	None	None	None	None
251	-10.5	-10.3	507.7	5.6	-7.6	8	3	126.6	9	24	2	Good	Good	None	None	None	High
252	-9.4	-9.3	507.7	5.6	-7.5	8	2	115.6	11	24	2	Good	Good	None	None	None	None
253	-9.9	-9.9	507.7	5.5	-7.5	8	2	115.6	10	24	2	Good	Good	None	None	None	None
254	-9.9	-9.9	507.7	5.5	-7.5	8	2	115.6	10	24	2	Good	Good	None	None	None	None
255	-11.3	-11.5	508.6	6.1	-9.2	7	1	107.7	7	29	2	Good	Good	None	High	None	None
256	-11.2	-11.4	508.6	6.1	-9.2	7	1	107.7	7	29	2	Good	Good	None	High	None	None
257	-10.7	-11.5	508.6	6.1	-9.2	7	1	107.7	7	29	2	Good	Good	None	High	None	None
258	-10.3	-9.8	508.6	2.1	-6.0	7	0	151.9	6	28	2	Good	Good	None	None	Low	None
259	-9.8	-9.7	509.6	4.8	-6.9	9	3	135.8	10	24	2	Low	Low	None	None	None	None
260	-9.5	-9.3	511.5	3.5	-5.2	5	2	83.9	7	24	2	Good	Good	High	None	None	None
261	-9.7	-9.6	512.6	3.3	-4.3	9	1	98.3	12	28	1	Good	Good	None	None	None	None
262	-9.2	-9.4	512.7	6.1	-6.3	6	0	112.0	13	26	2	Good	Good	None	None	Low	None
263	-9.2	-9.4	512.7	6.1	-6.3	6	0	112.0	13	26	2	Good	Good	None	None	Low	None
264	-10.1	-10.0	513.4	3.8	-5.5	9	1	95.5	5	22	1	Good	Good	None	None	None	None
265	-9.7	-9.6	513.5	5.6	-8.1	6	1	94.3	7	23	2	Good	Good	None	None	High	Low
266	-12.0	-11.9	513.6	5.3	-8.5	9	1	114.9	7	29	2	Good	Good	High	None	None	High
267	-9.5	-9.4	513.6	2.3	-3.5	10	1	111.2	12	28	1	Good	Good	None	None	None	None
268	-9.5	-9.4	513.6	2.3	-3.5	10	1	111.2	12	28	1	Good	Good	None	None	None	None
269	-10.4	-10.4	513.6	3.3	-4.9	10	1	119.0	8	31	1	Good	Good	None	None	Low	None
270	-10.0	-9.8	514.0	5.9	-7.2	6	0	82.6	10	27	2	Good	Good	None	None	None	None
271	-10.5	-10.4	514.6	3.5	-5.3	8	0	115.2	5	35	1	Good	Good	None	None	None	None
272	-8.2	-8.2	514.6	5.5	-6.0	8	0	107.6	12	23	2	Good	Good	None	None	Low	None
273	-10.7	-10.3	516.6	4.1	-5.6	9	1	102.2	10	27	2	Good	Good	None	None	None	None

274	-10.2	-10.2	516.6	3.0	-4.3	9	1	98.3	11	28	1	Good	Good	None	None	None	None
275	-9.6	-9.6	516.6	2.9	-4.2	9	1	94.4	12	28	1	Good	Good	None	None	None	None
276	-9.5	-9.4	516.7	7.5	-6.5	5	1	51.4	6	18	2	Good	Good	High	None	Low	Low
277	-8.2	-8.1	516.7	5.6	-6.6	7	0	123.7	11	23	2	Good	Good	None	None	None	None
278	-8.4	-8.5	516.7	6.5	-7.6	8	1	112.8	15	17	2	Good	Good	None	None	None	High
279	-8.0	-8.1	516.7	6.6	-7.5	8	1	112.8	16	17	2	Good	Good	None	None	None	High
280	-9.7	-9.5	517.7	1.5	-4.2	9	2	95.6	12	28	1	Good	Good	None	None	None	None
281	-9.4	-9.8	517.7	7.3	-6.9	6	1	85.2	9	23	2	Good	Good	None	None	None	None
282	-10.8	-10.2	517.8	6.4	-7.8	7	0	85.3	4	30	2	Good	Good	High	None	None	None
283	-8.8	-8.6	519.1	6.1	-6.8	7	0	98.4	10	23	2	Good	Good	None	None	None	None
284	-11.0	-10.7	519.4	7.6	-8.4	6	1	73.0	7	29	2	Good	Good	High	High	High	Low
285	-11.0	-10.7	519.4	7.6	-8.4	6	1	73.0	7	29	2	Good	Good	High	High	High	Low
286	-9.6	-9.6	519.5	5.5	-6.4	6	2	76.7	11	16	2	Good	Good	None	None	None	None
287	-9.1	-8.8	519.5	1.8	-4.2	10	2	149.7	11	22	1	Low	Low	None	None	None	None
288	-11.6	-11.6	519.6	5.5	-6.2	7	1	85.8	10	30	2	Good	Good	None	None	Low	None
289	-10.0	-10.0	519.7	6.9	-8.4	7	2	106.4	11	24	2	Good	Good	None	None	None	High
290	-10.0	-9.3	519.9	5.5	-8.2	6	1	94.3	7	23	2	Good	Good	None	None	None	None
291	-9.9	-9.8	520.7	4.4	-4.7	8	1	113.4	11	28	1	Good	Good	None	None	None	None
292	-8.6	-9.2	521.6	4.3	-5.7	7	2	104.2	11	25	1	Good	Good	High	High	None	Low
293	-10.3	-10.3	521.7	5.9	-7.9	8	2	115.6	10	24	2	Good	Good	None	None	None	High
294	-9.4	-9.2	521.7	6.1	-7.7	8	2	115.6	12	24	2	Good	Good	None	None	None	None
295	-9.6	-9.6	521.7	6.1	-7.7	8	2	115.6	12	24	2	Good	Good	None	None	High	None
296	-9.9	-9.8	521.7	6.0	-7.9	8	2	115.6	11	24	2	Good	Good	None	None	None	None
297	-11.4	-11.4	522.6	6.7	-9.4	7	1	107.7	9	29	2	Good	Good	None	High	None	None
298	-8.6	-8.9	522.7	5.8	-7.4	8	1	112.8	13	23	2	Good	Good	None	None	None	None
299	-10.7	-10.5	523.5	6.1	-8.8	5	1	86.4	5	24	2	Good	Good	None	High	None	None
300	-9.6	-9.6	523.7	5.1	-7.2	9	2	124.8	11	24	2	Good	Good	None	None	None	None
301	-10.1	-10.3	524.6	3.8	-7.4	11	3	172.4	9	26	3	Good	Good	None	None	None	None

302	-10.1	-10.3	524.6	3.8	-7.4	11	3	172.4	9	26	3	Good	Good	None	None	None	None
303	-10.6	-10.2	524.7	6.0	-6.2	7	0	67.2	9	31	2	Good	Good	None	None	High	Low
304	-9.2	-8.9	527.4	3.6	-6.4	10	2	137.1	8	22	1	Good	Good	High	High	High	High
305	-9.5	-9.5	527.5	4.2	-6.1	9	1	95.5	7	22	1	Good	Good	None	None	None	None
306	-10.4	-10.7	528.6	3.9	-5.4	10	2	126.4	8	31	2	Good	Good	None	None	Low	None
307	-9.8	-9.3	529.1	5.6	-7.6	8	1	112.8	11	23	2	Good	Good	None	None	None	None
308	-9.3	-9.4	529.6	5.7	-5.9	8	2	100.8	11	27	2	Good	Good	None	None	None	High
309	-9.8	-9.9	530.6	3.4	-4.6	9	1	98.3	12	28	1	Good	Good	None	None	None	None
310	-9.8	-9.6	530.6	5.2	-6.3	8	1	86.3	11	26	2	Good	Good	None	None	None	None
311	-9.8	-9.3	530.6	4.5	-5.3	8	1	86.3	11	26	1	Good	Good	None	None	None	None
312	-9.9	-10.3	530.7	3.2	-4.4	9	1	94.4	12	28	1	Good	Good	None	None	None	None
313	-9.9	-10.3	530.7	3.2	-4.4	9	1	94.4	12	28	1	Good	Good	None	None	None	None
314	-10.1	-9.9	530.7	3.2	-4.6	9	1	94.4	11	28	1	Good	Good	None	None	None	None
315	-8.2	-8.2	530.7	7.1	-7.7	8	1	112.8	17	17	2	Good	Good	None	None	None	High
316	-8.2	-8.2	530.7	7.1	-7.7	8	1	112.8	17	17	2	Good	Good	None	None	None	High
317	-10.3	-9.8	531.7	1.9	-4.4	9	2	95.6	12	28	1	Good	Good	None	None	None	None
318	-8.4	-9.6	534.1	6.5	-5.5	6	1	65.4	14	24	2	Good	Good	None	None	None	None
319	-9.5	-9.4	535.7	6.5	-8.0	8	2	115.6	13	24	2	Good	Good	None	None	None	High
320	-9.5	-9.4	535.7	6.5	-8.0	8	2	115.6	13	24	2	Good	Good	None	None	None	High
321	-9.4	-9.2	535.7	6.5	-8.0	8	2	115.6	13	24	2	Good	Good	None	None	None	High
322	-9.4	-9.5	535.7	6.4	-8.1	8	2	115.6	12	24	2	Good	Good	None	None	None	High
323	-10.1	-10.2	535.7	6.3	-8.2	8	2	115.6	11	24	2	Good	Good	None	None	None	High
324	-10.0	-10.1	535.7	6.3	-8.1	8	2	115.6	11	24	2	Good	Good	None	None	None	High
325	-10.8	-10.3	537.1	6.3	-6.0	7	0	79.5	11	27	2	Good	Good	None	None	High	Low
326	-10.0	-9.9	538.7	3.6	-4.4	9	1	94.4	12	29	1	Good	Good	None	None	None	None
327	-10.1	-11.6	539.2	6.0	-7.4	6	1	69.3	7	24	2	Good	Good	High	High	High	None
328	-10.1	-11.6	539.2	6.0	-7.4	6	1	69.3	7	24	2	Good	Good	High	High	High	None
329	-9.8	-9.3	541.7	7.1	-5.7	6	1	65.4	15	24	2	Good	Good	None	None	None	High

330	-10.0	-9.9	544.6	5.5	-6.6	8	1	86.3	11	26	2	Good	Good	None	High	None	None
331	-11.3	-11.5	544.7	5.5	-6.0	4	2	42.4	10	28	2	Good	Good	None	None	None	None
332	-11.3	-11.5	544.7	5.5	-6.0	4	2	42.4	10	28	2	Good	Good	None	None	None	None
333	-10.3	-12.0	550.0	6.5	-7.0	7	1	90.9	8	31	2	Good	Good	None	None	None	High
334	-9.3	-9.4	552.3	7.8	-7.9	4	1	50.7	8	15	2	Good	Good	None	Low	Low	Low
335	-9.3	-9.4	552.3	7.8	-7.9	4	1	50.7	8	15	2	Good	Good	None	Low	Low	Low
336	-9.3	-9.3	556.5	7.7	-9.6	6	0	102.4	9	25	2	Good	Good	None	High	High	High
337	-10.1	-10.8	556.6	3.7	-4.7	9	1	94.4	12	29	1	Good	Good	None	None	None	None
338	-9.6	-8.9	558.5	6.0	-7.9	6	1	124.5	7	25	2	Good	Good	High	High	None	Low
339	-9.4	-10.2	560.7	5.1	-5.0	8	3	118.0	12	26	2	Good	Good	None	None	None	None
340	-9.9	-9.5	562.4	5.8	-7.3	6	2	112.7	7	22	2	Good	Good	None	High	None	Low
341	-9.4	-9.3	566.5	7.2	-8.9	6	0	102.4	9	25	2	Good	Good	High	None	None	None
342	-11.0	-10.9	578.9	7.6	-7.7	5	0	65.5	10	26	2	Good	Good	High	None	None	None
343	-11.0	-10.9	578.9	7.6	-7.7	5	0	65.5	10	26	2	Good	Good	High	None	None	None
344	-10.7	-10.8	578.9	7.6	-7.7	5	0	65.5	10	26	2	Good	Good	High	None	None	None
345	-11.0	-10.4	582.8	6.9	-6.7	6	0	78.9	7	29	2	Good	Good	None	None	None	High
346	-11.0	-11.1	582.8	6.9	-6.7	6	0	78.9	7	29	2	Good	Good	None	None	None	High
347	-11.0	-11.1	582.8	6.9	-6.7	6	0	78.9	7	29	2	Good	Good	None	None	None	High
348	-11.6	-11.6	582.8	6.9	-6.7	6	0	78.9	7	29	2	Good	Good	None	None	None	High
349	-9.6	-9.2	587.0	12.4	-9.7	2	0	51.6	17	21	2	Good	Good	None	None	None	None
350	-11.3	-11.1	588.7	4.7	-7.0	11	0	120.3	4	36	2	Good	Good	None	None	None	None
351	-11.9	-12.0	588.8	5.3	-6.2	7	2	94.5	6	30	1	Good	Good	High	High	None	None
352	-12.0	-12.0	588.8	5.3	-6.2	7	2	94.5	6	30	1	Good	Good	High	High	None	None
353	-11.9	-12.0	588.8	5.3	-6.2	7	2	94.5	6	30	1	Good	Good	High	High	None	None
354	-12.0	-12.0	588.8	5.3	-6.2	7	2	94.5	6	30	1	Good	Good	High	High	None	None
355	-9.9	-10.0	591.5	6.7	-7.7	7	0	102.7	8	31	2	Good	Good	High	High	None	High
356	-12.0	-11.6	597.4	8.8	-9.9	3	1	38.3	4	34	2	Good	Good	High	High	High	High
357	-8.5	-8.6	608.3	8.3	-7.8	4	0	44.8	17	1	2	Good	Good	None	High	High	High

358	-7.5	-7.5	609.4	13.6	-9.0	4	0	52.6	33	5	2	Good	Good	High	High	High	High
359	-10.2	-10.0	620.7	5.4	-6.1	9	1	119.6	11	29	2	Good	Good	None	None	Low	None
360	-11.4	-11.4	628.8	7.4	-9.2	7	1	150.7	9	37	2	Good	Good	None	None	None	None
361	-10.2	-10.2	643.6	5.5	-8.2	4	0	47.9	6	19	2	Good	Good	None	None	None	High
362	-10.2	-10.3	644.8	2.3	-5.6	11	1	143.9	9	36	2	Good	Good	None	None	None	None
363	-10.2	-10.3	644.8	2.3	-5.6	11	1	143.9	9	36	2	Good	Good	None	None	None	None
364	-8.9	-9.1	648.8	5.5	-5.3	11	2	162.7	17	21	2	Low	Low	None	None	None	High
365	-8.8	-8.8	656.0	13.3	-11.2	4	3	69.6	27	20	2	Good	Good	High	High	None	High
366	-10.4	-10.7	690.1	6.4	-9.1	4	0	47.9	5	25	2	Good	Good	None	High	High	None
367	-11.6	-11.4	690.1	7.3	-10.4	8	2	118.7	12	32	2	Good	Good	High	High	Low	Low
368	-8.6	-9.4	708.6	11.1	-10.7	7	1	82.1	18	26	2	Good	Good	High	None	Low	High
369	-8.6	-9.0	728.9	5.2	-6.1	12	2	216.4	27	17	3	Low	Low	None	None	None	None
370	-8.6	-9.0	728.9	5.2	-6.1	12	2	216.4	27	17	3	Low	Low	None	None	None	None
371	-8.6	-9.0	728.9	5.2	-6.1	12	2	216.4	27	17	3	Low	Low	None	None	None	None
372	-8.6	-9.0	728.9	5.2	-6.1	12	2	216.4	27	17	3	Low	Low	None	None	None	None
373	-8.6	-9.0	728.9	5.2	-6.1	12	2	216.4	27	17	3	Low	Low	None	None	None	None
374	-8.2	-8.2	739.2	12.7	-7.6	7	7	141.6	31	3	3	Low	Low	None	None	None	High
375	-7.9	-8.0	739.2	12.7	-7.6	7	7	141.6	31	3	3	Low	Low	None	None	None	High
376	-12.4	-13.7	775.0	5.4	-10.4	10	8	160.9	5	44	3	Good	Good	None	High	High	None
377	-12.4	-13.7	775.0	5.4	-10.4	10	8	160.9	5	44	3	Good	Good	None	High	High	None
378	-8.7	-8.3	799.3	5.5	-9.6	13	1	169.7	10	48	3	Low	Low	None	None	High	None
379	-10.6	-9.9	863.4	22.1	-11.7	4	1	47.9	29	20	2	Good	Good	None	None	High	None
380	-10.6	-9.9	863.4	22.1	-11.7	4	1	47.9	29	20	2	Good	Good	None	None	High	None
381	-9.9	-10.0	863.4	22.1	-10.9	4	0	52.6	31	18	2	Good	Good	None	None	None	None

Notes: (i) Rapamycin crystallographic structure; (ii) Rapamycin docking structure; cLogP: logarithm of the partition coefficient between n-octanol and water log (coctanol/cwater); LogS: logarithm of the solubility measured in mol/L; HBD: Hydrogen Bound Donor; HBA: Hydrogen Bound Acceptor; tPSA: Topological Polar Surface Area in $Å^2$; RotB: Rotable Bounds; RigB: Rigid Bounds.

Supplemental Material 3

RMSF values from each residue of the simulated systems.

			System (FKBP12:X:FRB)									
RESIDUE	**POCKET**	**FKBP12:FRB**	**i**	**ii**	**A**	**B**	**C**	**D**	**E**	**F**	**G**	**H**
GLY1	No	2.62	0.35	0.19	0.22	0.19	0.34	0.28	0.20	0.40	0.46	0.21
VAL2	No	2.28	0.20	0.21	0.20	0.21	0.35	0.26	0.24	0.31	0.28	0.20
GLN3	No	2.62	0.21	0.18	0.21	0.29	0.20	0.34	0.19	0.25	0.21	0.27
VAL4	No	1.96	0.20	0.18	0.18	0.26	0.20	0.25	0.22	0.28	0.20	0.40
GLU5	No	2.21	0.26	0.24	0.26	0.25	0.35	0.21	0.22	0.40	0.33	0.34
THR6	No	1.92	0.22	0.21	0.20	0.30	0.24	0.23	0.25	0.33	0.22	0.39
ILE7	No	2.02	0.24	0.20	0.24	0.30	0.29	0.37	0.30	0.32	0.33	0.29
SER8	No	3.07	0.25	0.21	0.20	0.29	0.18	0.21	0.24	0.26	0.23	0.19
PRO9	No	3.82	0.29	0.25	0.20	0.20	0.25	0.32	0.27	0.21	0.27	0.22
GLY10	No	4.85	0.24	0.27	0.28	0.26	0.17	0.57	0.23	0.20	0.21	0.19
ASP11	No	6.41	0.23	0.21	0.34	0.38	0.19	0.20	0.17	0.26	0.24	0.26
GLY12	No	5.39	0.26	0.24	0.36	0.46	0.21	0.21	0.19	0.30	0.20	0.17
ARG13	No	6.30	0.38	0.31	0.42	0.29	0.21	0.37	0.27	0.26	0.23	0.22
THR14	No	4.33	0.28	0.21	0.87	0.20	0.19	0.17	0.18	0.27	0.27	0.18
PHE15	No	4.24	0.29	0.29	0.38	0.21	0.22	0.25	0.25	0.28	0.30	0.23
PRO16	No	4.39	0.27	0.23	0.27	0.21	0.21	0.17	0.23	0.30	0.20	0.24
LYS17	No	4.99	0.35	0.23	0.46	0.28	0.22	0.27	0.35	0.25	0.28	0.26
ARG18	No	5.89	0.26	0.19	0.27	0.25	0.29	0.34	0.25	0.39	0.28	0.35
GLY19	No	4.78	0.19	0.26	0.23	0.23	0.29	0.25	0.23	0.21	0.15	0.16
GLN20	No	4.25	0.20	0.21	0.21	0.28	0.23	0.32	0.29	0.23	0.23	0.21
THR21	Yes	3.71	0.19	0.21	0.22	0.22	0.23	0.25	0.28	0.34	0.20	0.19
CYS22	No	3.07	0.21	0.19	0.23	0.25	0.23	0.25	0.25	0.30	0.22	0.26
VAL23	No	2.24	0.16	0.19	0.17	0.20	0.17	0.18	0.23	0.19	0.21	0.18
VAL24	No	1.83	0.15	0.18	0.17	0.22	0.21	0.20	0.16	0.19	0.20	0.18
HIS25	No	1.76	0.16	0.31	0.23	0.43	0.31	0.59	0.23	0.34	0.25	0.18
TYR26	Yes	2.34	0.21	0.19	0.26	0.21	0.31	0.26	0.25	0.24	0.19	0.15
THR27	No	1.54	0.23	0.23	0.26	0.20	0.26	0.33	0.21	0.20	0.24	0.20
GLY28	No	1.83	0.14	0.15	0.26	0.17	0.19	0.23	0.21	0.22	0.23	0.16
MET29	No	2.03	0.21	0.46	0.37	0.33	0.26	0.31	0.30	0.61	0.32	0.51
LEU30	No	2.59	0.18	0.21	0.25	0.19	0.20	0.21	0.25	0.26	0.21	0.23
GLU31	No	3.15	0.22	0.26	0.28	0.20	0.25	0.36	0.44	0.38	0.26	0.26
ASP32	No	3.26	0.19	0.20	0.32	0.19	0.16	0.20	0.23	0.41	0.24	0.18
GLY33	No	3.24	0.15	0.24	0.36	0.19	0.21	0.18	0.35	0.45	0.22	0.22
LYS34	No	3.36	0.17	0.32	0.35	0.19	0.33	0.25	0.32	0.34	0.21	0.46
LYS35	No	2.88	0.19	0.31	0.35	0.25	0.32	0.23	0.26	0.20	0.25	0.21
PHE36	Yes	2.79	0.19	0.30	0.31	0.28	0.26	0.18	0.25	0.20	0.25	0.21
ASP37	Yes	2.77	0.21	0.34	0.28	0.28	0.37	0.29	0.33	0.23	0.28	0.18
SER38	No	2.31	0.19	0.35	0.31	0.33	0.22	0.27	0.20	0.22	0.20	0.17
SER39	No	2.30	0.22	0.28	0.23	0.20	0.36	0.34	0.32	0.34	0.19	0.13
ARG40	No	3.64	0.18	0.29	0.28	0.20	0.31	0.26	0.24	0.27	0.21	0.17
ASP41	No	3.52	0.21	0.30	0.32	0.35	0.28	0.23	0.21	0.20	0.25	0.27
ARG42	Yes	4.40	0.31	0.33	0.64	0.61	0.28	0.31	0.49	0.30	0.51	0.43
ASN43	No	5.36	0.23	0.31	0.36	0.33	0.30	0.23	0.34	0.25	0.39	0.23
LYS44	Yes	4.71	0.23	0.31	0.20	0.55	0.28	0.18	0.26	0.18	0.42	0.27
PRO45	Yes	3.27	0.20	0.20	0.27	0.50	0.28	0.19	0.26	0.26	0.45	0.16
PHE46	Yes	2.64	0.18	0.19	0.34	0.25	0.27	0.23	0.36	0.34	0.45	0.22
LYS47	Yes	3.30	0.34	0.29	0.47	0.31	0.28	0.23	0.29	0.25	0.41	0.24
PHE48	Yes	3.55	0.21	0.20	0.24	0.37	0.21	0.22	0.26	0.31	0.26	0.23
MET49	Yes	4.49	0.22	0.21	0.25	0.25	0.64	0.43	0.37	0.18	0.21	0.27

LEU50	No	4.65	0.23	0.20	0.20	0.23	0.27	0.20	0.21	0.20	0.18	0.27
GLY51	No	5.59	0.22	0.29	0.27	0.21	0.28	0.32	0.57	0.48	0.19	0.48
LYS52	Yes	6.59	0.33	0.30	0.25	0.38	0.19	0.22	0.36	0.27	0.17	0.37
GLN53	Yes	5.79	0.19	0.26	0.28	0.22	0.20	0.21	0.43	0.30	0.25	0.28
GLU54	Yes	5.73	0.19	0.30	0.37	0.25	0.39	0.33	0.26	0.25	0.45	0.38
VAL55	Yes	3.70	0.18	0.57	0.20	0.26	0.31	0.29	0.20	0.29	0.27	0.39
ILE56	Yes	3.79	0.25	0.39	0.19	0.21	0.18	0.31	0.20	0.27	0.19	0.20
ARG57	No	3.36	0.28	0.30	0.25	0.21	0.26	0.29	0.25	0.29	0.22	0.24
GLY58	No	2.19	0.16	0.16	0.18	0.14	0.15	0.17	0.17	0.19	0.16	0.14
TRP59	Yes	2.57	0.21	0.21	0.29	0.17	0.26	0.34	0.25	0.36	0.23	0.19
GLU60	No	3.92	0.34	0.33	0.43	0.39	0.44	0.47	0.38	0.38	0.17	0.29
GLU61	No	3.27	0.31	0.28	0.29	0.22	0.20	0.33	0.38	0.25	0.26	0.22
GLY62	No	2.52	0.18	0.16	0.29	0.16	0.18	0.21	0.28	0.20	0.23	0.18
VAL63	No	2.83	0.21	0.17	0.31	0.21	0.22	0.26	0.21	0.29	0.20	0.24
ALA64	No	2.78	0.23	0.18	0.41	0.23	0.24	0.27	0.19	0.22	0.23	0.25
GLN65	No	4.13	0.28	0.34	0.33	0.29	0.33	0.32	0.28	0.19	0.54	0.38
MET66	No	2.77	0.21	0.20	0.28	0.22	0.19	0.22	0.20	0.23	0.20	0.24
SER67	No	2.76	0.19	0.18	0.27	0.20	0.15	0.22	0.22	0.23	0.17	0.30
VAL68	No	2.71	0.21	0.21	0.29	0.19	0.17	0.25	0.25	0.19	0.25	0.48
GLY69	No	2.18	0.40	0.21	0.25	0.19	0.18	0.23	0.22	0.21	0.29	0.37
GLN70	No	2.22	0.19	0.23	0.24	0.20	0.16	0.34	0.23	0.25	0.18	0.30
ARG71	No	2.25	0.32	0.26	0.34	0.28	0.21	0.19	0.25	0.29	0.22	0.46
ALA72	No	1.00	0.19	0.18	0.19	0.19	0.19	0.22	0.23	0.28	0.20	0.15
LYS73	No	1.78	0.18	0.27	0.18	0.23	0.27	0.37	0.22	0.32	0.24	0.24
LEU74	No	1.29	0.18	0.19	0.21	0.23	0.26	0.29	0.27	0.32	0.24	0.19
THR75	No	1.45	0.17	0.18	0.22	0.18	0.23	0.18	0.17	0.18	0.19	0.16
ILE76	No	1.35	0.17	0.17	0.20	0.15	0.47	0.18	0.17	0.21	0.19	0.17
SER77	No	1.76	0.19	0.19	0.27	0.19	0.23	0.19	0.16	0.25	0.20	0.20
PRO78	No	1.83	0.15	0.35	0.28	0.25	0.28	0.30	0.16	0.31	0.21	0.26
ASP79	No	2.69	0.17	0.37	0.29	0.50	0.27	0.48	0.23	0.33	0.44	0.82
TYR80	No	2.70	0.19	0.22	0.23	0.17	0.29	0.23	0.28	0.30	0.26	0.21
ALA81	No	2.20	0.15	0.29	0.24	0.17	0.27	0.18	0.27	0.27	0.22	0.22
TYR82	Yes	2.62	0.20	0.46	0.36	0.21	0.29	0.36	0.26	0.37	0.27	0.22
GLY83	No	2.43	0.19	0.31	0.27	0.19	0.22	0.20	0.20	0.51	0.21	0.23
ALA84	No	3.15	0.19	0.29	0.25	0.27	0.18	0.28	0.26	0.45	0.27	0.26
THR85	No	3.60	0.25	0.24	0.23	0.29	0.18	0.34	0.31	0.33	0.25	0.24
GLY86	No	4.20	0.28	0.29	0.23	0.28	0.16	0.32	0.29	0.25	0.32	0.26
HIS87	Yes	5.17	0.23	0.36	0.23	0.28	0.36	0.33	0.22	0.44	0.69	0.37
PRO88	No	4.57	0.35	0.26	0.42	0.38	0.25	0.46	0.28	0.36	0.41	0.46
GLY89	No	5.07	0.39	0.22	0.59	0.37	0.24	0.18	0.25	0.20	0.32	0.42
ILE90	Yes	3.74	0.24	0.26	0.49	0.37	0.37	0.18	0.31	0.18	0.39	0.48
ILE91	Yes	2.83	0.23	0.24	0.23	0.26	0.21	0.20	0.27	0.24	0.28	0.33
PRO92	No	2.86	0.23	0.23	0.20	0.27	0.18	0.27	0.27	0.21	0.25	0.34
PRO93	No	2.63	0.18	0.20	0.22	0.24	0.17	0.26	0.26	0.25	0.29	0.33
HIS94	No	2.49	0.21	0.27	0.25	0.35	0.25	0.33	0.30	0.38	0.28	0.46
ALA95	No	1.79	0.18	0.22	0.24	0.22	0.21	0.23	0.26	0.24	0.27	0.35
THR96	No	1.73	0.15	0.20	0.20	0.22	0.17	0.19	0.30	0.29	0.18	0.32
LEU97	No	1.51	0.17	0.17	0.19	0.17	0.18	0.18	0.20	0.22	0.17	0.21
VAL98	No	1.39	0.16	0.18	0.20	0.18	0.19	0.28	0.20	0.30	0.20	0.18
PHE99	Yes	1.37	0.17	0.24	0.20	0.18	0.21	0.36	0.26	0.34	0.21	0.21
ASP100	No	1.21	0.21	0.21	0.29	0.19	0.35	0.30	0.26	0.39	0.21	0.24
VAL101	No	1.12	0.17	0.18	0.22	0.21	0.22	0.26	0.50	0.49	0.23	0.16
GLU102	No	1.57	0.25	0.23	0.19	0.24	0.20	0.24	0.20	0.28	0.19	0.15
LEU103	No	2.08	0.21	0.20	0.23	0.18	0.18	0.18	0.20	0.18	0.19	0.20

LEU104	No	2.21	0.20	0.23	0.21	0.21	0.20	0.21	0.23	0.25	0.29	0.17
LYS105	No	3.01	0.27	0.36	0.25	0.31	0.29	0.33	0.33	0.28	0.43	0.18
LEU106	No	3.49	0.20	0.20	0.22	0.21	0.20	0.23	0.28	0.26	0.23	0.36
GLU107	Yes	4.02	0.35	0.30	0.44	0.28	0.23	0.29	0.34	0.35	0.27	0.19
ARG108	No	5.69	0.41	0.33	0.47	0.57	0.37	0.58	0.36	0.40	0.46	0.29
VAL109	No	4.03	0.26	0.37	0.36	0.34	0.50	0.41	0.30	0.46	0.31	0.29
ALA110	No	3.95	0.42	0.40	0.31	0.34	0.37	0.33	0.38	0.40	0.31	0.48
ILE111	No	4.23	0.35	0.38	0.21	0.32	0.37	0.23	0.23	0.35	0.40	0.24
LEU112	No	3.71	0.43	0.26	0.20	0.28	0.38	0.28	0.29	0.31	0.26	0.27
TRP113	No	2.76	0.24	0.25	0.29	0.26	0.27	0.22	0.25	0.34	0.27	0.18
HIS114	No	3.29	0.27	0.34	0.17	0.20	0.76	0.52	0.36	0.33	0.55	0.17
GLU115	No	3.62	0.24	0.20	0.18	0.30	0.29	0.22	0.36	0.23	0.27	0.36
MET116	No	3.08	0.46	0.51	0.37	0.54	0.38	0.43	0.40	0.33	0.59	0.43
TRP117	No	2.15	0.20	0.22	0.24	0.17	0.20	0.19	0.19	0.34	0.25	0.26
HIS118	No	3.26	0.20	0.15	0.27	0.24	0.19	0.17	0.19	0.16	0.22	0.20
GLU119	No	3.82	0.16	0.16	0.32	0.29	0.18	0.18	0.45	0.20	0.29	0.50
GLY120	No	2.66	0.13	0.14	0.17	0.19	0.16	0.20	0.13	0.16	0.25	0.21
LEU121	Yes	2.26	0.15	0.18	0.20	0.26	0.21	0.22	0.21	0.24	0.28	0.21
GLU122	Yes	3.65	0.29	0.20	0.27	0.43	0.34	0.34	0.41	0.33	0.35	0.26
GLU123	No	3.29	0.16	0.16	0.27	0.30	0.18	0.17	0.22	0.28	0.27	0.19
ALA124	No	2.30	0.14	0.16	0.16	0.14	0.14	0.15	0.15	0.26	0.17	0.17
SER125	Yes	2.70	0.19	0.25	0.23	0.25	0.20	0.19	0.23	0.58	0.24	0.18
ARG126	Yes	3.93	0.23	0.43	0.24	0.43	0.31	0.21	0.23	0.58	0.27	0.27
LEU127	No	3.00	0.23	0.23	0.24	0.19	0.19	0.21	0.22	0.24	0.27	0.17
TYR128	No	2.39	0.21	0.18	0.23	0.25	0.21	0.32	0.36	0.27	0.38	0.22
PHE129	Yes	2.96	0.26	0.27	0.25	0.33	0.27	0.40	0.29	0.38	0.31	0.27
GLY130	Yes	3.46	0.20	0.21	0.22	0.30	0.41	0.20	0.27	0.27	0.22	0.24
GLU131	No	4.19	0.23	0.21	0.20	0.39	0.32	0.26	0.44	0.33	0.25	0.23
ARG132	Yes	4.09	0.22	0.29	0.34	0.44	0.52	0.27	0.25	0.31	0.30	0.56
ASN133	No	3.10	0.17	0.18	0.36	0.19	0.32	0.15	0.26	0.29	0.37	0.15
VAL134	No	2.61	0.23	0.19	0.25	0.19	0.37	0.22	0.24	0.21	0.33	0.16
LYS135	No	3.86	0.33	0.28	0.21	0.17	0.30	0.16	0.40	0.27	0.29	0.22
GLY136	No	2.84	0.20	0.19	0.17	0.16	0.28	0.14	0.23	0.20	0.28	0.18
MET137	No	1.98	0.24	0.25	0.27	0.18	0.38	0.18	0.45	0.30	0.32	0.21
PHE138	No	2.55	0.27	0.38	0.30	0.52	0.50	0.34	0.42	0.30	0.54	0.26
GLU139	No	3.54	0.20	0.22	0.17	0.23	0.43	0.19	0.31	0.24	0.28	0.51
VAL140	No	2.84	0.25	0.44	0.56	0.32	0.37	0.30	0.33	0.44	0.49	0.36
LEU141	No	2.07	0.36	0.25	0.30	0.28	0.26	0.23	0.32	0.56	0.47	0.39
GLU142	No	2.90	0.19	0.24	0.18	0.25	0.23	0.16	0.25	0.26	0.44	0.18
PRO143	No	2.96	0.17	0.19	0.17	0.17	0.21	0.15	0.22	0.28	0.33	0.19
LEU144	No	2.47	0.36	0.25	0.21	0.22	0.25	0.22	0.23	0.40	0.29	0.21
HIS145	No	1.94	0.20	0.17	0.18	0.22	0.18	0.16	0.18	0.19	0.26	0.20
ALA146	No	2.84	0.19	0.17	0.23	0.18	0.19	0.17	0.16	0.23	0.24	0.13
MET147	No	3.39	0.26	0.24	0.30	0.19	0.20	0.57	0.18	0.45	0.34	0.17
MET148	No	2.25	0.42	0.31	0.39	0.30	0.32	0.33	0.27	0.55	0.23	0.50
GLU149	No	3.26	0.27	0.27	0.38	0.34	0.26	0.19	0.29	0.31	0.58	0.22
ARG150	No	4.18	0.26	0.36	0.38	0.23	0.41	0.22	0.29	0.36	0.47	0.21
GLY151	No	3.37	0.21	0.35	0.21	0.20	0.25	0.18	0.28	0.35	0.22	0.21
PRO152	No	3.01	0.19	0.25	0.25	0.26	0.28	0.20	0.21	0.42	0.22	0.21
GLN153	No	4.17	0.24	0.22	0.41	0.18	0.27	0.18	0.24	0.38	0.28	0.21
THR154	No	3.62	0.22	0.17	0.26	0.20	0.27	0.15	0.29	0.23	0.26	0.21
LEU155	No	3.31	0.46	0.35	0.53	0.25	0.24	0.18	0.48	0.28	0.61	0.44
LYS156	No	3.67	0.33	0.20	0.20	0.27	0.79	0.19	0.24	0.24	0.27	0.27
GLU157	No	3.11	0.17	0.19	0.22	0.25	0.26	0.15	0.20	0.26	0.25	0.17

THR158	No	2.53	0.28	0.19	0.20	0.22	0.17	0.15	0.17	0.23	0.18	0.19
SER159	No	2.58	0.24	0.25	0.22	0.21	0.20	0.30	0.17	0.18	0.31	0.34
PHE160	No	2.25	0.24	0.22	0.17	0.19	0.16	0.17	0.15	0.27	0.20	0.23
ASN161	No	2.01	0.20	0.17	0.17	0.26	0.16	0.18	0.17	0.19	0.22	0.24
GLN162	No	2.58	0.22	0.25	0.19	0.27	0.18	0.17	0.16	0.21	0.19	0.19
ALA163	No	2.24	0.19	0.18	0.16	0.36	0.22	0.23	0.17	0.19	0.15	0.19
TYR164	No	2.33	0.22	0.25	0.23	0.23	0.25	0.26	0.18	0.23	0.29	0.25
GLY165	No	1.57	0.22	0.24	0.36	0.26	0.35	0.28	0.22	0.19	0.20	0.29
ARG166	No	3.23	0.44	0.28	0.38	0.27	0.37	0.26	0.43	0.25	0.38	0.28
ASP167	No	1.81	0.18	0.16	0.23	0.20	0.30	0.18	0.21	0.20	0.18	0.19
LEU168	No	1.17	0.20	0.16	0.22	0.18	0.22	0.17	0.15	0.18	0.19	0.20
MET169	No	1.85	0.21	0.37	0.26	0.39	0.23	0.20	0.31	0.26	0.31	0.24
GLU170	No	1.98	0.18	0.20	0.23	0.22	0.55	0.15	0.15	0.23	0.37	0.22
ALA171	No	1.02	0.16	0.14	0.23	0.19	0.17	0.15	0.12	0.14	0.20	0.18
GLN172	No	1.65	0.24	0.18	0.25	0.23	0.18	0.20	0.27	0.16	0.19	0.23
GLU173	No	2.32	0.25	0.17	0.19	0.30	0.27	0.16	0.20	0.32	0.21	0.29
TRP174	No	1.98	0.17	0.25	0.21	0.29	0.20	0.18	0.16	0.34	0.32	0.25
CYS175	No	1.33	0.17	0.21	0.26	0.21	0.21	0.24	0.28	0.21	0.25	0.25
ARG176	No	2.27	0.39	0.25	0.35	0.35	0.29	0.29	0.27	0.28	0.54	0.25
LYS177	No	2.22	0.17	0.24	0.17	0.22	0.23	0.17	0.19	0.20	0.23	0.28
TYR178	No	1.90	0.23	0.28	0.28	0.36	0.23	0.23	0.27	0.19	0.41	0.38
MET179	No	2.48	0.26	0.45	0.26	0.47	0.31	0.24	0.40	0.25	0.31	0.37
LYS180	No	2.80	0.22	0.32	0.35	0.40	0.40	0.20	0.32	0.34	0.40	0.64
SER181	No	2.75	0.29	0.47	0.17	0.27	0.23	0.19	0.29	0.21	0.67	0.53
GLY182	No	2.67	0.31	0.42	0.25	0.25	0.30	0.27	0.48	0.25	0.25	0.61
ASN183	No	3.10	0.19	0.53	0.36	0.43	0.36	0.74	0.50	0.62	0.22	0.49
VAL184	No	3.07	0.39	0.44	0.54	0.46	0.48	0.45	0.24	0.32	0.22	0.56
LYS185	Yes	2.67	0.30	0.37	0.22	0.38	0.30	0.26	0.49	0.24	0.30	0.39
ASP186	No	2.25	0.21	0.45	0.21	0.56	0.44	0.23	0.27	0.31	0.25	0.29
LEU187	No	1.66	0.19	0.27	0.26	0.25	0.31	0.24	0.33	0.20	0.23	0.26
THR188	Yes	2.04	0.19	0.23	0.20	0.23	0.27	0.22	0.33	0.17	0.22	0.26
GLN189	Yes	2.17	0.24	0.29	0.29	0.30	0.24	0.29	0.31	0.24	0.45	0.34
ALA190	No	1.25	0.14	0.13	0.17	0.19	0.23	0.15	0.17	0.12	0.23	0.18
TRP191	Yes	1.61	0.17	0.21	0.19	0.16	0.38	0.16	0.29	0.21	0.31	0.20
ASP192	Yes	2.43	0.16	0.22	0.28	0.21	0.22	0.17	0.29	0.13	0.42	0.27
LEU193	Yes	1.87	0.16	0.22	0.24	0.21	0.18	0.19	0.23	0.23	0.22	0.25
TYR194	Yes	1.37	0.15	0.16	0.17	0.16	0.17	0.14	0.21	0.14	0.23	0.19
TYR195	Yes	3.41	0.21	0.17	0.26	0.25	0.15	0.25	0.30	0.13	0.33	0.47
HIS196	Yes	2.96	0.21	0.22	0.26	0.29	0.22	0.18	0.32	0.22	0.25	0.24
VAL197	No	2.33	0.16	0.19	0.19	0.18	0.17	0.16	0.23	0.16	0.21	0.18
PHE198	Yes	3.13	0.17	0.19	0.22	0.19	0.17	0.31	0.25	0.18	0.22	0.24
ARG199	Yes	4.27	0.23	0.35	0.52	0.46	0.20	0.24	0.29	0.28	0.37	0.33
ARG200	Yes	3.66	0.39	0.25	0.32	0.48	0.22	0.22	0.24	0.34	0.57	0.21
ILE201	No	3.10	0.23	0.19	0.30	0.28	0.20	0.24	0.18	0.19	0.22	0.23
SER202	Yes	5.04	0.23	0.21	0.41	0.29	0.28	0.21	0.18	0.28	0.23	0.15

Notes: FKBP12:X:FRB systems: (FKBP12:FRB) only protein fractions; (i) Rapamycin crystallographic structure; (ii) Rapamycin docking structure; (A/B/C/D/E/F/G/H) ligands; Pocket: residue belongs or not to the binding pocket in FKBP12:FRB interface; RMSF plotted as Å.

Supplemental Material 4

The binding energy contribution values of the simulated systems.

		System (FKBP12:X:FRB)									
RESIDUE	**Pocket**	**i**	**ii**	**A**	**B**	**C**	**D**	**E**	**F**	**G**	**H**
GLY1	No	0.18	0.23	0.16	0.19	0.08	0.02	0.08	0.08	0.08	0.09
VAL2	No	0.00	-0.01	0.00	0.00	0.00	0.00	0.00	0.00	-0.01	0.00
GLN3	No	-0.02	-0.01	-0.01	-0.01	-0.01	-0.02	-0.01	0.00	-0.01	-0.01
VAL4	No	0.02	0.01	0.01	0.00	0.01	0.00	0.00	0.00	0.00	0.00
GLU5	No	-0.06	-0.06	-0.01	-0.14	-0.09	-0.02	-0.05	-0.03	-0.07	-0.08
THR6	No	-0.01	0.00	-0.01	0.00	-0.01	0.00	0.00	0.00	0.00	0.00
ILE7	No	0.02	0.03	0.01	0.01	0.02	0.01	0.01	0.01	0.01	0.01
SER8	No	0.00	0.00	0.00	0.00	0.00	0.00	0.00	0.00	0.00	0.00
PRO9	No	0.00	0.00	0.00	0.00	0.00	0.00	0.00	0.00	0.00	0.00
GLY10	No	0.01	0.01	0.01	0.00	0.00	0.00	0.00	0.00	0.01	0.00
ASP11	No	-0.02	-0.06	0.02	-0.05	-0.04	-0.07	-0.06	-0.07	-0.18	-0.02
GLY12	No	0.01	0.02	0.01	0.01	0.01	0.01	0.00	0.01	0.00	0.01
ARG13	No	-0.02	-0.03	-0.05	0.02	0.02	0.04	0.03	0.04	0.13	-0.02
THR14	No	0.00	-0.01	0.00	0.00	0.00	0.00	0.00	0.00	0.00	0.00
PHE15	No	0.00	0.00	0.01	0.00	0.00	-0.01	0.00	0.00	-0.01	0.00
PRO16	No	0.01	0.01	0.00	0.00	0.00	0.01	0.00	0.01	0.00	-0.01
LYS17	No	0.04	0.00	-0.02	0.03	-0.01	0.10	0.08	0.08	0.24	-0.07
ARG18	No	0.08	0.23	0.11	0.09	-0.03	0.10	0.19	0.23	0.21	0.03
GLY19	No	0.03	0.03	0.02	0.02	0.00	-0.01	0.01	0.02	-0.01	0.02
GLN20	No	-0.03	-0.07	-0.03	-0.02	-0.01	0.00	-0.02	-0.03	0.01	-0.01
THR21	Yes	-0.03	-0.05	-0.01	0.00	0.00	-0.04	-0.02	-0.01	-0.03	0.00
CYS22	No	-0.05	-0.03	-0.02	-0.04	-0.02	-0.03	-0.03	-0.02	-0.05	-0.07
VAL23	No	0.00	0.01	0.01	0.00	0.00	0.00	0.01	0.00	0.00	0.01
VAL24	No	-0.14	-0.09	-0.04	-0.06	-0.05	-0.04	-0.16	-0.14	-0.08	-0.14
HIS25	No	0.10	0.08	0.04	-0.02	0.05	-0.02	0.09	0.06	0.04	0.11
TYR26	Yes	-2.86	-1.13	-0.01	0.56	-0.37	-0.21	-0.92	-0.95	-0.99	-1.57
THR27	No	-0.10	-0.06	-0.02	-0.02	-0.01	-0.03	-0.04	-0.08	-0.02	-0.08
GLY28	No	-0.12	-0.06	0.00	-0.01	0.02	0.01	0.00	-0.02	0.00	-0.04
MET29	No	-0.12	-0.10	-0.05	-0.04	-0.11	-0.07	-0.01	-0.04	-0.01	-0.09
LEU30	No	-0.03	-0.01	0.01	0.00	-0.01	-0.01	-0.01	-0.01	-0.01	0.00
GLU31	No	-0.06	-0.04	-0.04	-0.13	-0.10	0.03	0.00	0.03	0.02	-0.07
ASP32	No	-0.12	-0.14	-0.08	-0.19	-0.18	0.01	0.01	0.04	0.04	-0.13
GLY33	No	0.01	0.02	0.01	0.01	0.01	0.01	0.00	0.01	0.00	0.00
LYS34	No	0.04	0.02	0.04	0.16	0.12	-0.07	-0.07	-0.10	-0.11	0.08
LYS35	No	0.17	0.26	0.08	0.27	0.25	0.01	0.01	-0.01	0.07	0.18
PHE36	Yes	-1.32	-0.20	-0.03	0.00	0.00	-0.08	-0.03	-0.04	-0.05	-0.06
ASP37	Yes	2.45	-0.36	-1.08	-0.95	-0.59	-0.26	-0.42	-0.18	0.74	2.04
SER38	No	-0.26	-0.03	-0.01	-0.04	0.00	-0.02	-0.01	-0.01	-0.01	-0.09
SER39	No	-0.05	0.02	0.02	0.00	0.07	0.00	0.06	0.04	0.02	0.06
ARG40	No	0.30	0.39	0.14	0.24	0.28	0.13	0.18	0.15	0.25	0.28
ASP41	No	-0.28	-0.38	-0.13	-0.33	-0.28	-0.01	0.01	0.02	-0.09	-0.22
ARG42	Yes	2.28	1.31	1.14	1.27	1.06	0.34	0.52	0.39	1.08	2.65
ASN43	No	-0.02	0.00	-0.01	0.00	0.00	-0.01	0.00	-0.01	0.00	0.00
LYS44	Yes	0.48	0.69	0.51	0.47	0.43	0.36	0.33	0.28	0.54	0.31
PRO45	Yes	-0.04	-0.04	-0.06	-0.02	-0.03	-0.03	0.00	0.01	-0.02	-0.03
PHE46	Yes	-1.77	-0.70	-0.64	-1.14	-1.10	-0.57	-0.98	-0.92	-1.23	-1.35
LYS47	Yes	0.36	0.51	0.23	-0.01	0.14	0.38	0.14	0.18	0.32	0.44
PHE48	Yes	-0.43	-0.18	-0.14	-0.42	-0.17	-0.26	-0.19	-0.23	-0.57	-0.32
MET49	Yes	-0.11	-0.14	-0.05	-0.11	-0.02	-0.13	-0.04	-0.06	-0.14	-0.12
LEU50	No	-0.02	-0.03	-0.01	0.00	0.00	-0.02	-0.02	-0.02	-0.02	-0.01

GLY51	No	0.04	0.01	0.04	0.02	0.03	0.01	0.03	0.02	-0.01	0.02
LYS52	Yes	-0.04	0.22	0.17	0.01	-0.03	0.20	0.26	0.21	0.29	-0.08
GLN53	Yes	-1.18	-0.38	-0.20	-0.11	0.03	-0.40	-0.21	-0.28	-0.12	-0.17
GLU54	Yes	-2.31	-1.54	-1.18	-0.82	-0.16	0.80	-2.42	-1.57	1.17	-0.04
VAL55	Yes	-1.58	-2.24	-0.64	-0.80	-0.06	-0.94	-0.98	-0.96	-1.09	-1.58
ILE56	Yes	-1.41	-1.40	-0.43	-0.17	-0.22	-0.86	-0.25	-0.18	-0.16	0.13
ARG57	No	0.84	0.60	0.18	0.15	-0.09	-0.06	0.09	0.11	0.05	0.04
GLY58	No	0.23	0.06	0.11	0.07	0.09	0.03	0.02	0.04	0.03	0.04
TRP59	Yes	-1.00	-0.60	0.35	0.34	-0.42	-0.42	-0.37	-0.23	-0.38	-0.11
GLU60	No	-0.93	-1.27	-0.60	-0.36	-0.15	-0.50	-0.67	-0.61	-0.27	-0.31
GLU61	No	-0.40	-0.58	-0.14	-0.18	0.00	-0.10	-0.17	-0.18	-0.16	-0.06
GLY62	No	0.09	0.07	0.05	0.03	0.05	0.02	0.01	0.02	0.01	0.02
VAL63	No	0.03	0.04	0.03	0.01	0.01	-0.01	-0.03	-0.01	-0.02	0.00
ALA64	No	0.04	0.05	0.03	0.02	0.02	0.01	0.01	0.02	0.00	0.01
GLN65	No	0.10	0.13	0.03	0.03	0.02	0.03	0.03	0.04	0.02	0.02
MET66	No	-0.03	-0.03	-0.01	-0.01	-0.03	-0.01	-0.02	-0.02	-0.01	-0.01
SER67	No	-0.01	-0.01	0.00	0.00	-0.01	0.00	0.00	0.00	0.00	0.00
VAL68	No	0.01	0.01	0.00	0.00	0.00	0.01	0.01	0.01	0.01	0.00
GLY69	No	0.02	0.02	0.01	0.00	0.01	0.01	0.01	0.01	0.01	0.01
GLN70	No	-0.03	-0.03	0.00	0.00	-0.02	-0.01	-0.02	-0.03	-0.02	-0.01
ARG71	No	0.13	0.21	0.03	0.17	0.18	0.07	0.09	0.08	0.16	0.16
ALA72	No	-0.03	-0.02	-0.01	-0.01	-0.02	-0.01	-0.01	-0.01	-0.01	-0.02
LYS73	No	0.13	0.21	0.03	0.16	0.17	0.04	0.04	0.04	0.08	0.11
LEU74	No	-0.09	-0.07	-0.05	-0.04	-0.09	-0.05	-0.06	-0.06	-0.04	-0.04
THR75	No	0.01	0.00	0.00	0.01	0.01	0.02	0.01	0.01	0.01	0.01
ILE76	No	-0.09	-0.07	-0.04	-0.02	-0.06	-0.06	-0.04	-0.04	-0.04	-0.03
SER77	No	-0.20	-0.10	-0.06	-0.06	-0.08	-0.06	-0.05	-0.05	-0.04	-0.04
PRO78	No	-0.08	-0.06	-0.06	-0.04	-0.03	-0.04	-0.03	-0.03	-0.02	-0.03
ASP79	No	-0.29	-0.36	-0.31	-0.22	-0.10	-0.01	-0.07	-0.06	-0.03	-0.11
TYR80	No	-0.50	-0.36	-0.13	-0.07	-0.08	-0.06	-0.05	-0.07	-0.05	-0.05
ALA81	No	-0.07	0.16	-0.10	-0.05	-0.04	-0.03	-0.02	-0.08	-0.01	-0.03
TYR82	Yes	0.06	0.44	-0.36	0.37	0.69	0.38	0.44	0.25	0.30	1.35
GLY83	No	-0.03	-0.06	-0.03	-0.01	-0.04	-0.02	-0.02	-0.02	-0.01	-0.02
ALA84	No	-0.01	0.00	0.00	-0.01	-0.01	-0.01	0.00	-0.01	0.00	0.00
THR85	No	-0.07	-0.08	-0.06	-0.02	-0.06	-0.02	-0.03	-0.02	-0.02	-0.03
GLY86	No	-0.07	-0.14	-0.12	-0.02	0.02	-0.03	-0.03	-0.03	-0.01	-0.04
HIS87	Yes	1.03	0.10	-0.30	-0.22	1.09	-0.13	0.00	-0.06	0.37	-0.12
PRO88	No	-0.23	-0.16	-0.12	-0.07	-0.12	-0.02	-0.04	-0.03	-0.07	-0.06
GLY89	No	0.01	0.03	0.01	0.00	0.00	0.02	0.01	0.02	0.01	0.01
ILE90	Yes	-1.25	-0.25	-0.02	-0.01	-0.17	-0.03	0.00	0.00	-0.03	-0.01
ILE91	Yes	-0.65	-0.29	-0.09	-0.04	-0.15	-0.09	-0.07	-0.06	-0.06	-0.08
PRO92	No	-0.06	-0.05	-0.05	-0.04	-0.06	-0.04	-0.03	-0.03	-0.03	-0.03
PRO93	No	0.01	0.01	0.03	0.01	0.01	0.01	0.01	0.01	0.00	0.01
HIS94	No	0.00	0.00	0.03	0.00	0.02	0.01	0.01	0.00	-0.01	0.02
ALA95	No	-0.07	-0.06	-0.04	-0.03	-0.05	-0.05	-0.02	-0.02	-0.02	-0.02
THR96	No	-0.02	-0.03	-0.01	-0.01	0.00	0.00	0.00	0.00	0.01	-0.01
LEU97	No	-0.28	-0.15	-0.05	-0.02	-0.08	-0.11	-0.05	-0.06	-0.06	-0.03
VAL98	No	-0.03	-0.04	-0.01	-0.01	-0.04	-0.02	-0.03	-0.02	-0.01	-0.03
PHE99	Yes	-1.59	-0.43	-0.06	-0.03	-0.35	-0.07	-0.51	-0.59	-0.50	-0.42
ASP100	No	-0.30	-0.38	-0.14	-0.25	-0.31	-0.12	-0.19	-0.18	-0.23	-0.28
VAL101	No	-0.04	-0.03	0.00	-0.01	-0.02	-0.02	-0.03	-0.03	-0.03	-0.03
GLU102	No	-0.26	-0.29	-0.08	-0.17	-0.18	-0.12	-0.13	-0.12	-0.25	-0.23
LEU103	No	0.01	0.01	0.00	0.00	0.01	0.00	0.00	0.00	0.00	0.00
LEU104	No	0.04	0.04	0.02	0.02	0.03	0.02	0.03	0.03	0.02	0.03

LYS105	No	0.13	0.31	0.04	0.03	0.08	0.15	0.07	0.11	0.30	0.15
LEU106	No	0.01	0.01	0.00	0.00	0.00	0.00	0.00	0.00	0.00	0.00
GLU107	Yes	-0.45	-0.77	-0.26	-0.20	-0.22	-0.73	-0.38	-0.45	-0.86	-0.24
ARG108	No	0.19	0.35	0.17	-0.04	0.02	0.19	0.16	0.17	-0.01	0.09
VAL109	No	0.00	-0.01	0.00	0.00	0.00	-0.01	0.00	0.00	0.00	0.00
ALA110	No	0.00	0.00	0.00	0.00	0.00	0.00	0.00	0.00	0.00	0.00
ILE111	No	-0.01	0.00	0.00	0.00	0.00	0.00	0.00	0.00	0.00	0.00
LEU112	No	-0.01	-0.02	-0.01	-0.01	0.00	-0.01	-0.02	-0.01	-0.01	-0.01
TRP113	No	-0.05	-0.08	-0.02	-0.03	-0.02	-0.05	-0.05	-0.05	-0.04	-0.04
HIS114	No	-0.08	-0.13	-0.03	-0.05	-0.03	-0.06	-0.06	-0.07	-0.05	-0.07
GLU115	No	-0.14	-0.37	-0.12	-0.02	-0.03	-0.30	-0.20	-0.23	-0.19	-0.03
MET116	No	-0.03	-0.06	-0.01	-0.02	0.00	-0.02	-0.02	-0.04	-0.02	-0.01
TRP117	No	-0.16	-0.21	-0.07	-0.13	-0.10	-0.16	-0.14	-0.15	-0.11	-0.16
HIS118	No	-0.18	-0.23	-0.09	-0.16	-0.14	-0.09	-0.15	-0.19	-0.07	-0.21
GLU119	No	-0.33	-0.74	-0.22	-0.10	-0.01	-0.45	-0.47	-0.42	-0.25	-0.21
GLY120	No	-0.12	-0.17	-0.09	-0.08	-0.04	-0.10	-0.12	-0.10	-0.09	-0.11
LEU121	Yes	-1.16	-1.30	-0.70	-1.13	-0.98	-0.89	-0.81	-0.77	-0.90	-1.08
GLU122	Yes	-1.59	-3.71	-0.95	-0.80	-0.09	1.23	-1.19	-1.88	-1.62	-0.73
GLU123	No	-0.76	-1.39	-0.44	-0.33	-0.12	-0.79	-0.79	-0.66	-0.34	-0.48
ALA124	No	-0.16	-0.13	-0.15	-0.06	-0.11	-0.13	-0.08	-0.10	-0.17	-0.09
SER125	Yes	0.17	0.23	-0.55	0.00	-0.20	-0.31	0.16	0.28	0.10	-0.12
ARG126	Yes	-0.06	1.02	0.14	0.19	-0.13	0.13	0.25	0.18	0.17	0.15
LEU127	No	-0.04	0.02	0.00	0.01	-0.04	0.02	0.02	0.03	0.03	0.04
TYR128	No	0.77	0.09	0.00	-0.04	-0.05	0.05	0.04	0.03	0.07	0.07
PHE129	Yes	-2.65	-2.43	-2.98	-1.75	-2.71	-2.11	-2.40	-2.58	-1.70	-1.89
GLY130	Yes	0.19	-0.20	-0.28	0.06	-0.36	0.26	0.25	0.23	0.08	0.17
GLU131	No	-0.52	-1.26	-0.42	-0.20	-0.01	-0.31	-0.57	-0.44	-0.09	-0.32
ARG132	Yes	0.77	1.33	1.82	0.88	0.86	0.71	0.69	0.71	0.22	0.85
ASN133	No	-0.04	-0.02	-0.07	-0.01	-0.09	-0.03	-0.02	-0.09	-0.08	-0.03
VAL134	No	-0.08	-0.08	-0.05	-0.04	-0.05	-0.05	-0.07	-0.07	-0.05	-0.06
LYS135	No	0.17	0.17	0.14	0.02	-0.04	-0.06	0.04	0.00	-0.15	0.08
GLY136	No	0.02	0.00	0.02	0.01	0.01	0.00	0.00	0.02	0.00	0.01
MET137	No	-0.18	-0.13	-0.10	-0.08	-0.06	-0.09	-0.10	-0.08	-0.11	-0.13
PHE138	No	0.00	-0.01	0.00	0.00	-0.01	-0.01	-0.02	0.01	-0.02	-0.01
GLU139	No	-0.28	-0.37	-0.19	-0.07	0.00	-0.08	-0.19	-0.14	0.07	-0.14
VAL140	No	0.03	0.06	0.02	0.03	0.02	0.03	0.03	0.03	0.01	0.03
LEU141	No	0.00	0.01	0.00	0.00	-0.01	0.01	0.01	0.00	-0.04	-0.01
GLU142	No	-0.30	-0.27	-0.15	-0.04	-0.07	-0.06	-0.11	-0.07	0.02	-0.13
PRO143	No	0.01	0.02	0.01	0.01	0.01	0.01	0.01	0.01	0.01	0.01
LEU144	No	0.02	0.04	0.01	0.02	0.01	0.02	0.03	0.02	0.01	0.02
HIS145	No	0.11	0.14	0.08	0.08	0.08	0.08	0.09	0.08	0.07	0.09
ALA146	No	0.02	0.02	0.01	0.01	0.01	0.01	0.02	0.02	0.01	0.01
MET147	No	0.01	0.04	0.02	0.02	0.01	0.03	0.02	0.03	0.02	0.02
MET148	No	0.03	0.04	0.02	0.01	0.02	0.02	0.03	0.02	0.01	0.02
GLU149	No	-0.15	-0.13	-0.08	0.02	-0.04	-0.03	-0.02	-0.01	0.02	-0.07
ARG150	No	0.13	0.13	0.08	-0.01	0.04	0.05	0.04	0.03	-0.01	0.06
GLY151	No	0.00	0.00	0.00	0.00	0.00	0.00	0.01	0.01	0.00	0.00
PRO152	No	0.01	0.01	0.00	0.00	0.00	0.01	0.01	0.01	0.00	0.00
GLN153	No	0.01	0.01	0.01	0.00	0.00	0.00	0.01	0.01	0.00	0.01
THR154	No	-0.01	-0.01	0.00	0.00	0.00	-0.01	0.00	0.00	-0.01	0.00
LEU155	No	-0.01	-0.01	0.00	0.00	0.00	-0.01	0.00	0.00	-0.01	0.00
LYS156	No	0.07	0.14	0.04	-0.05	0.04	0.14	0.05	0.08	0.09	0.00
GLU157	No	-0.16	-0.22	-0.09	-0.02	-0.05	-0.15	-0.10	-0.12	-0.10	-0.07
THR158	No	-0.02	-0.01	-0.01	-0.01	0.00	-0.01	-0.01	-0.01	-0.01	-0.01

SER159	No	-0.02	-0.01	-0.01	-0.01	0.00	-0.01	-0.01	-0.01	-0.01	-0.01
PHE160	No	-0.01	-0.01	-0.01	-0.01	-0.01	-0.01	0.00	-0.01	-0.02	-0.01
ASN161	No	0.00	0.00	0.00	0.01	0.00	0.02	0.01	0.01	0.00	0.01
GLN162	No	-0.01	-0.02	0.00	0.00	0.00	-0.01	-0.01	-0.01	-0.01	-0.01
ALA163	No	-0.01	-0.01	0.00	0.00	0.00	0.00	0.00	0.00	-0.01	-0.01
TYR164	No	-0.03	-0.05	-0.03	-0.02	-0.04	-0.02	-0.03	-0.02	-0.04	-0.04
GLY165	No	-0.02	-0.03	-0.02	-0.02	-0.02	-0.02	-0.02	-0.02	-0.01	-0.02
ARG166	No	0.16	0.14	0.05	-0.02	0.07	0.05	-0.03	0.00	0.04	0.07
ASP167	No	-0.46	-0.65	-0.30	-0.30	-0.33	-0.36	-0.30	-0.28	-0.41	-0.34
LEU168	No	-0.04	-0.06	-0.04	-0.04	-0.04	-0.03	-0.03	-0.02	-0.04	-0.04
MET169	No	0.01	0.02	-0.01	0.01	-0.01	0.01	0.00	0.00	0.00	-0.01
GLU170	No	-0.33	-0.47	-0.21	-0.21	-0.22	-0.15	-0.12	-0.09	-0.16	-0.23
ALA171	No	-0.04	-0.02	-0.02	-0.02	-0.02	0.00	-0.01	0.00	-0.01	-0.02
GLN172	No	-0.03	-0.03	-0.02	-0.02	-0.01	-0.01	-0.03	-0.01	-0.01	-0.01
GLU173	No	-0.25	-0.26	-0.14	-0.10	-0.11	-0.05	-0.05	-0.03	-0.02	-0.13
TRP174	No	-0.06	-0.02	-0.02	-0.04	-0.02	0.00	0.00	-0.01	0.00	-0.02
CYS175	No	-0.06	-0.02	-0.03	-0.03	-0.03	-0.01	0.00	-0.01	-0.01	-0.04
ARG176	No	0.25	0.25	0.14	0.10	0.11	0.08	0.06	0.07	0.04	0.14
LYS177	No	0.33	0.38	0.20	0.22	0.21	0.10	0.11	0.04	0.13	0.21
TYR178	No	0.00	0.01	0.02	0.03	0.02	0.02	0.02	0.03	0.03	0.03
MET179	No	0.05	0.04	0.03	0.03	0.03	0.04	0.04	0.04	0.03	0.03
LYS180	No	0.22	0.15	0.09	0.11	0.09	-0.04	-0.03	-0.06	-0.07	0.09
SER181	No	0.01	0.03	0.01	0.01	0.01	0.01	0.01	0.01	0.02	0.01
GLY182	No	0.02	0.01	0.00	0.00	0.00	0.02	0.00	0.01	0.03	-0.01
ASN183	No	0.02	0.02	0.00	0.00	0.01	-0.01	0.02	0.01	0.04	-0.01
VAL184	No	-0.33	-0.20	-0.07	-0.10	-0.10	-0.06	-0.06	-0.05	-0.09	-0.08
LYS185	Yes	2.21	1.12	0.76	0.91	0.93	0.11	0.12	0.00	0.29	0.45
ASP186	No	-0.72	-0.67	-0.31	-0.43	-0.37	-0.13	-0.15	-0.09	-0.14	-0.30
LEU187	No	-0.17	-0.17	-0.11	-0.11	-0.13	-0.10	-0.12	-0.10	-0.13	-0.15
THR188	Yes	-0.32	-0.23	-0.15	-0.21	-0.25	-0.07	-0.09	-0.11	-0.19	-0.16
GLN189	Yes	-0.15	-0.14	-0.08	-0.11	-0.12	-0.03	0.03	-0.03	-0.04	-0.07
ALA190	No	-0.04	-0.06	-0.05	-0.05	-0.12	-0.08	-0.06	-0.05	-0.10	-0.08
TRP191	Yes	-2.61	-2.24	-1.41	-1.91	-1.94	-0.75	-1.23	-1.54	-1.37	-1.94
ASP192	Yes	-1.33	-1.67	-1.17	-0.27	-1.47	-0.63	-0.85	-0.69	-1.56	1.67
LEU193	Yes	-0.13	-0.07	-0.01	-0.07	-0.03	-0.04	-0.04	-0.06	-0.05	-0.12
TYR194	Yes	-0.20	-0.33	-0.05	-0.37	-0.34	0.00	-0.13	-0.30	-0.17	-0.22
TYR195	Yes	-2.40	-2.08	-1.81	-3.21	-1.71	-1.57	-1.86	-1.90	-2.55	-2.49
HIS196	Yes	-0.25	-0.26	-0.09	-0.20	-0.07	-0.10	-0.11	-0.13	-0.15	-0.42
VAL197	No	0.02	-0.03	0.00	0.00	0.02	0.04	0.04	0.01	-0.06	0.01
PHE198	Yes	-1.13	-0.86	-0.47	-0.49	-0.60	-0.76	-0.28	-0.63	-0.97	-0.73
ARG199	Yes	1.07	1.08	0.63	0.90	0.49	0.85	0.77	0.76	0.81	1.30
ARG200	Yes	0.49	0.67	0.24	0.31	0.21	0.53	0.34	0.32	0.45	0.33
ILE201	No	0.01	0.00	-0.02	0.00	0.01	0.04	0.01	0.01	-0.02	0.02
SER202	Yes	-0.30	-0.70	-0.16	-0.02	-0.04	-0.64	-0.30	-0.43	-0.60	-0.01

Notes: FKBP12:X:FRB systems: (i) Rapamycin crystallographic structure; (ii) Rapamycin docking structure; (A/B/C/D/E/F/G/H) ligands; Pocket: residue belongs or not to the binding pocket in FKBP12:FRB interface; Energy plotted as kcal/mol.

Supplemental Material 5

Radius of gyration of Cα protein portions FKBP12:FRB system.

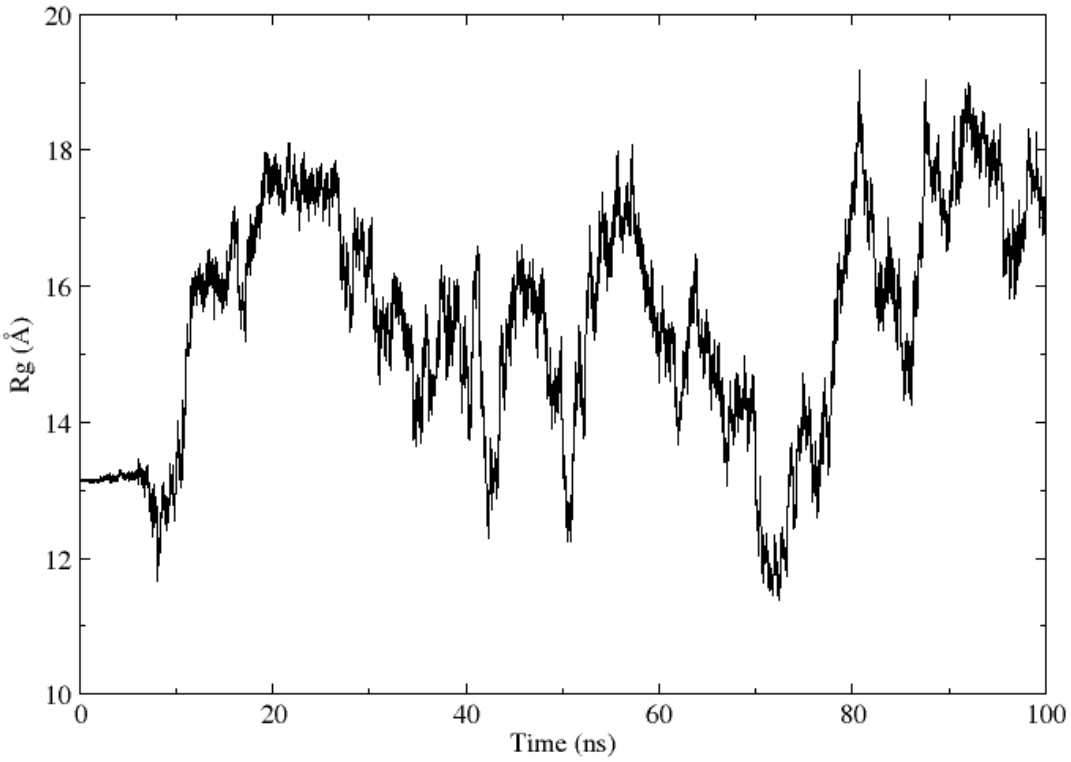

Supplemental Material 6

Radius of gyration plots of Cα protein portions of complexes FKBP12:X:FRB systems. In black line, ligand (X) complex; in green line, crystallographic rapamycin complex and, in red, docking rapamycin complex.

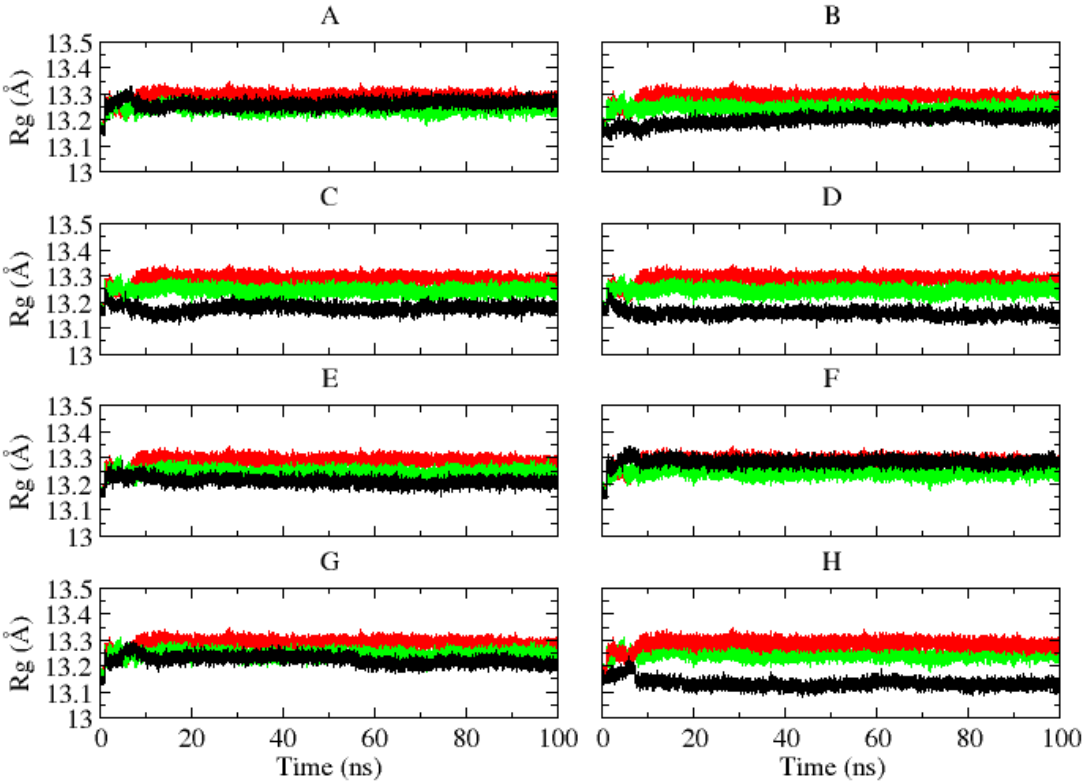

4 CONCLUSÃO

As técnicas computacionais são amplamente utilizadas na indústria farmacêutica para reduzir o tempo e os recursos financeiros no processo de descoberta e desenvolvimento de fármacos. No presente trabalho apresentamos um passo inicial para encontrar novas moléculas para atuar como potenciais inibidores não competitivos ao ATP para controle da via da mTOR. Ao final, conseguimos propor oito moléculas apresentando melhores perfis energéticos e farmacocinéticos do que o inibidor natural, a rapamicina. Além disso, as simulações de DM demonstraram que todos os ligantes induzem uma rigidez da estrutura protéica (FKBP12:FRB) e que essa característica também é observada para a rapamicina. De mesma forma, mudanças conformacionais foram confirmadas pela análise PCA e FEL, o que nos permite compreender características importantes da associação da rapamicina com FKBP12:FRB. Além disso, conseguimos descrever os resíduos PHE46, GLU122, PHE129, ASP192 e TYR195 como os principais contribuintes para a ligação. Todavia, o próximo passo é realizar estudos experimentais (*in vitro*) para confirmar o perfil de inibição desses ligantes.

5 ANEXOS

5.1 Orientações e regras de submissão à revista

JOURNAL OF MOLECULAR GRAPHICS AND MODELLING

AUTHOR INFORMATION PACK

TABLE OF CONTENTS

ISSN: 1093-3263

DESCRIPTION

The *Journal of Molecular Graphics and Modelling* is devoted to the publication of papers on the uses of **computers** in theoretical investigations of molecular structure, function, interaction, and design. The scope of the journal includes all aspects of **molecular modeling** and **computational chemistry**, including, for instance, the study of molecular shape and properties, molecular simulations, protein and polymer engineering, drug design, materials design, structure-activity and structure-property relationships, database mining, and compound library design.

As a primary research journal, *JMGM* seeks to bring new knowledge to the attention of our readers. As such, submissions to the journal need to not only report results, but must draw conclusions and explore implications of the work presented. Authors are strongly encouraged to bear this in mind when preparing manuscripts. Routine applications of standard modelling approaches, providing only very limited new scientific insight, will not meet our criteria for publication. Reproducibility of reported calculations is an important issue. Wherever possible, we urge authors to enhance their papers with Supplementary Data, for example, in QSAR studies machine-readable versions of molecular datasets or in the development of new force-field parameters versions of the topology and force field parameter files. Routine applications of existing methods that do not lead to genuinely new insight will not be considered.

JMGM is published in association with two of the largest and most active professional societies in the field: the Molecular Graphics and Modelling Society (MGMS) and the Computers in Chemistry (COMP) Division of the American Chemical Society. Several thousand computational chemists worldwide belong to these two societies and any research topic that may of interest to the membership is within the wide scope of the journal. It is not necessary to be a member of these professional societies to publish in the journal.

Published in association with the Molecular Graphics and Modelling Society www.mgms.org and the ACS Division of Computers in Chemistry.

mgms525012.jpg CompLogo525012.jpg

AUDIENCE

Researchers in computer graphics, molecular modelling, and automation for chemical engineering, engineered materials, and pharmaceutical research.

IMPACT FACTOR

2016: 1.754 © Thomson Reuters Journal Citation Reports 2017

ABSTRACTING AND INDEXING

Biotechnology Citation Index Elsevier BIOBASE
Chemical Abstracts Chemistry Citation Index
Computer and Information Systems Abstracts Journal Current Contents
MEDLINE®
Research Alert Science Citation Index Scisearch
Scopus

EDITORIAL BOARD

GUIDE FOR AUTHORS

Your Paper Your Way

We now differentiate between the requirements for new and revised submissions. You may choose to submit your manuscript as a single Word or PDF file to be used in the refereeing process. Only when your paper is at the revision stage, will you be requested to put your paper in to a 'correct format' for acceptance and provide the items required for the publication of your article.
To find out more, please visit the Preparation section below.

INTRODUCTION

Published in Affiliation with the Molecular Graphics and Modelling Society and the ACS Division of Computers in Chemistry Former title: *Journal of Molecular Graphics*

Scope

The *Journal of Molecular Graphics and Modelling* is devoted to the publication of papers on the uses of computers in theoretical investigations of molecular structure, function, interaction, and design. The scope of the journal includes all aspects of molecular modeling and computational chemistry, including, for instance, the study of molecular shape and properties, molecular simulations, protein and polymer engineering, drug design, materials design, structure-activity and structure-property relationships, database mining, and compound library design.

As a primary research journal, *JMGM* seeks to bring new knowledge to the attention of our readers. As such, submissions to the journal need to not only report results, but must draw conclusions and explore implications of the work presented. Authors are strongly encouraged to bear this in mind when preparing manuscripts.

JMGM is published in association with two of the largest and most active professional societies in the field: the Molecular Graphics and Modelling Society (MGMS) and the Computers in Chemistry (COMP) Division of the American Chemical Society. Several thousand computational chemists worldwide belong to these two societies and any research topic that may of interest to the membership is within the wide scope of the journal. It is not necessary to be a member of these professional societies to publish in the journal.

Programs

Descriptions of programs will not be accepted for publication by JMGM, but descriptions of **algorithms** are acceptable.

Supplementary Information

Authors should carefully develop manuscripts with brevity and clarity in mind, and as much material as possible should be deposited online as Supplementary Information. Consider placing items that are not REQUIRED for understanding the main conclusions of the paper, but are necessary for the reasons of repeatability and more detailed analysis in this category.

Types of papers

The editors also welcome authoritative review articles or commentaries on any aspect of molecular modeling and computational chemistry. If you are interested in contributing such material, you should first contact one of the Editors.

Structural Data

For papers describing structures of biological macromolecules, the atomic coordinates and the related experimental data (structure factor amplitudes/intensities and/or NMR restraints) must be deposited at a member site of the Worldwide Protein Data Bank (http://www.wwpdb.org): RCSB PDB (http://www.pdb.org), MSD-EBI (http://www.ebi.ac.uk/pdbe/), PDBj (http://www.pdbj.org, or BMRB (http://www.bmrb.wisc.edu). Manuscripts must carry a statement that coordinates and structure factors (or NMR restraints) have been deposited in the Protein Data Bank. The accession number(s) must be cited in the manuscript at the end of the Materials and Methods section. Authors must agree to release the atomic coordinates and experimental data immediately upon publication.

It is increasingly common for coordinates to be deposited in the Protein Data Bank without an associated publication. Before submission to JSB, authors are expected to search the Protein Data Bank for related structures using one or more alignment programs and report the outcome. Prior deposition of related coordinates, without an associated publication, does not necessarily preclude publication in JMGM. The primary criteria for publication of a structure in JMGM are that it provides novel structural insights or important new functional and biological insights that are likely to be of general interest.

Page Charges

This journal has no page charges.

Submission checklist

You can use this list to carry out a final check of your submission before you send it to the journal for review. Please check the relevant section in this Guide for Authors for more details.

Ensure that the following items are present:

One author has been designated as the corresponding author with contact details:
- E-mail address
- Full postal address

All necessary files have been uploaded:
Manuscript:
- Include keywords
- All figures (include relevant captions)
- All tables (including titles, description, footnotes)
- Ensure all figure and table citations in the text match the files provided
- Indicate clearly if color should be used for any figures in print *Graphical Abstracts / Highlights files* (where applicable) *Supplemental files* (where applicable)

Further considerations
- Manuscript has been 'spell checked' and 'grammar checked'
- All references mentioned in the Reference List are cited in the text, and vice versa
- Permission has been obtained for use of copyrighted material from other sources (including the Internet)
- A competing interests statement is provided, even if the authors have no competing interests to declare
- Journal policies detailed in this guide have been reviewed
- Referee suggestions and contact details provided, based on journal requirements

For further information, visit our Support Center.

BEFORE YOU BEGIN

Ethics in publishing

Please see our information pages on Ethics in publishing and Ethical guidelines for journal publication.

Declaration of interest

All authors must disclose any financial and personal relationships with other people or organizations that could inappropriately influence (bias) their work. Examples of potential conflicts of interest include employment, consultancies, stock ownership, honoraria, paid expert testimony, patent applications/ registrations, and grants or other funding. If there are no conflicts of interest then please state this: 'Conflicts of interest: none'. More information.

Submission declaration and verification

Submission of an article implies that the work described has not been published previously (except in the form of an abstract or as part of a published lecture or academic thesis or as an electronic preprint, see 'Multiple, redundant or concurrent publication' section of our ethics policy for more information), that it is not under consideration for publication elsewhere, that its publication is approved by all authors and tacitly or explicitly by the responsible authorities where the work was

carried out, and that, if accepted, it will not be published elsewhere in the same form, in English or in any other language, including electronically without the written consent of the copyright-holder. To verify originality, your article may be checked by the originality detection service CrossCheck.

Changes to authorship

Authors are expected to consider carefully the list and order of authors **before** submitting their manuscript and provide the definitive list of authors at the time of the original submission. Any addition, deletion or rearrangement of author names in the authorship list should be made only **before** the manuscript has been accepted and only if approved by the journal Editor. To request such a change, the Editor must receive the following from the **corresponding author**: (a) the reason for the change in author list and (b) written confirmation (e-mail, letter) from all authors that they agree with the addition, removal or rearrangement. In the case of addition or removal of authors, this includes confirmation from the author being added or removed.

Only in exceptional circumstances will the Editor consider the addition, deletion or rearrangement of authors **after** the manuscript has been accepted. While the Editor considers the request, publication of the manuscript will be suspended. If the manuscript has already been published in an online issue, any requests approved by the Editor will result in a corrigendum.

Copyright

Upon acceptance of an article, authors will be asked to complete a 'Journal Publishing Agreement' (see more information on this). An e-mail will be sent to the corresponding author confirming receipt of the manuscript together with a 'Journal Publishing Agreement' form or a link to the online version of this agreement.

Subscribers may reproduce tables of contents or prepare lists of articles including abstracts for internal circulation within their institutions. Permission of the Publisher is required for resale or distribution outside the institution and for all other derivative works, including compilations and translations. If excerpts from other copyrighted works are included, the author(s) must obtain written permission from the copyright owners and credit the source(s) in the article. Elsevier has preprinted forms for use by authors in these cases.

For open access articles: Upon acceptance of an article, authors will be asked to complete an 'Exclusive License Agreement' (more information). Permitted third party reuse of open access articles is determined by the author's choice of user license.

Author rights

As an author you (or your employer or institution) have certain rights to reuse your work. More information.

Elsevier supports responsible sharing

Find out how you can share your research published in Elsevier journals.

Role of the funding source

You are requested to identify who provided financial support for the conduct of the research and/or preparation of the article and to briefly describe the role of the sponsor(s), if any, in study design; in the collection, analysis and interpretation of data; in the writing of the report; and in the decision to submit the article for publication. If the funding source(s) had no such involvement then this should be stated.

Funding body agreements and policies

Elsevier has established a number of agreements with funding bodies which allow authors to comply with their funder's open access policies. Some funding bodies will reimburse the author for the Open Access Publication Fee. Details of existing agreements are available online.

Open access

This journal offers authors a choice in publishing their research:

Subscription

- Articles are made available to subscribers as well as developing countries and patient groups through our universal access programs.
- No open access publication fee payable by authors.

Open access

- Articles are freely available to both subscribers and the wider public with permitted reuse.

- An open access publication fee is payable by authors or on their behalf, e.g. by their research funder or institution.

Regardless of how you choose to publish your article, the journal will apply the same peer review criteria and acceptance standards.

For open access articles, permitted third party (re)use is defined by the following Creative Commons user licenses:

Creative Commons Attribution (CC BY)
Lets others distribute and copy the article, create extracts, abstracts, and other revised versions, adaptations or derivative works of or from an article (such as a translation), include in a collective work (such as an anthology), text or data mine the article, even for commercial purposes, as long as they credit the author(s), do not represent the author as endorsing their adaptation of the article, and do not modify the article in such a way as to damage the author's honor or reputation.

Creative Commons Attribution-NonCommercial-NoDerivs (CC BY-NC-ND)
For non-commercial purposes, lets others distribute and copy the article, and to include in a collective work (such as an anthology), as long as they credit the author(s) and provided they do not alter or modify the article.

The open access publication fee for this journal is **USD 2600**, excluding taxes. Learn more about Elsevier's pricing policy: http://www.elsevier.com/openaccesspricing.

Green open access
Authors can share their research in a variety of different ways and Elsevier has a number of green open access options available. We recommend authors see our green open access page for further information. Authors can also self-archive their manuscripts immediately and enable public access from their institution's repository after an embargo period. This is the version that has been accepted for publication and which typically includes author-incorporated changes suggested during submission, peer review and in editor-author communications. Embargo period: For subscription articles, an appropriate amount of time is needed for journals to deliver value to subscribing customers before an article becomes freely available to the public. This is the embargo period and it begins from the date the article is formally published online in its final and fully citable form. Find out more.

This journal has an embargo period of 24 months.

Elsevier Publishing Campus
The Elsevier Publishing Campus (www.publishingcampus.com) is an online platform offering free lectures, interactive training and professional advice to support you in publishing your research. The College of Skills training offers modules on how to prepare, write and structure your article and explains how editors will look at your paper when it is submitted for publication. Use these resources, and more, to ensure that your submission will be the best that you can make it.

Language (usage and editing services)
Please write your text in good English (American or British usage is accepted, but not a mixture of these). Authors who feel their English language manuscript may require editing to eliminate possible grammatical or spelling errors and to conform to correct scientific English may wish to use the English Language Editing service available from Elsevier's WebShop.

Submission

Our online submission system guides you stepwise through the process of entering your article details and uploading your files. The system converts your article files to a single PDF file used in the peer-review process. Editable files (e.g., Word, LaTeX) are required to typeset your article for final publication. All correspondence, including notification of the Editor's decision and requests for revision, is sent by e-mail.

For submitting your manuscripts to the *Journal of Molecular Graphics and Modelling* please go to our Elsevier Editorial System (EES) Website at: http://ees.elsevier.com/jmgm .

Referees

The names, affiliation and email addresses of five potential Referees are required (no generic mail addresses such as gmail or hotmail are allowed). Appropriate Referees should be knowledgeable about the subject and have potential interest in the work. Referees should have no close connection with any of the authors and be from institutions other than (and preferably countries other than) those of any of the Authors. Articles will not be considered for publication if this requirement is not met.

PREPARATION

NEW SUBMISSIONS

Submission to this journal proceeds totally online and you will be guided stepwise through the creation and uploading of your files. The system automatically converts your files to a single PDF file, which is used in the peer-review process.

As part of the Your Paper Your Way service, you may choose to submit your manuscript as a single file to be used in the refereeing process. This can be a PDF file or a Word document, in any format or lay-out that can be used by referees to evaluate your manuscript. It should contain high enough quality figures for refereeing. If you prefer to do so, you may still provide all or some of the source files at the initial submission. Please note that individual figure files larger than 10 MB must be uploaded separately.

References

There are no strict requirements on reference formatting at submission. References can be in any style or format as long as the style is consistent. Where applicable, author(s) name(s), journal title/book title, chapter title/article title, year of publication, volume number/book chapter and the pagination must be present. Use of DOI is highly encouraged. The reference style used by the journal will be applied to the accepted article by Elsevier at the proof stage. Note that missing data will be highlighted at proof stage for the author to correct.

Formatting requirements

There are no strict formatting requirements but all manuscripts must contain the essential elements needed to convey your manuscript, for example Abstract, Keywords, Introduction, Materials and Methods, Results, Conclusions, Artwork and Tables with Captions.

If your article includes any Videos and/or other Supplementary material, this should be included in your initial submission for peer review purposes.

Divide the article into clearly defined sections.

Figures and tables embedded in text

Please ensure the figures and the tables included in the single file are placed next to the relevant text in the manuscript, rather than at the bottom or the top of the file. The corresponding caption should be placed directly below the figure or table.

Peer review

This journal operates a single blind review process. All contributions will be initially assessed by the editor for suitability for the journal. Papers deemed suitable are then typically sent to a minimum of two independent expert reviewers to assess the scientific quality of the paper. The Editor is responsible for the final decision regarding acceptance or rejection of articles. The Editor's decision is final. More information on types of peer review.

REVISED SUBMISSIONS

Use of word processing software

Regardless of the file format of the original submission, at revision you must provide us with an editable file of the entire article. Keep the layout of the text as simple as possible. Most formatting codes will be removed and replaced on processing the article. The electronic text should be prepared in a way very similar to that of conventional manuscripts (see also the Guide to Publishing with Elsevier). See also the section on Electronic artwork.

To avoid unnecessary errors you are strongly advised to use the 'spell-check' and 'grammar-check' functions of your word processor.

LaTeX

You are recommended to use the Elsevier article class elsarticle.cls to prepare your manuscript and BibTeX to generate your bibliography.

Our LaTeX site has detailed submission instructions, templates and other information.

Essential title page information

- ***Title.*** Concise and informative. Titles are often used in information-retrieval systems. Avoid abbreviations and formulae where possible.
- ***Author names and affiliations.*** Please clearly indicate the given name(s) and family name(s) of each author and check that all names are accurately spelled. Present the authors' affiliation addresses (where the actual work was done) below the names. Indicate all affiliations with a lower-case superscript letter immediately after the author's name and in front of the appropriate address. Provide the full postal address of each affiliation, including the country name and, if available, the e-mail address of each author.
- ***Corresponding author.*** Clearly indicate who will handle correspondence at all stages of refereeing and publication, also post-publication. **Ensure that the e-mail address is given and that contact details are kept up to date by the corresponding author.**
- ***Present/permanent address.*** If an author has moved since the work described in the article was done, or was visiting at the time, a 'Present address' (or 'Permanent address') may be indicated as a footnote to that author's name. The address at which the author actually did the work must be retained as the main, affiliation address. Superscript Arabic numerals are used for such footnotes.

Graphical abstract

A graphical abstract is mandatory for this journal. It should summarize the contents of the article in a concise, pictorial form designed to capture the attention of a wide readership online. Authors must provide images that clearly represent the work described in the article. Graphical abstracts should be submitted as a separate file in the online submission system. Image size: please provide an image with a minimum of 531 × 1328 pixels (h × w) or proportionally more. The image should be readable at a size of 5 × 13 cm using a regular screen resolution of 96 dpi. Preferred file types: TIFF, EPS, PDF or MS Office files. You can view Example Graphical Abstracts on our information site.
Authors can make use of Elsevier's Illustration Services to ensure the best presentation of their images also in accordance with all technical requirements.

Highlights

Highlights are mandatory for this journal. They consist of a short collection of bullet points that convey the core findings of the article and should be submitted in a separate editable file in the online submission system. Please use 'Highlights' in the file name and include 3 to 5 bullet points (maximum 85 characters, including spaces, per bullet point). You can view example Highlights on our information site.

Keywords

Immediately after the abstract provide a minimum of 5 keywords. These keywords will be used for indexing purposes.

Formatting of funding sources

List funding sources in this standard way to facilitate compliance to funder's requirements:

Funding: This work was supported by the National Institutes of Health [grant numbers xxxx, yyyy]; the Bill & Melinda Gates Foundation, Seattle, WA [grant number zzzz]; and the United States Institutes of Peace [grant number aaaa].

It is not necessary to include detailed descriptions on the program or type of grants and awards. When funding is from a block grant or other resources available to a university, college, or other research institution, submit the name of the institute or organization that provided the funding.

If no funding has been provided for the research, please include the following sentence:

This research did not receive any specific grant from funding agencies in the public, commercial, or not-for-profit sectors.

Nomenclature and Units

Use of Systeme Internationale (SI) units is encouraged; provide a conversion factor in parentheses at the first mention of non-SI units. Biochemical nomenclature should conform to that recommended by the IUPAC-IUB Commission, and enzymes should be referred to by their recommended names and numbers.

Mathematical and Technical Terms

Write mathematical, Greek and other symbols carefully using, for instance, a Symbol font. Explain the meaning of all symbols and acronyms in the text where they first occur. Identify Greek letters at their first mention by writing their names in English words in the margin. If you use several symbols, a list of definitions -- not necessarily for publication -- will be useful to and ensure the accuracy of the production editors. Identify all vectors, tensors, and matrices in bold. The journal is read by an international audience; therefore authors should attempt to make their work clear to diverse readers. Note the following points:

- Use a zero before decimal quantities less than one, e.g., 0.376, not .376.
- Group numbers consisting of more than three numerals in threes separated by spaces, rather than commas.
- Use fractional exponents instead of root signs, e.g., (3x + 9y)**1/2, not the square root symbol. (Here ** indicates that 1/2 is an exponent).
- Specify whether logarithms are to base 10 or base e.
- Write simple mathematical fractions in the text on one line, e.g., L(N - l)/L(l), not as a stacked fraction. If the fraction is complicated with superscripts and subscripts, then present it in a manner consistent with maximum clarity.

Footnotes

Footnotes should be used sparingly. Number them consecutively throughout the article. Many word processors build footnotes into the text, and this feature may be used. Should this not be the case, indicate the position of footnotes in the text and present the footnotes themselves separately at the end of the article.

Artwork *Electronic artwork General points*

- Make sure you use uniform lettering and sizing of your original artwork.
- Preferred fonts: Arial (or Helvetica), Times New Roman (or Times), Symbol, Courier.
- Number the illustrations according to their sequence in the text.
- Use a logical naming convention for your artwork files.
- Indicate per figure if it is a single, 1.5 or 2-column fitting image.
- For Word submissions only, you may still provide figures and their captions, and tables within a single file at the revision stage.
- Please note that individual figure files larger than 10 MB must be provided in separate source files.

A detailed guide on electronic artwork is available.

You are urged to visit this site; some excerpts from the detailed information are given here.

Formats

Regardless of the application used, when your electronic artwork is finalized, please 'save as' or convert the images to one of the following formats (note the resolution requirements for line drawings, halftones, and line/halftone combinations given below):

EPS (or PDF): Vector drawings. Embed the font or save the text as 'graphics'.

TIFF (or JPG): Color or grayscale photographs (halftones): always use a minimum of 300 dpi. TIFF (or JPG): Bitmapped line drawings: use a minimum of 1000 dpi.

TIFF (or JPG): Combinations bitmapped line/half-tone (color or grayscale): a minimum of 500 dpi is required.

Please do not:

- Supply files that are optimized for screen use (e.g., GIF, BMP, PICT, WPG); the resolution is too low.
- Supply files that are too low in resolution.
- Submit graphics that are disproportionately large for the content.

Color artwork

Please make sure that artwork files are in an acceptable format (TIFF (or JPEG), EPS (or PDF) or MS Office files) and with the correct resolution. If, together with your accepted article, you submit usable color figures then Elsevier will ensure, at no additional charge, that these figures will appear in color online (e.g., ScienceDirect and other sites) in addition to color reproduction in print. Further information on the preparation of electronic artwork.

Figure captions
Ensure that each illustration has a caption. A caption should comprise a brief title (**not** on the figure itself) and a description of the illustration. Keep text in the illustrations themselves to a minimum but explain all symbols and abbreviations used.

Tables

Please submit tables as editable text and not as images. Tables can be placed either next to the relevant text in the article, or on separate page(s) at the end. Number tables consecutively in accordance with their appearance in the text and place any table notes below the table body. Be sparing in the use of tables and ensure that the data presented in them do not duplicate results described elsewhere in the article. Please avoid using vertical rules and shading in table cells.

References

Citation in text
Please ensure that every reference cited in the text is also present in the reference list (and vice versa). Any references cited in the abstract must be given in full. Unpublished results and personal communications are not recommended in the reference list, but may be mentioned in the text. If these references are included in the reference list they should follow the standard reference style of the journal and should include a substitution of the publication date with either 'Unpublished results' or 'Personal communication'. Citation of a reference as 'in press' implies that the item has been accepted for publication.

Reference links
Increased discoverability of research and high quality peer review are ensured by online links to the sources cited. In order to allow us to create links to abstracting and indexing services, such as Scopus, CrossRef and PubMed, please ensure that data provided in the references are correct. Please note that incorrect surnames, journal/book titles, publication year and pagination may prevent link creation. When copying references, please be careful as they may already contain errors. Use of the DOI is encouraged.

A DOI can be used to cite and link to electronic articles where an article is in-press and full citation details are not yet known, but the article is available online. A DOI is guaranteed never to change, so you can use it as a permanent link to any electronic article. An example of a citation using DOI for an article not yet in an issue is: VanDecar J.C., Russo R.M., James D.E., Ambeh W.B., Franke M. (2003). Aseismic continuation of the Lesser Antilles slab beneath northeastern Venezuela. Journal of Geophysical Research, https://doi.org/10.1029/2001JB000884. Please note the format of such citations should be in the same style as all other references in the paper.

Data references
This journal encourages you to cite underlying or relevant datasets in your manuscript by citing them in your text and including a data reference in your Reference List. Data references should include the following elements: author name(s), dataset title, data repository, version (where available), year, and global persistent identifier. Add [dataset] immediately before the reference so we can properly identify it as a data reference. The [dataset] identifier will not appear in your published article.

[dataset] M. Oguro, S. Imahiro, S. Saito, T. Nakashizuka, Mortality data for Japanese oak wilt disease and surrounding forest compositions, Mendeley Data, v1, 2015. http://dx.doi.org/10.17632/xwj98nb39r.1.

Reference management software
Most Elsevier journals have their reference template available in many of the most popular reference management software products. These include all products that support Citation Style Language styles, such as Mendeley and Zotero, as well as EndNote. Using the word processor plug-ins from these products, authors only need to select the appropriate journal template when preparing their article, after which citations and bibliographies will be automatically formatted in the journal's style. If no template is yet available for this journal, please follow the format of the sample references and citations as shown in this Guide.

Users of Mendeley Desktop can easily install the reference style for this journal by clicking the following link:
http://open.mendeley.com/use-citation-style/journal-of-molecular-graphics-and-modelling
When preparing your manuscript, you will then be able to select this style using the Mendeley plug-ins for Microsoft Word or LibreOffice.

Reference formatting
There are no strict requirements on reference formatting at submission. References can be in any style or format as long as the style is consistent. Where applicable, author(s) name(s), journal title/book title, chapter title/article title, year of publication, volume number/book chapter and the pagination must be present. Use of DOI is highly encouraged. The reference style used by the journal will be applied to the accepted article by Elsevier at the proof stage. Note that missing data will be highlighted at proof stage for the author to correct. If you do wish to format the references yourself they should be arranged according to the following examples:

Reference Style

1. D.C. Spellmeyer, A.K. Wong, M.J.. Bower, and J.M. Blaney, Conformational analysis using distance geometry methods. J. Mol. Graphics Modell. 15 (1997) 18-36.

2. S.A. Best, K.M. Merz, Jr., and C.H. Reynolds, Free energy perturbation study of octanol/water partition coefficients: Comparison with continuum GB/SA calculations. J. Phys. Chem. B 103 (199) 714-726.

3. J. Gao, Methods and applications of combined quantum mechanical and molecular mechanical potentials. In: Reviews in computational chemistry, K.B. Lipkowitz and D.B. Boyd, Eds., VCH Publishers, New York, 1995, Vol. 7, pp. 119-185.

4. M.P. Allen and D.J. Tildesley, Computer simulation of liquids. Clarendon, Oxford, 1987.

5. Spartan, version 4.1.1, 1993, Wavefunction, Inc., Irvine, Calif.

Commercial products, including computer programs, are to be mentioned in the text of the manuscript and not normally referenced. If required the reference should list the first author et al. only.

Video

Elsevier accepts video material and animation sequences to support and enhance your scientific research. Authors who have video or animation files that they wish to submit with their article are strongly encouraged to include links to these within the body of the article. This can be done in the same way as a figure or table by referring to the video or animation content and noting in the body text where it should be placed. All submitted files should be properly labeled so that they directly relate to the video file's content. In order to ensure that your video or animation material is directly usable, please provide the files in one of our recommended file formats with a preferred maximum size of 150 MB in total. Any single file should not exceed 50 MB. Video and animation files supplied will be published online in the electronic version of your article in Elsevier Web products, including ScienceDirect. Please supply 'stills' with your files: you can choose any frame from the video or animation or make a separate image. These will be used instead of standard icons and will personalize the link to your video data. For more detailed instructions please visit our video instruction pages. Note: since video and animation cannot be embedded in the print version of the journal, please provide text for both the electronic and the print version for the portions of the article that refer to this content.

Supplementary data
Elsevier accepts electronic supplementary material to support and enhance your scientific research. Supplementary files offer the author additional possibilities to publish supporting applications, high-resolution images, machine-readable files of datasets (especially compounds) sound clips and more. Supplementary files supplied will be published online alongside the electronic version of your article in Elsevier Web products, including ScienceDirect: http://www.sciencedirect.com. In order to ensure that your submitted material is directly usable, please provide the data in one of our recommended file formats. Authors should submit the material in electronic format together with the article and supply a concise and descriptive caption for each file. For more detailed instructions please visit our artwork instruction pages at http://www.elsevier.com/artworkinstructions.

RESEARCH DATA

This journal encourages and enables you to share data that supports your research publication where appropriate, and enables you to interlink the data with your published articles. Research data refers to the results of observations or experimentation that validate research findings. To facilitate reproducibility and data reuse, this journal also encourages you to share your software, code, models, algorithms, protocols, methods and other useful materials related to the project.

Below are a number of ways in which you can associate data with your article or make a statement about the availability of your data when submitting your manuscript. If you are sharing data in one of these ways, you are encouraged to cite the data in your manuscript and reference list. Please refer to the "References" section for more information about data citation. For more information on depositing, sharing and using research data and other relevant research materials, visit the research data page.

Data linking
If you have made your research data available in a data repository, you can link your article directly to the dataset. Elsevier collaborates with a number of repositories to link articles on ScienceDirect with relevant repositories, giving readers access to underlying data that gives them a better understanding of the research described.

There are different ways to link your datasets to your article. When available, you can directly link your dataset to your article by providing the relevant information in the submission system. For more information, visit the database linking page.

For supported data repositories a repository banner will automatically appear next to your published article on ScienceDirect.

In addition, you can link to relevant data or entities through identifiers within the text of your manuscript, using the following format: Database: xxxx (e.g., TAIR: AT1G01020; CCDC: 734053; PDB: 1XFN).

Mendeley Data
This journal supports Mendeley Data, enabling you to deposit any research data (including raw and processed data, video, code, software, algorithms, protocols, and methods) associated with your manuscript in a free-to-use, open access repository. During the submission process, after uploading your manuscript, you will have the opportunity to upload your relevant datasets directly to *Mendeley Data*. The datasets will be listed and directly accessible to readers next to your published article online.

For more information, visit the Mendeley Data for journals page.

Data in Brief
You have the option of converting any or all parts of your supplementary or additional raw data into one or multiple data articles, a new kind of article that houses and describes your data. Data articles ensure that your data is actively reviewed, curated, formatted, indexed, given a DOI and publicly available to all upon publication. You are encouraged to submit your article for *Data in Brief* as an additional item directly alongside the revised version of your manuscript. If your research article is accepted, your data article will automatically be transferred over to *Data in Brief* where it will be editorially reviewed and published in the open access data journal, *Data in Brief*. Please note an open access fee of 500 USD is payable for publication in *Data in Brief*. Full details can be found on the Data in Brief website. Please use this template to write your Data in Brief.

MethodsX
You have the option of converting relevant protocols and methods into one or multiple MethodsX articles, a new kind of article that describes the details of customized research methods. Many researchers spend a significant amount of time on developing methods to fit their specific needs or setting, but often without getting credit for this part of their work. MethodsX, an open access journal, now publishes this information in order to make it searchable, peer reviewed, citable and reproducible. Authors are encouraged to submit their MethodsX article as an additional item directly alongside the revised version of their manuscript. If your research article is accepted, your methods article will automatically be transferred over to MethodsX where it will be editorially reviewed. Please note an open access fee is payable for publication in MethodsX. Full details can be found on the MethodsX website. Please use this template to prepare your MethodsX article.

Data statement
To foster transparency, we encourage you to state the availability of your data in your submission. This may be a requirement of your funding body or institution. If your data is unavailable to access or unsuitable to post, you will have the opportunity to indicate why during the submission process, for example by stating that the research data is confidential. The statement will appear with your published article on ScienceDirect. For more information, visit the Data Statement page.

ARTICLE ENRICHMENTS

AudioSlides

The journal encourages authors to create an AudioSlides presentation with their published article. AudioSlides are brief, webinar-style presentations that are shown next to the online article on ScienceDirect. This gives authors the opportunity to summarize their research in their own words and to help readers understand what the paper is about. More information and examples are available. Authors of this journal will automatically receive an invitation e-mail to create an AudioSlides presentation after acceptance of their paper.

Chemical Compound Viewer (Reaxys)

You can enrich your article with visual representations, links and details for those chemical structures that you define as the main chemical compounds described. Please follow the instructions to learn how to do this.

3D molecular models

You can enrich your online articles by providing 3D molecular models (optional) in PDB, PSE or MOL/MOL2 format, which will be visualized using the interactive viewer embedded within the article. Using the viewer, it will be possible to zoom into the model, rotate and pan the model, and change display settings. Submitted models will also be available for downloading from your online article on ScienceDirect. Each molecular model will have to be uploaded to the online submission system separately, via the '3D molecular models' submission category. More information.

Interactive plots

This journal enables you to show an Interactive Plot with your article by simply submitting a data file. Full instructions.

Interactive Network Viewer

This journal enables you to enrich your online article by including interactive network diagrams created with the latest version of Cytoscape. Each network should be exported from Cytoscape as a ZIP file containing a pair of network (.cyjs) and visual style (.json) files, which is most easily done using the green "SD" button. The recommended maximum file size of a dataset is 150 MB or less.
Once the article is accepted, your ZIP datasets will appear as supplementary material on ScienceDirect and will be visualized inside the Cytoscape application which is displayed alongside your article. Readers will then be able to interactively explore your networks while reading the article. Please note that you must use the latest available version of Cytoscape. More information.

AFTER ACCEPTANCE

Online proof correction

Corresponding authors will receive an e-mail with a link to our online proofing system, allowing annotation and correction of proofs online. The environment is similar to MS Word: in addition to editing text, you can also comment on figures/tables and answer questions from the Copy Editor. Web-based proofing provides a faster and less error-prone process by allowing you to directly type your corrections, eliminating the potential introduction of errors.
If preferred, you can still choose to annotate and upload your edits on the PDF version. All instructions for proofing will be given in the e-mail we send to authors, including alternative methods to the online version and PDF.
We will do everything possible to get your article published quickly and accurately. Please use this proof only for checking the typesetting, editing, completeness and correctness of the text, tables and figures. Significant changes to the article as accepted for publication will only be considered at this stage with permission from the Editor. It is important to ensure that all corrections are sent back to us in one communication. Please check carefully before replying, as inclusion of any subsequent corrections cannot be guaranteed. Proofreading is solely your responsibility.

Offprints

The corresponding author will, at no cost, receive a customized Share Link providing 50 days free access to the final published version of the article on ScienceDirect. The Share Link can be used for sharing the article via any communication channel, including email and social media. For an extra charge, paper offprints can be ordered via the offprint order form which is sent once the article is accepted for publication. Both corresponding and co-authors may order offprints at any time via Elsevier's Webshop. Corresponding authors who have published their article open access do not receive a Share Link as their final published version of the article is available open access on ScienceDirect and can be shared through the article DOI link.

AUTHOR INQUIRIES

Visit the Elsevier Support Center to find the answers you need. Here you will find everything from Frequently Asked Questions to ways to get in touch.
You can also check the status of your submitted article or find out when your accepted article will be published.

5.2 Carta de aceite de publicação do artigo

Gmail Roger Kist <rogerkist@gmail.com>

Your manuscript JMGM_2017_608_R1 has been accepted

Jamie Platts (Journal of Molecular Graphics and Modelling) 21 de dezembro de 2017
<EviseSupport@elsevier.com> 08:57
Responder a: platts@cardiff.ac.uk
Para: rogerkist@gmail.com

Ref: JMGM_2017_608_R1
Title: Searching for potential mTOR inhibitors: ligand-based drug design, docking and molecular dynamics studies of rapamycin binding site
Journal: Journal of Molecular Graphics and Modelling

Dear Mr. Kist,

I am pleased to inform you that your paper has been accepted for publication. My own comments as well as any reviewer comments are appended to the end of this letter. Now that your manuscript has been accepted for publication it will proceed to copy-editing and production.

Thank you for submitting your work to Journal of Molecular Graphics and Modelling. We hope you consider us again for future submissions.

Kind regards,

Jamie Platts
Editor
Journal of Molecular Graphics and Modelling

Comments from the editors and reviewers:
- Reviewer 2

- All revisions made, accept

Have questions or need assistance?
For further assistance, please visit our Customer Support site. Here you can search for solutions on a range of topics, find answers to frequently asked questions, and learn more about EVISE® via interactive tutorials. You can also talk 24/5 to our customer support team by phone and 24/7 by live chat and email.

5.3 Registro do projeto na Comissão de Pesquisa da UFCSPA

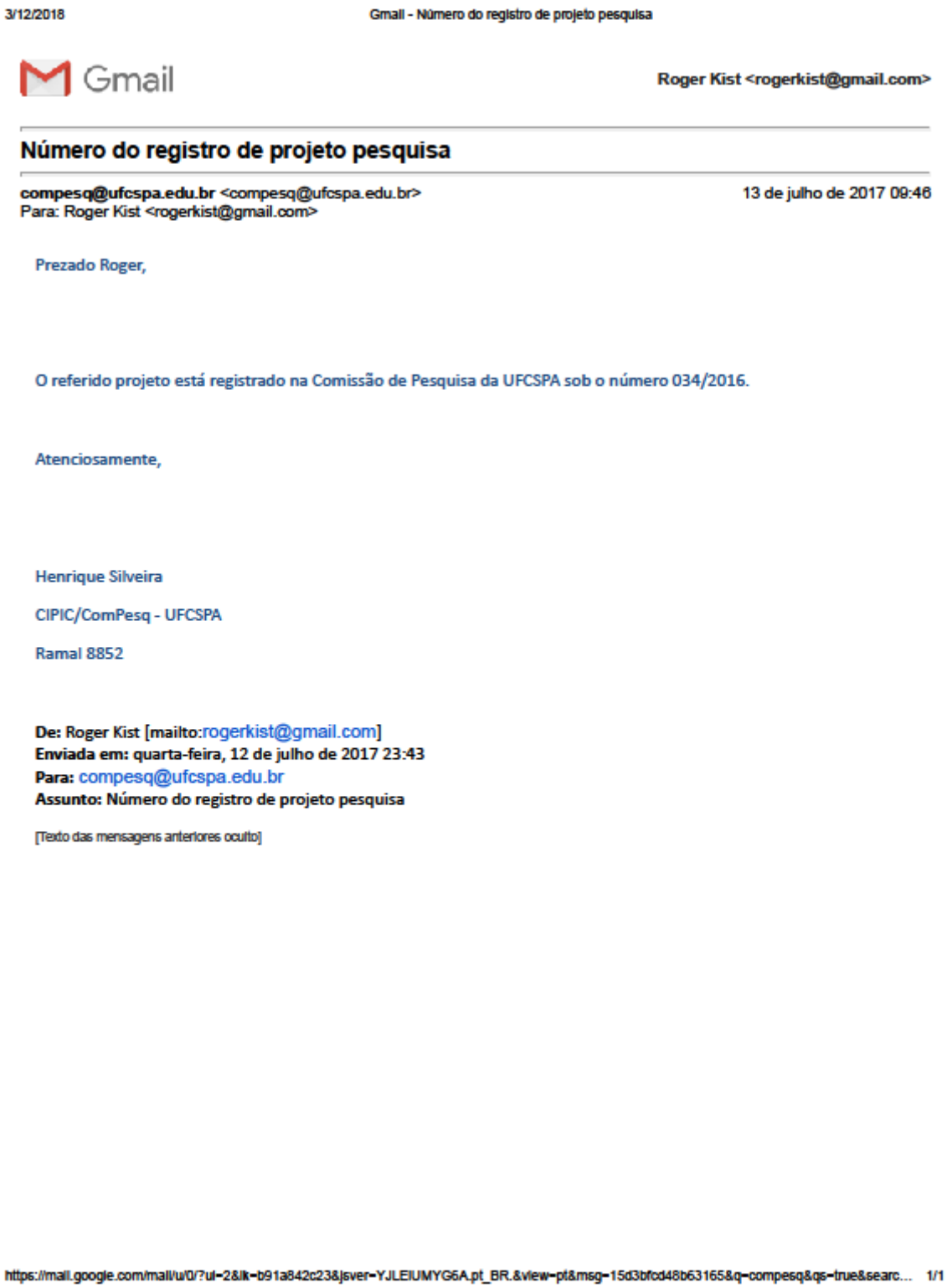

3/12/2018 Gmail - Número do registro de projeto pesquisa

Gmail

Roger Kist <rogerkist@gmail.com>

Número do registro de projeto pesquisa

compesq@ufcspa.edu.br <compesq@ufcspa.edu.br> 13 de julho de 2017 09:46
Para: Roger Kist <rogerkist@gmail.com>

Prezado Roger,

O referido projeto está registrado na Comissão de Pesquisa da UFCSPA sob o número 034/2016.

Atenciosamente,

Henrique Silveira

CIPIC/ComPesq - UFCSPA

Ramal 8852

De: Roger Kist [mailto:rogerkist@gmail.com]
Enviada em: quarta-feira, 12 de julho de 2017 23:43
Para: compesq@ufcspa.edu.br
Assunto: Número do registro de projeto pesquisa

[Texto das mensagens anteriores oculto]

https://mail.google.com/mail/u/0/?ui=2&ik=b91a842c23&jsver=YJLEIUMYG6A.pt_BR.&view=pt&msg=15d3bfcd48b63165&q=compesq&qs=true&searc... 1/1

5.4 Fluxograma metodológico empregado no trabalho